ISM Dynamics and Star Formation

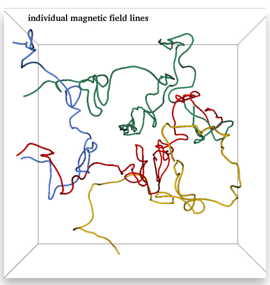


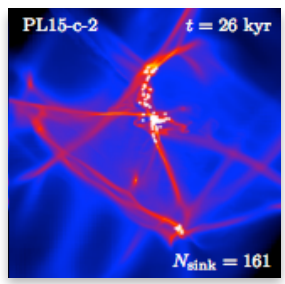

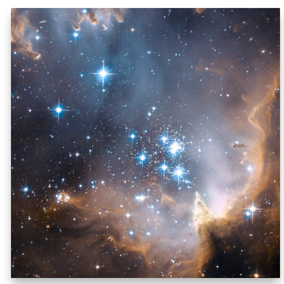
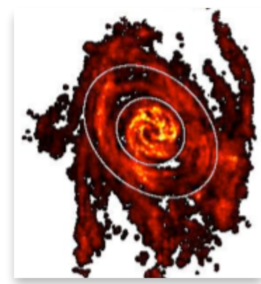
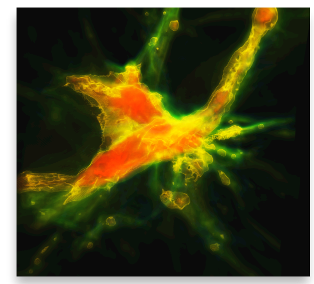

Ralf Klessen

Zentrum für Astronomie der Universität Heidelberg
Institut für Theoretische Astrophysik

thanks to ...

... people in the star formation group at Heidelberg University:

Christian Baczynski, Erik Bertram, Frank Bigiel, Carla June Carroll, Diane Cormier, Simon Glover, Dimitrious Gouliermis, Lionel Haemmerle, Juan Ibanez, Jan-Pieter Paardekooper, Anna Schauer, Jennifer Schober, Rahul Shetty, Daniel Whalen, Katharina Wollenberg

... former group members:

Robi Banerjee, Paul Clark, Christoph Federrath, Philipp Girichidis, Tilman Hartwig, Lukas Konstandin, Thomas Peters, Dominik Schleicher, Rowan Smith, László Szűcs. . .

... many collaborators abroad!

Deutsche Forschungsgemeinschaft DFG

ISM-SPP DFG Priority Program 1573 Interstellar Medium

BADEN-WÜRTTEMBERG STIFTUNG Wir stiften Zukunft

HGSFP

IMPRS

erc European Research Council

agenda

- remarks on star formation theory
  - historic remarks
  - current understanding
- applications / controversies / puzzles
  - global star formation relations: *do we understand them?*
  - molecular gas: *are we sure we see all H_2 gas?*
  - filaments: *is there a universal width?*

NGC 3324 (Hubble, NASA/ESA)


theoretical
remarks

decrease in spatial scale / increase in density


Andromeda (R. Gendler)


NGC 602 in LMC (Hubble)


Proplyd in Orion (Hubble)

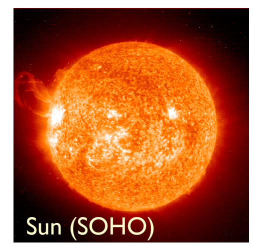
Sun (SOHO)


Earth

- density
  - density of ISM: few particles per cm^3
  - density of molecular cloud: few 100 particles per cm^3
  - density of Sun: 1.4 g/cm^3
- spatial scale
  - size of molecular cloud: few 10s of pc
  - size of young cluster: ~ 1 pc
  - size of Sun: 1.4×10^{10} cm

decrease in spatial scale / increase in density


Andromeda (R. Gendler)


NGC 602 in LMC (Hubble)


Proplyd in Orion (Hubble)

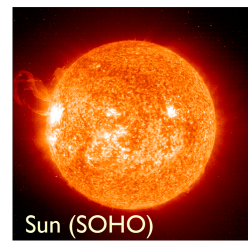
Sun (SOHO)


Earth

- contracting force
  - only force that can do this compression is *GRAVITY*
- opposing forces
  - there are several processes that can oppose gravity
  - *GAS PRESSURE*
  - *TURBULENCE*
  - *MAGNETIC FIELDS*
  - *RADIATION PRESSURE*

Modern star formation theory is based on the complex interplay between *all* these processes.

early theoretical models

- *Jeans (1902):* Interplay between self-gravity and thermal pressure
  - stability of homogeneous spherical density enhancements against gravitational collapse
  - dispersion relation:

$$\boxed{\omega^2 = c_s^2 k^2 - 4\pi G \rho_0}$$

  - instability when $\omega^2 < 0$
  - minimal mass: $\boxed{M_J = \frac{1}{6}\pi^{-5/2} G^{-3/2} \rho_0^{-1/2} c_s^3 \propto \rho_0^{-1/2} T^{+3/2}}$

Sir James Jeans, 1877 - 1946

first approach to turbulence

- *von Weizsäcker (1943, 1951)* and *Chandrasekhar (1951):* concept of ***MICROTURBULENCE***
  - BASIC ASSUMPTION: separation of scales between dynamics and turbulence

    $\ell_{\mathrm{turb}} \ll \ell_{\mathrm{dyn}}$

  - then turbulent velocity dispersion contributes to effective soundspeed:

    $$\boxed{c_c^2 \mapsto c_c^2 + \sigma_{rms}^2}$$

  - → Larger effective Jeans masses → more stability
  - BUT: *(1) turbulence depends on k:* $\sigma_{rms}^2(k)$

    (2) supersonic turbulence → $\sigma_{rms}^2(k) >> c_s^2$ *usually*

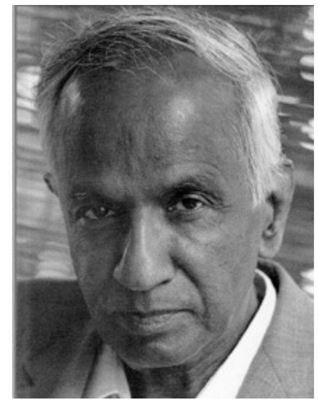

S. Chandrasekhar, 1910 - 1995

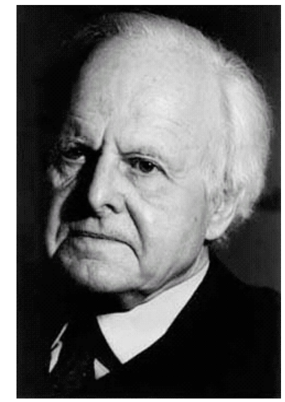

C.F. von Weiszäcker, 1912 - 2007

problems of early dynamical theory

- molecular clouds are *highly Jeans-unstable,*
  yet, they do *NOT* form stars at high rate
  and with high efficiency (Zuckerman & Evans 1974 conundrum)
  (the observed global SFE in molecular clouds is *~5%*)
  → *something prevents large-scale collapse.*
- all throughout the early 1990's, molecular clouds
  had been thought to be long-lived quasi-equilibrium
  entities.
- molecular clouds are *magnetized*

magnetic star formation

- *Mestel & Spitzer (1956):* Magnetic fields can prevent collapse*!!!*
  - Critical mass for gravitational collapse in presence of B-field

$$M_{cr} = \frac{5^{3/2}}{48\pi^2} \frac{B^3}{G^{3/2}\rho^2}$$

  - Critical mass-to-flux ratio (Mouschovias & Spitzer 1976)

$$\left[\frac{M}{\Phi}\right]_{cr} = \frac{\zeta}{3\pi}\left[\frac{5}{G}\right]^{1/2}$$

  - Ambipolar diffusion can initiate collapse

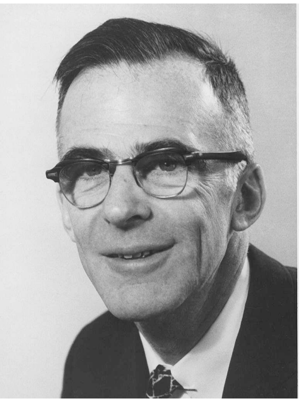

Lyman Spitzer, Jr., 1914 - 1997

“standard theory” of star formation

- BASIC ASSUMPTION: Stars form from magnetically highly subcritical cores
- Ambipolar diffusion slowly increases (M/Φ): $\tau_{AD} \approx 10\tau_{ff}$
- Once $(M/\Phi) > (M/\Phi)_{crit}$: dynamical collapse of SIS
  - Shu (1977) collapse solution
  - $dM/dt = 0.975\ c_s^3/G = \text{const.}$
- Was (in principle) only intended for isolated, low-mass stars

Frank Shu, 1943 -

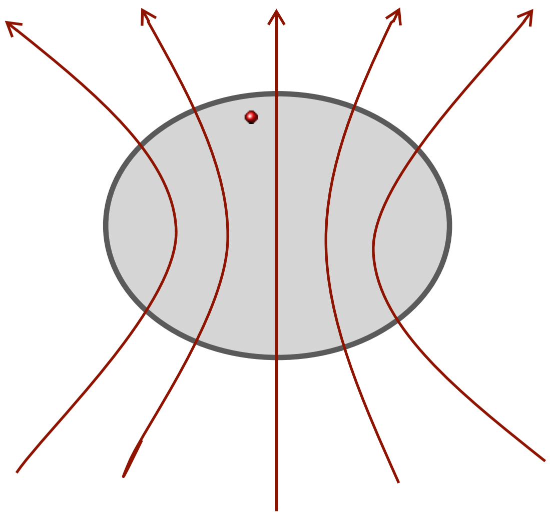

problems of “standard theory”

- Observed B-fields are weak, at most marginally critical (Crutcher 1999, Bourke et al. 2001)
- Magnetic fields cannot prevent decay of turbulence
(Mac Low et al. 1998, Stone et al. 1998, Padoan & Nordlund 1999)
- Structure of prestellar cores
(e.g. Bacman et al. 2000, Alves et al. 2001)
- Strongly time varying dM/dt
(e.g. Hendriksen et al. 1997, André et al. 2000)
- More extended infall motions than predicted by the standard model
(Williams & Myers 2000, Myers et al. 2000)
- Most stars form as binaries
(e.g. Lada 2006)
- As many prestellar cores as protostellar cores in SF regions (e.g. André et al 2002)
- Molecular cloud clumps are chemically young
(Bergin & Langer 1997, Pratap et al 1997, Aikawa et al 2001)
- Stellar age distribution small ($\tau_{ff} << \tau_{AD}$)
(Ballesteros-Paredes et al. 1999, Elmegreen 2000, Hartmann 2001)
- Strong theoretical criticism of the SIS as starting condition for gravitational collapse
(e.g. Whitworth et al 1996, Nakano 1998, as summarized in Klessen & Mac Low 2004)
- Standard AD-dominated theory is incompatible with observations
(Crutcher et al. 2009, 2010ab, Bertram et al. 2011)

(see e.g. Mac Low & Klessen, 2004, Rev. Mod. Phys., 76, 125-194, Klessen & Glover 2014, Saas Fee Lecture, arXiv:1412.5182, 1-191)

properties of turbulence

- laminar flows turn *turbulent* at *high* *Reynolds* numbers

$$Re = \frac{\text{advection}}{\text{dissipation}} = \frac{VL}{\nu}$$

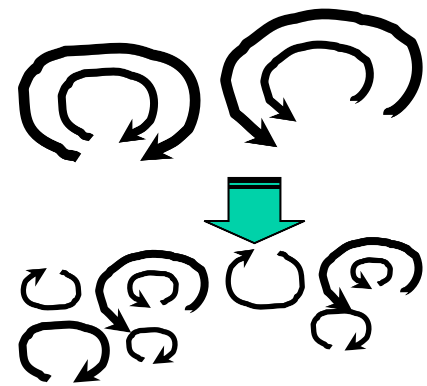

V= typical velocity on scale L, $\nu = \eta/\rho$ = kinematic viscosity,
turbulence for Re > 1000 → typical values in ISM 10^8-10^{10}

- Navier-Stokes equation (transport of momentum)

$$\rho \frac{d\vec{v}}{dt} = \rho\left(\frac{\partial \vec{v}}{\partial t} + (\vec{v}\cdot\vec{\nabla})\vec{v}\right) = -\vec{\nabla}P + \eta\,\vec{\nabla}^2\vec{v} + \left(\frac{\eta}{3} + \zeta\right)\vec{\nabla}(\vec{\nabla}\cdot\vec{v})$$

shear viscosity

bulk viscosity

$$\sigma_{ij} \equiv \eta\left(\frac{\partial v_i}{\partial x_j} + \frac{\partial v_j}{\partial x_i} - \frac{2}{3}\,\delta_{ij}\frac{\partial v_k}{\partial x_k}\right) + \zeta\delta_{ij}\frac{\partial v_k}{\partial x_k}$$

viscous stress tensor

properties of turbulence

- laminar flows turn *turbulent* at *high* *Reynolds* numbers

$$Re = \frac{\text{advection}}{\text{dissipation}} = \frac{VL}{\nu}$$

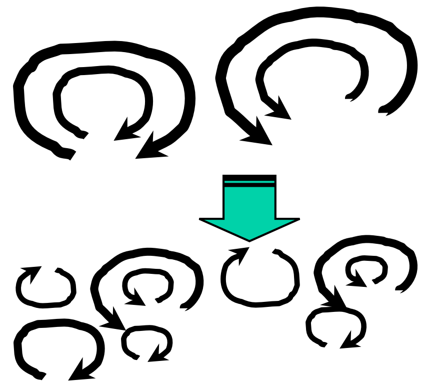

V= typical velocity on scale L, $\nu = \eta/\rho$ = kinematic viscosity,
turbulence for Re > 1000 → typical values in ISM 10^8-10^{10}

- vortex streching --> turbulence is intrinsically anisotropic
(only on large scales you may get
homogeneity & isotropy in a statistical sense;
see Landau & Lifschitz, Chandrasekhar, Taylor, etc.)

(ISM turbulence: shocks & B-field
cause additional inhomogeneity)

turbulent cascade in the ISM

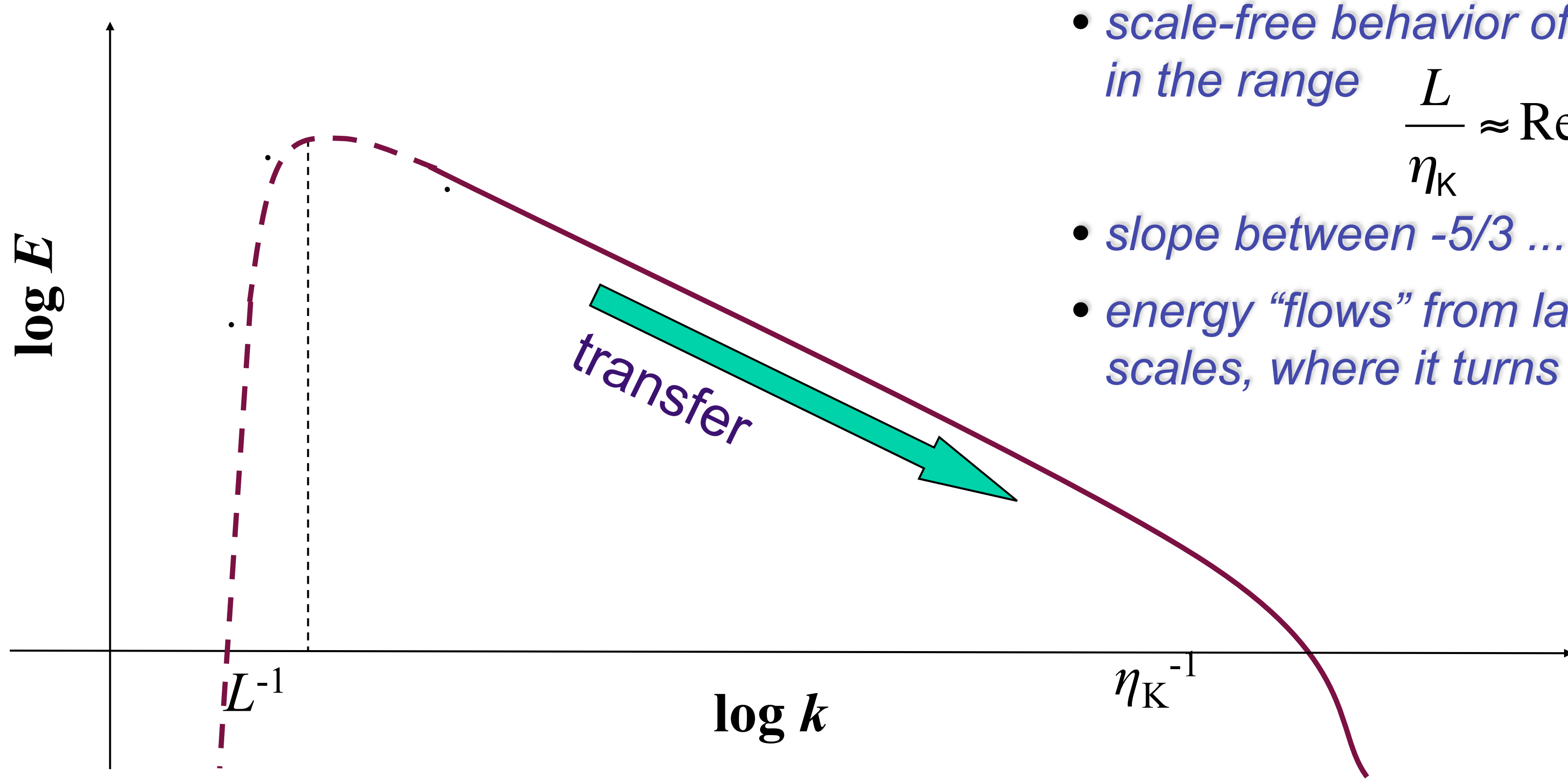

- *scale-free behavior of turbulence in the range* $\dfrac{L}{\eta_K} \approx \mathrm{Re}^{3/4}$
- *slope between -5/3 ... -2*
- *energy "flows" from large to small scales, where it turns into heat*

energy source & scale *NOT known* (supernovae, winds, spiral density waves?)

dissipation scale not known (ambipolar diffusion, molecular diffusion?)

turbulent cascade in the ISM

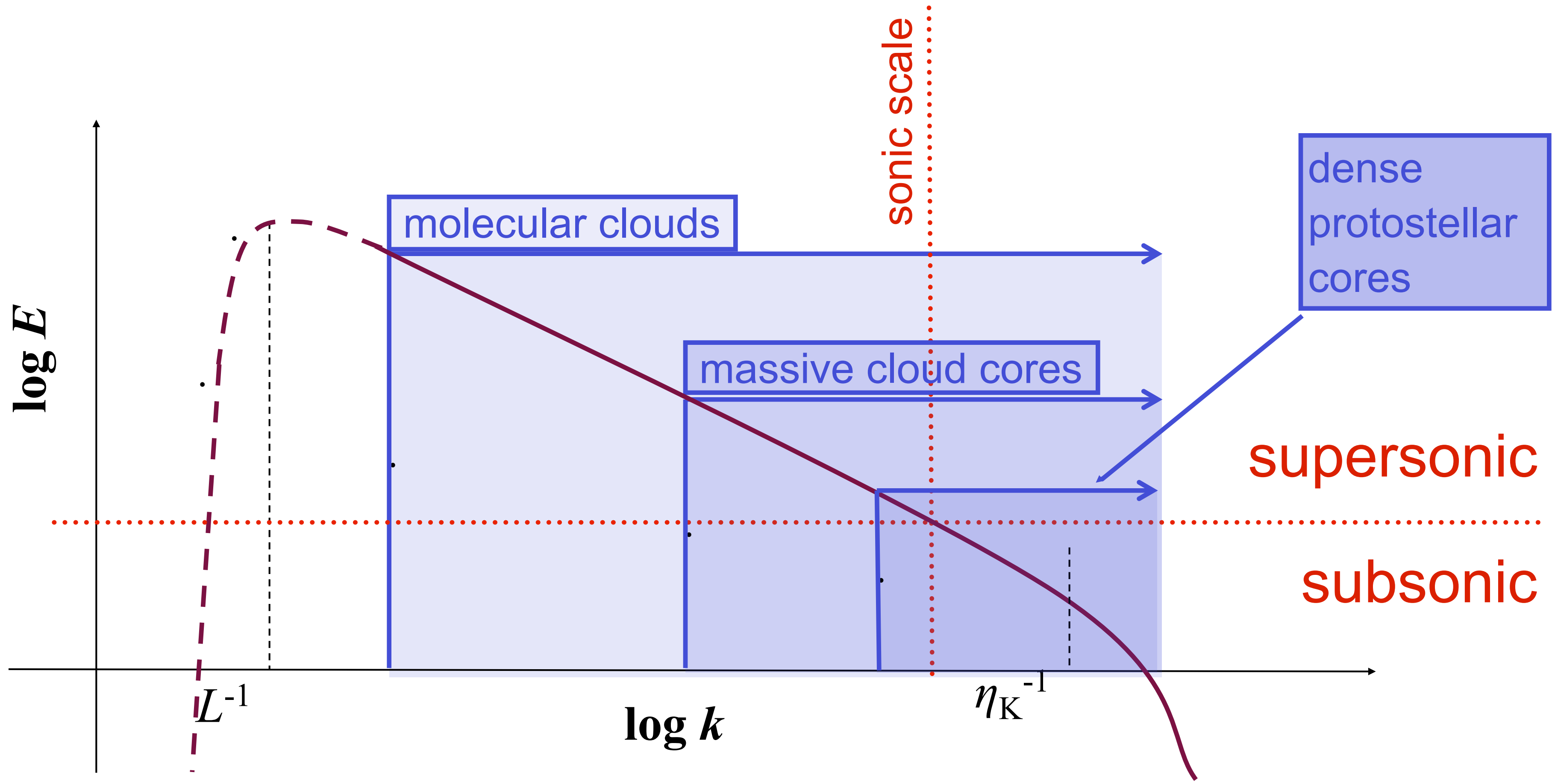

energy source & scale *NOT known* (supernovae, winds, spiral density waves?)

$\sigma_{rms} << 1$ km/s
$M_{rms} \leq 1$
$L \approx 0.1$ pc

dissipation scale not known (ambipolar diffusion, molecular diffusion?)

gravoturbulent star formation

- BASIC ASSUMPTION:

star formation is controlled by interplay between supersonic turbulence and self-gravity

- turbulence plays a *dual role*:
  - on *large scales* it *provides support*
  - on *small scales* it can *trigger collapse*
- some predictions:
  - dynamical star formation timescale τ_{ff}
  - high binary fraction
  - complex spatial structure of embedded star clusters
  - and many more . . .

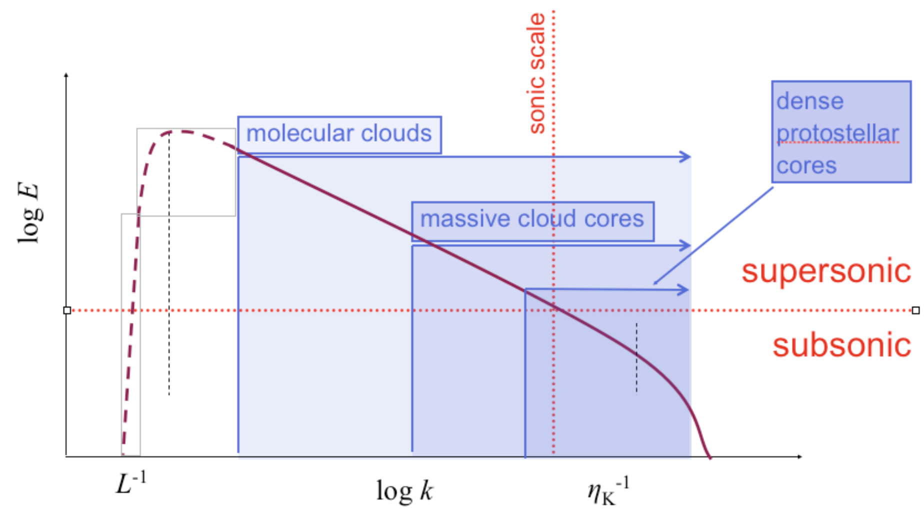

Mac Low & Klessen, 2004, Rev. Mod. Phys., 76, 125-194
McKee & Ostriker, 2007, ARAA, 45, 565
Klessen & Glover 2014, Saas Fee Lecture, arXiv:1412.5182, 1-191

gravoturbulent star formation

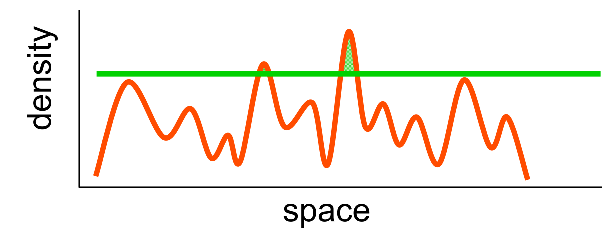

- interstellar gas is highly *inhomogeneous*
  - *gravitational instability*
  - *thermal instability*
  - *turbulent compression* (in shocks $\delta\rho/\rho \propto \mathcal{M}^2$; in atomic gas: $\mathcal{M} \approx 1...3$)
- cold *molecular clouds* can form rapidly in high-density regions at *stagnation points* of *convergent large-scale flows*
  - chemical *phase transition*: atomic → molecular
  - process is *modulated* by large-scale *dynamics* in the galaxy
- inside *cold clouds:* turbulence is highly supersonic ($\mathcal{M} \approx 1...20$)
  → *turbulence* creates large density contrast,
  gravity selects for collapse

→ ***GRAVOTUBULENT FRAGMENTATION***

- *turbulent cascade:* local compression *within* a cloud provokes collapse → formation of individual *stars* and *star clusters*

(e.g. Mac Low & Klessen, 2004, Rev. Mod. Phys., 76, 125-194)

molecular cloud formation

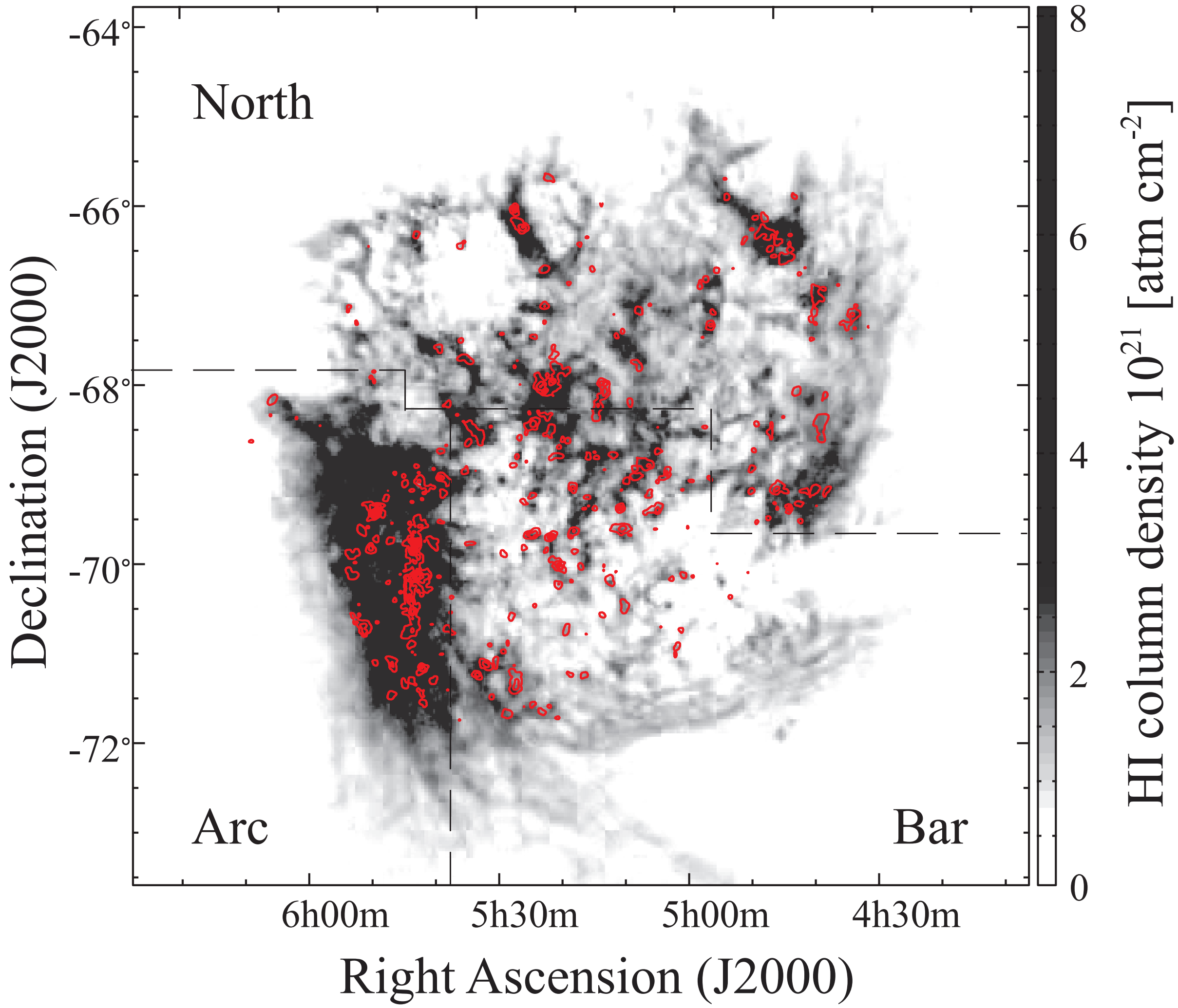

Idea:

Molecular clouds form at *stagnation points* of large-scale convergent flows, mostly triggered by global (or external) perturbations. Their internal turbulence is driven by accretion, i.e. by the process of cloud formation

- molecular clouds grow in mass
- this is inferred by looking at molecular clouds in different evolutionary phases in the LMC (Fukui et al. 2008, 2009)

Fukui et al. (2009)

zooming in ...

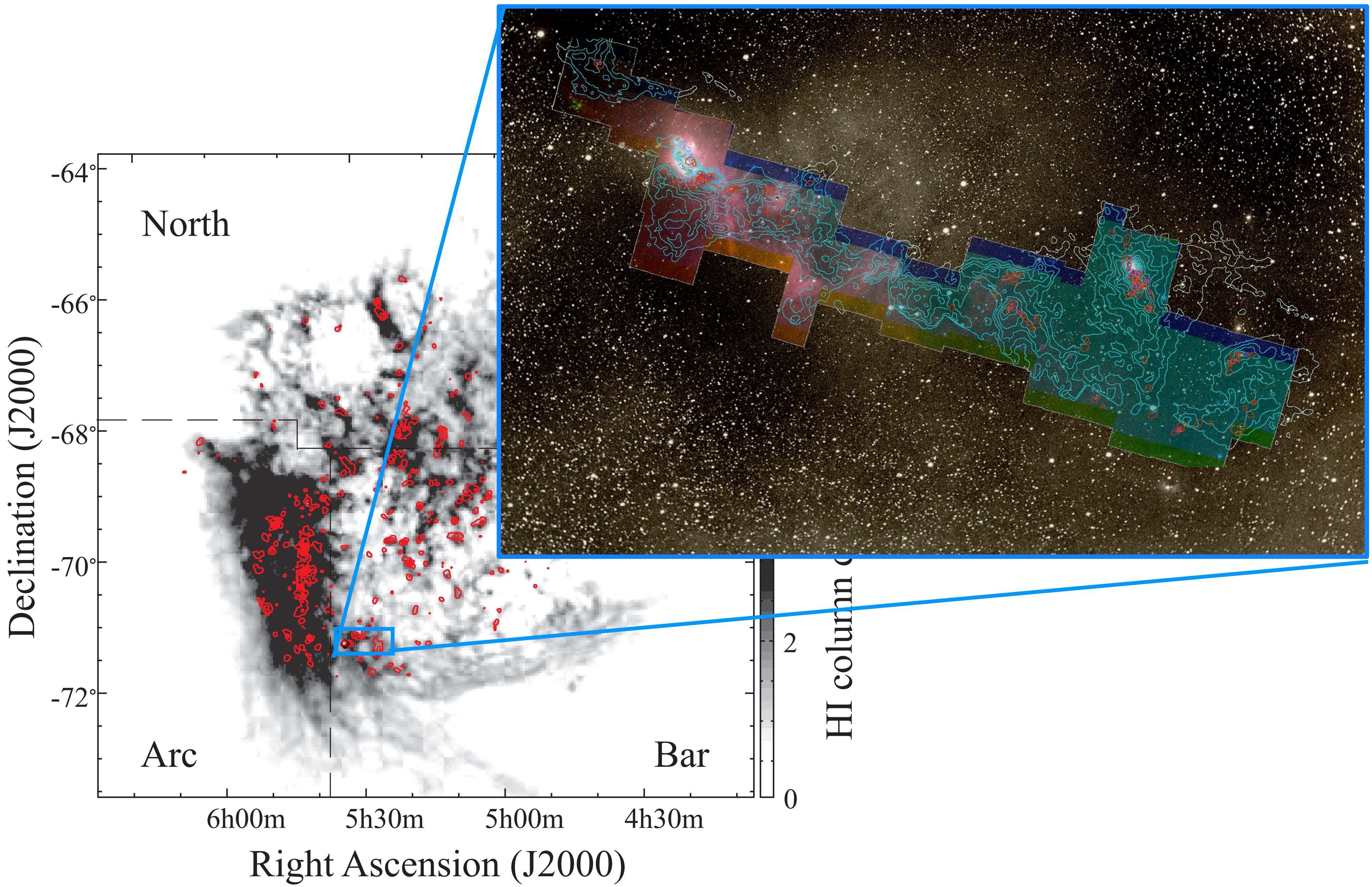

-64°
-66°
-68°
-70°
-72°
North
Arc
Bar
Declination (J2000)
6h00m
5h30m
5h00m
4h30m
Right Ascension (J2000)
HI column
2
0

position-position-velocity structure of the Perseus cloud

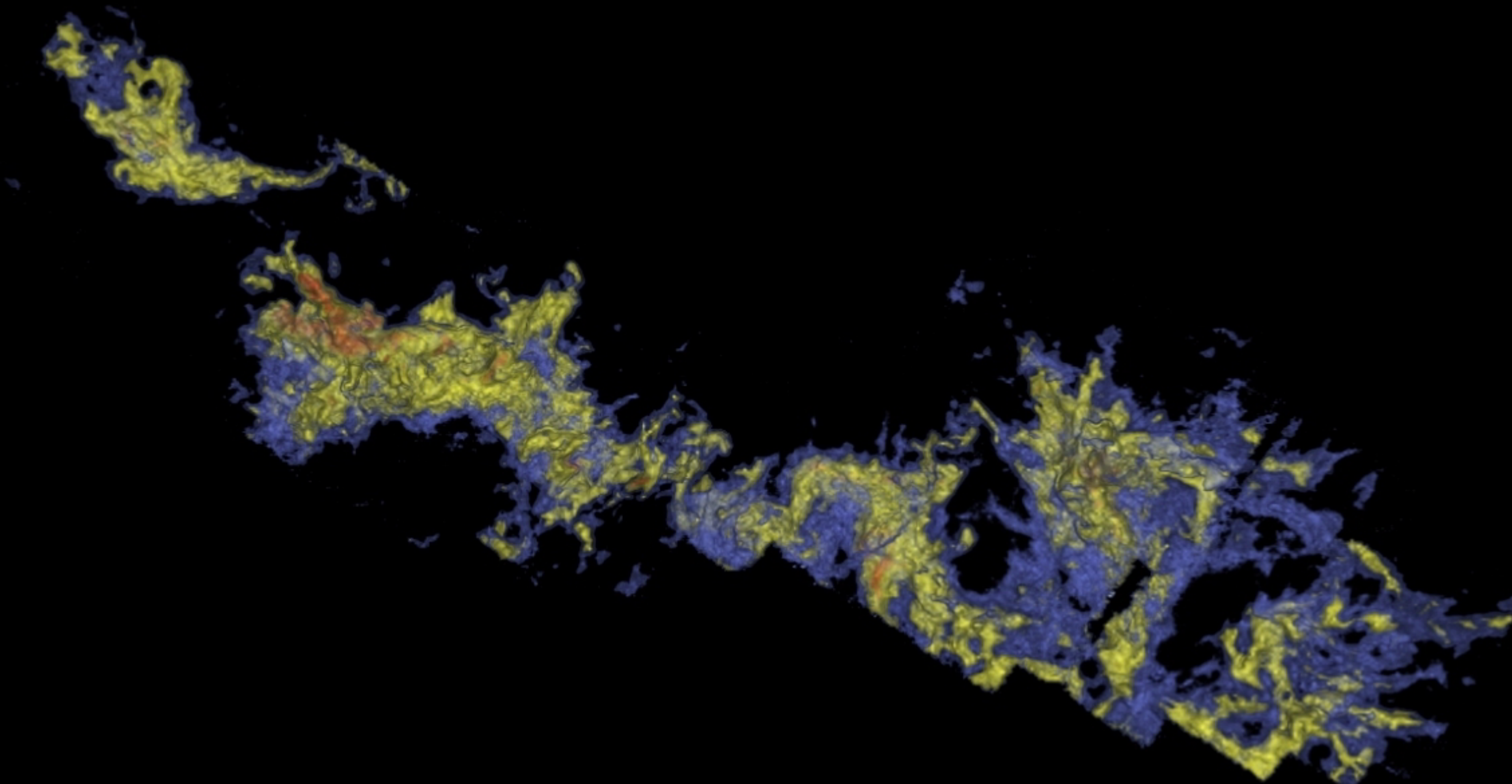

image from Alyssa Goodman: COMPLETE survey

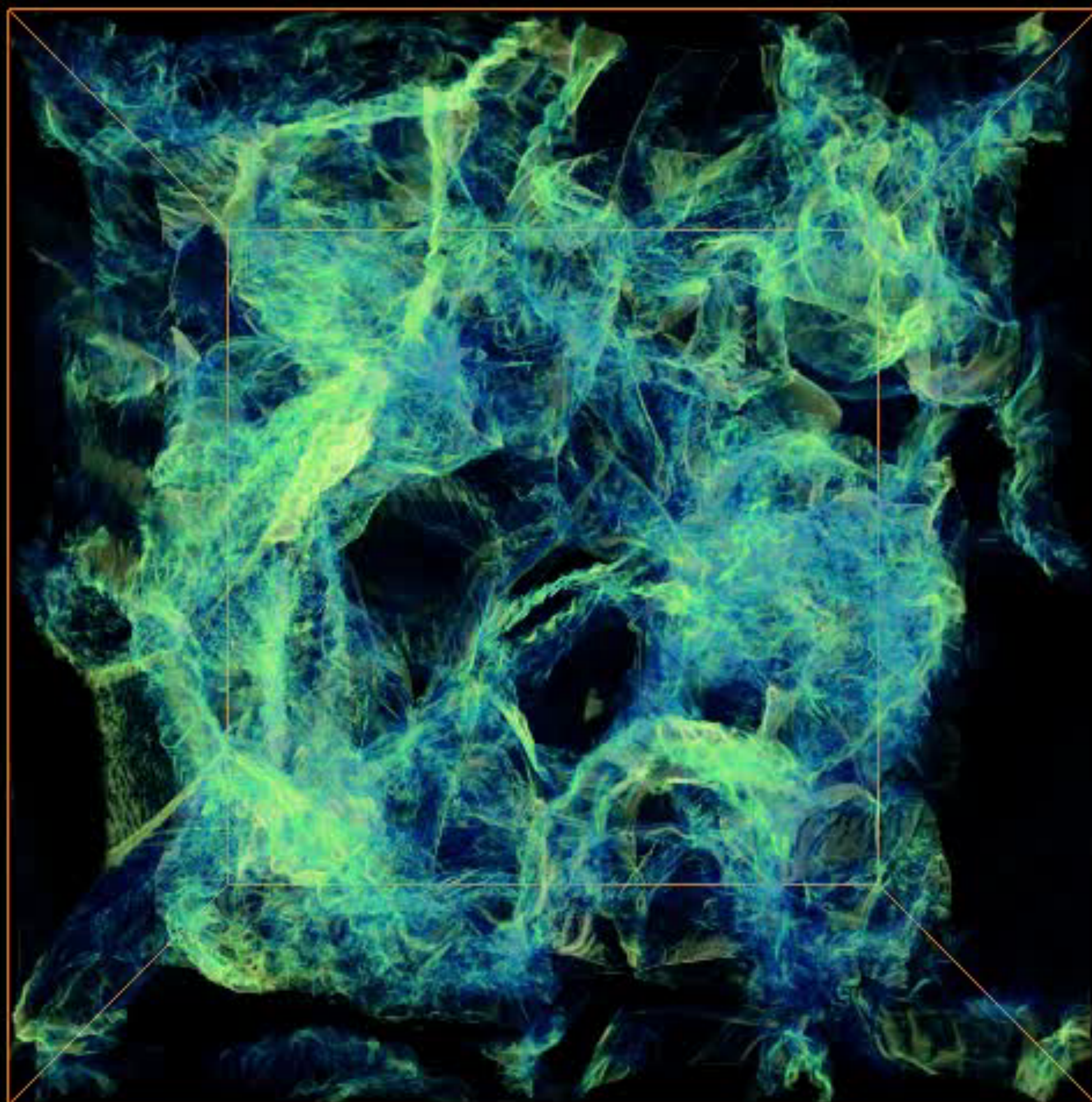

Schmidt et al. (2009, A&A, 494, 127)

caveat of numerical simulations

- most astrophysical turbulence simulations use an ***LES*** approach to model the flow
- principal problem: only large scale flow properties
  - Reynolds number: Re = LV/ν ***(Re_{nature} >> Re_{model})***
  - dynamic range much smaller than true physical one
  - need *subgrid model* (often only dissipation)
  - but what to do for more complex when processes on subgrid scale determine large-scale dynamics
    (chemical reactions, nuclear burning, etc)
  - Turbulence is “space filling” --> difficulty for AMR (don’t know what criterion to use for refinement)
- how *large* a Reynolds number do we need to catch basic dynamics right?

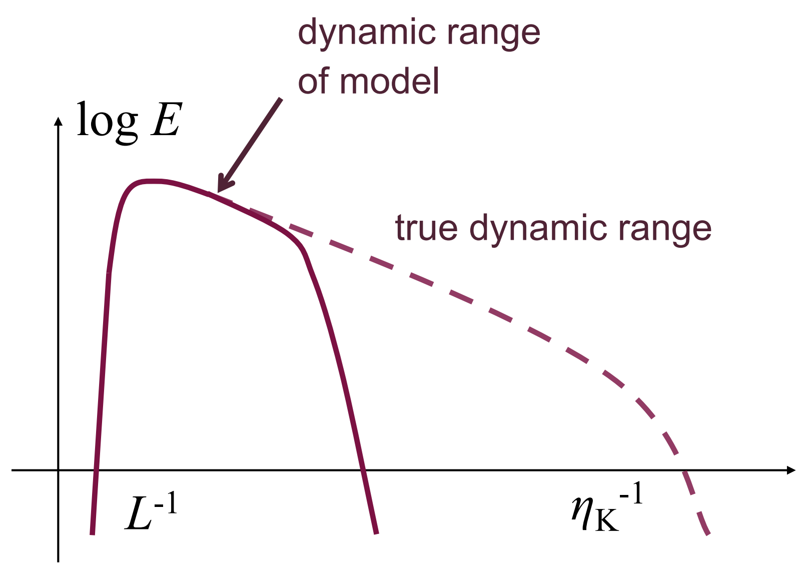


including detailed
chemistry

chemical model 0

- 32 chemical species
  - 17 in instantaneous equilibrium:

H^-, H_2^+, H_3^+, CH^+, CH_2^+, OH^+, H_2O^+, H_3O^+, CO^+, HOC^+, O^-, C^- and O_2^+

  - 19 full non-equilibrium evolution

e^-, H^+, H, H_2, He, He^+, C, C^+, O, O^+, OH, H_2O, CO,

C_2, O_2, HCO^+, CH, CH_2 and CH_3^+

- 218 reactions
- various heating and cooling processes

long series of publications by Simon Glover and collaborators, e.g. Glover & Mac Low (2007ab), Glover, Federrath, Mac Low, Klessen (2010), Glover & Clark (2012, 2013), Clark & Clover (2012, 2013)

chemical model 1

Process	Reference(s)
Cooling:	
C fine structure lines	Atomic data – Silva & Viegas (2002)
	Collisional rates (H) – Abrahamsson, Krems & Dalgarno (2007)
	Collisional rates (H_2) – Schroder et al. (1991)
	Collisional rates (e^-) – Johnson et al. (1987)
	Collisional rates (H^+) – Roueff & Le Bourlot (1990)
C^+ fine structure lines	Atomic data – Silva & Viegas (2002)
	Collisional rates (H_2) – Flower & Launay (1977)
	Collisional rates (H, $T < 2000$ K) – Hollenbach & McKee (1989)
	Collisional rates (H, $T > 2000$ K) – Keenan et al. (1986)
	Collisional rates (e^-) – Wilson & Bell (2002)
O fine structure lines	Atomic data – Silva & Viegas (2002)
	Collisional rates (H) – Abrahamsson, Krems & Dalgarno (2007)
	Collisional rates (H_2) – see Glover & Jappsen (2007)
	Collisional rates (e^-) – Bell, Berrington & Thomas (1998)
	Collisional rates (H^+) – Pequignot (1990, 1996)
H_2 rovibrational lines	Le Bourlot, Pineau des Forêts & Flower (1999)
CO and H_2O rovibrational lines	Neufeld & Kaufman (1993); Neufeld, Lepp & Melnick (1995)
OH rotational lines	Pavlovski et al. (2002)
Gas-grain energy transfer	Hollenbach & McKee (1989)
Recombination on grains	Wolfire et al. (2003)
Atomic resonance lines	Sutherland & Dopita (1993)
H collisional ionization	Abel et al. (1997)
H_2 collisional dissociation	See Table B1
Compton cooling	Cen (1992)
Heating:	
Photoelectric effect	Bakes & Tielens (1994); Wolfire et al. (2003)
H_2 photodissociation	Black & Dalgarno (1977)
UV pumping of H_2	Burton, Hollenbach & Tielens (1990)
H_2 formation on dust grains	Hollenbach & McKee (1989)
Cosmic ray ionization	Goldsmith & Langer (1978)

(Glover, Federrath, Mac Low, Klessen, 2010, MNRS, 404, 2)

chemical model 2

Table B1. List of collisional gas-phase reactions included in our chemical model.

No.	Reaction	Rate coefficient ($cm^3 s^{-1}$)	Notes	Ref.
1	$H + e^- \rightarrow H^- + \gamma$	$k_1 = \mathrm{dex}[-17.845 + 0.762 \log T + 0.1523(\log T)^2$		1
		$- 0.03274(\log T)^3]$	$T \leqslant 6000$ K	
		$= \mathrm{dex}[-16.420 + 0.1998(\log T)^2$		
		$- 5.447 \times 10^{-3}(\log T)^4$		
		$+ 4.0415 \times 10^{-5}(\log T)^6]$	$T > 6000$ K	
2	$H^- + H \rightarrow H_2 + e^-$	$k_2 = 1.5 \times 10^{-9}$	$T \leqslant 300$ K	2
		$= 4.0 \times 10^{-9} T^{-0.17}$	$T > 300$ K	
3	$H + H^+ \rightarrow H_2^+ + \gamma$	$k_3 = \mathrm{dex}[-19.38 - 1.523 \log T$		3
		$+ 1.118(\log T)^2 - 0.1269(\log T)^3]$		
4	$H + H_2^+ \rightarrow H_2 + H^+$	$k_4 = 6.4 \times 10^{-10}$		4
5	$H^- + H^+ \rightarrow H + H$	$k_5 = 2.4 \times 10^{-6} T^{-1/2}(1.0 + T/20000)$		5
6	$H_2^+ + e^- \rightarrow H + H$	$k_6 = 1.0 \times 10^{-8}$	$T \leqslant 617$ K	6
		$= 1.32 \times 10^{-6} T^{-0.76}$	$T > 617$ K	
7	$H_2 + H^+ \rightarrow H_2^+ + H$	$k_7 = [-3.3232183 \times 10^{-7}$		7
		$+ 3.3735382 \times 10^{-7} \ln T$		
		$- 1.4491368 \times 10^{-7}(\ln T)^2$		
		$+ 3.4172805 \times 10^{-8}(\ln T)^3$		
		$- 4.7813720 \times 10^{-9}(\ln T)^4$		
		$+ 3.9731542 \times 10^{-10}(\ln T)^5$		
		$- 1.8171411 \times 10^{-11}(\ln T)^6$		
		$+ 3.5311932 \times 10^{-13}(\ln T)^7]$		
		$\times \exp\left(\frac{-21237.15}{T}\right)$		
8	$H_2 + e^- \rightarrow H + H + e^-$	$k_8 = 3.73 \times 10^{-9} T^{0.1121} \exp\left(\frac{-99430}{T}\right)$		8
9	$H_2 + H \rightarrow H + H + H$	$k_{9,1} = 6.67 \times 10^{-12} T^{1/2} \exp\left[-(1 + \frac{63590}{T})\right]$		9
		$k_{9,h} = 3.52 \times 10^{-9} \exp\left(-\frac{43900}{T}\right)$		10
		$n_{cr,H} = \mathrm{dex}\left[3.0 - 0.416 \log\left(\frac{T}{10000}\right) - 0.327\left\{\log\left(\frac{T}{10000}\right)\right\}^2\right]$		10
10	$H_2 + H_2 \rightarrow H_2 + H + H$	$k_{10,1} = \frac{5.996 \times 10^{-30} T^{4.1881}}{(1.0 + 6.761 \times 10^{-6} T)^{5.6881}} \exp\left(-\frac{54657.4}{T}\right)$		11
		$k_{10,h} = 1.3 \times 10^{-9} \exp\left(-\frac{53300}{T}\right)$		12
		$n_{cr,H_2} = \mathrm{dex}\left[4.845 - 1.3 \log\left(\frac{T}{10000}\right) + 1.62\left\{\log\left(\frac{T}{10000}\right)\right\}^2\right]$		12
11	$H + e^- \rightarrow H^+ + e^- + e^-$	$k_{11} = \exp[-3.271396786 \times 10^1$		13
		$+ 1.35365560 \times 10^1 \ln T_e$		
		$- 5.73932875 \times 10^0(\ln T_e)^2$		
		$+ 1.56315498 \times 10^0(\ln T_e)^3$		
		$- 2.87705600 \times 10^{-1}(\ln T_e)^4$		
		$+ 3.48255977 \times 10^{-2}(\ln T_e)^5$		
		$- 2.63197617 \times 10^{-3}(\ln T_e)^6$		
		$+ 1.11954395 \times 10^{-4}(\ln T_e)^7$		
		$- 2.03914985 \times 10^{-6}(\ln T_e)^8]$		
12	$H^+ + e^- \rightarrow H + \gamma$	$k_{12,A} = 1.269 \times 10^{-13}\left(\frac{315614}{T}\right)^{1.503}$	Case A	14
		$\times [1.0 + \left(\frac{604625}{T}\right)^{0.470}]^{-1.923}$		
		$k_{12,B} = 2.753 \times 10^{-14}\left(\frac{315614}{T}\right)^{1.500}$	Case B	14
		$\times [1.0 + \left(\frac{115188}{T}\right)^{0.407}]^{-2.242}$		
13	$H^- + e^- \rightarrow H + e^- + e^-$	$k_{13} = \exp[-1.801849334 \times 10^1$		13
		$+ 2.36085220 \times 10^0 \ln T_e$		
		$- 2.82744300 \times 10^{-1}(\ln T_e)^2$		
		$+ 1.62331664 \times 10^{-2}(\ln T_e)^3$		
		$- 3.36501203 \times 10^{-2}(\ln T_e)^4$		
		$+ 1.17832978 \times 10^{-2}(\ln T_e)^5$		
		$- 1.65619470 \times 10^{-3}(\ln T_e)^6$		
		$+ 1.06827520 \times 10^{-4}(\ln T_e)^7$		
		$- 2.63128581 \times 10^{-6}(\ln T_e)^8]$		

(Glover, Federrath, Mac Low, Klessen, 2010, MNRS, 404, 2)

chemical model 2

(Glover, Federrath, Mac Low, Klessen, 2010, MNRS, 404, 2)

Table B1.

No.	Reaction			
1	H +			
2	H^-			
3	H +			
4	H +			
5	H^-			
6	H_2^+			
7	H_2			
8	H_2			
9	H_2			
10	H_2			
11	H +			
12	H^+			
13	H^-			
14	$H^- + H \rightarrow H + H + e^-$	$k_{14} = 2.5634 \times 10^{-9} T_e^{1.78186}$	$T_e \leqslant 0.1$ eV	13
		$= \exp[-2.0372609 \times 10^1$		
		$+ 1.13944933 \times 10^0 \ln T_e$		
		$- 1.4210135 \times 10^{-1} (\ln T_e)^2$		
		$+ 8.4644554 \times 10^{-3} (\ln T_e)^3$		
		$- 1.$[illegible]$7641 \times 10^{-3} (\ln T_e)^4$		
		$+ 2.012$[illegible]$ \times 10^{-4} (\ln T_e)^5$		
		$+ 8.6639632 \times 10^{-5} (\ln T_e)^6$		
		$- 2.5850097 \times 10^{-5} (\ln T_e)^7$		
		$+ 2.4555012 \times 10^{-6} (\ln T_e)^8$		
		$- 8.0683825 \times 10^{-8} (\ln T_e)^9]$	$T_e > 0.1$ eV	
15	$H^- + H^+ \rightarrow H_2^+ + e^-$	$k_{15} = 6.9 \times 10^{-9} T^{-0.35}$	$T \leqslant 8000$ K	15
		$= 9.6 \times 10^{-7} T^{-0.90}$	$T > 8000$ K	
16	$He + e^- \rightarrow He^+ + e^- + e^-$	$k_{16} = \exp[-4.409864886 \times 10^1$		13
		$+ 2.391596563 \times 10^1 \ln T_e$		
		$- 1.07532302 \times 10^1 (\ln T_e)^2$		
		$+ 3.05803875 \times 10^0 (\ln T_e)^3$		
		$- 5.6851189 \times 10^{-1} (\ln T_e)^4$		
		$+ 6.79539123 \times 10^{-2} (\ln T_e)^5$		
		$- 5.0090561 \times 10^{-3} (\ln T_e)^6$		
		$+ 2.06723616 \times 10^{-4} (\ln T_e)^7$		
		$- 3.64916141 \times 10^{-6} (\ln T_e)^8]$		
17	$He^+ + e^- \rightarrow He + \gamma$	$k_{17,rr,A} = 10^{-11} T^{-0.5} [12.72 - 1.615 \log T$	Case A	16
		$- 0.3162 (\log T)^2 + 0.0493 (\log T)^3]$		
		$k_{17,rr,B} = 10^{-11} T^{-0.5} [11.19 - 1.676 \log T$	Case B	16
		$- 0.2852 (\log T)^2 + 0.04433 (\log T)^3]$		
		$k_{17,di} = 1.9 \times 10^{-3} T^{-1.5} \exp\left(-\frac{473421}{T}\right)$		
		$\times \left[1.0 + 0.3 \exp\left(-\frac{94684}{T}\right)\right]$		17
18	$He^+ + H \rightarrow He + H^+$	$k_{18} = 1.25 \times 10^{-15} \left(\frac{T}{300}\right)^{0.25}$		18
19	$He + H^+ \rightarrow He^+ + H$	$k_{19} = 1.26 \times 10^{-9} T^{-0.75} \exp\left(-\frac{127500}{T}\right)$	$T \leqslant 10000$ K	19
		$= 4.0 \times 10^{-37} T^{4.74}$	$T > 10000$ K	
20	$C^+ + e^- \rightarrow C + \gamma$	$k_{20} = 4.67 \times 10^{-12} \left(\frac{T}{300}\right)^{-0.6}$	$T \leqslant 7950$ K	20
		$= 1.23 \times 10^{-17} \left(\frac{T}{300}\right)^{2.49} \exp\left(\frac{21845.6}{T}\right)$	$7950 \text{ K} < T \leqslant 21140$ K	
		$= 9.62 \times 10^{-8} \left(\frac{T}{300}\right)^{-1.37} \exp\left(\frac{-115786.2}{T}\right)$	$T > 21140$ K	
21	$O^+ + e^- \rightarrow O + \gamma$	$k_{21} = 1.30 \times 10^{-10} T^{-0.64}$	$T \leqslant 400$ K	21
		$= 1.41 \times 10^{-10} T^{-0.66} + 7.4 \times 10^{-4} T^{-1.5}$		
		$\times \exp\left(-\frac{175000}{T}\right) \left[1.0 + 0.062 \times \exp\left(-\frac{145000}{T}\right)\right]$	$T > 400$ K	
22	$C + e^- \rightarrow C^+ + e^- + e^-$	$k_{22} = 6.85 \times 10^{-8} (0.193 + u)^{-1} u^{0.25} e^{-u}$	$u = 11.26/T_e$	22
23	$O + e^- \rightarrow O^+ + e^- + e^-$	$k_{23} = 3.59 \times 10^{-8} (0.073 + u)^{-1} u^{0.34} e^{-u}$	$u = 13.6/T_e$	22
24	$O^+ + H \rightarrow O + H^+$	$k_{24} = 4.99 \times 10^{-11} T^{0.405} + 7.54 \times 10^{-10} T^{-0.458}$		23
25	$O + H^+ \rightarrow O^+ + H$	$k_{25} = [1.08 \times 10^{-11} T^{0.517}$		24
		$+ 4.00 \times 10^{-10} T^{0.00669}] \exp\left(-\frac{227}{T}\right)$		
26	$O + He^+ \rightarrow O^+ + He$	$k_{26} = 4.991 \times 10^{-15} \left(\frac{T}{10000}\right)^{0.3794} \exp\left(-\frac{T}{1121000}\right)$		25
		$+ 2.780 \times 10^{-15} \left(\frac{T}{10000}\right)^{-0.2163} \exp\left(\frac{T}{815800}\right)$		
27	$C + H^+ \rightarrow C^+ + H$	$k_{27} = 3.9 \times 10^{-16} T^{0.213}$		24
28	$C^+ + H \rightarrow C + H^+$	$k_{28} = 6.08 \times 10^{-14} \left(\frac{T}{10000}\right)^{1.96} \exp\left(-\frac{170000}{T}\right)$		24
29	$C + He^+ \rightarrow C^+ + He$	$k_{29} = 8.58 \times 10^{-17} T^{0.757}$	$T \leqslant 200$ K	26
		$= 3.25 \times 10^{-17} T^{0.968}$	$200 < T \leqslant 2000$ K	
		$= 2.77 \times 10^{-19} T^{1.597}$	$T > 2000$ K	
30	$H_2 + He \rightarrow H + H + He$	$k_{30,l} = \mathrm{dex}[-27.029 + 3.801 \log(T) - 29487/T]$		27
		$k_{30,h} = \mathrm{dex}[-2.729 - 1.75 \log(T) - 23474/T]$		
		$n_{cr,He} = \mathrm{dex}\left[5.0792(1.0 - 1.23 \times 10^{-5}(T - 2000)\right]$		27
31	$OH + H \rightarrow O + H + H$	$k_{31} = 6.0 \times 10^{-9} \exp\left(-\frac{50900}{T}\right)$		28
32	$HOC^+ + H_2 \rightarrow HCO^+ + H_2$	$k_{32} = 3.8 \times 10^{-10}$		29
33	$HOC^+ + CO \rightarrow HCO^+ + CO$	$k_{33} = 4.0 \times 10^{-10}$		30
34	$C + H_2 \rightarrow CH + H$	$k_{34} = 6.64 \times 10^{-10} \exp\left(-\frac{11700}{T}\right)$		31
35	$CH + H \rightarrow C + H_2$	$k_{35} = 1.31 \times 10^{-10} \exp\left(-\frac{80}{T}\right)$		32

chemical model 2

Table B1.

No.	Reaction	Rate coefficient		Ref.
14	$H^- + H \rightarrow H + H + e^-$	$k_{14} = 2.5634 \times 10^{-9} T_e^{1.78186}$	$T_e \leqslant 0.1$ eV	13
36	$CH + H_2 \rightarrow CH_2 + H$	$k_{36} = 5.46 \times 10^{-10} \exp\left(-\frac{1943}{T}\right)$		33
37	$CH + C \rightarrow C_2 + H$	$k_{37} = 6.59 \times 10^{-11}$		34
38	$CH + O \rightarrow CO + H$	$k_{38} = 6.6 \times 10^{-11}$	$T \leqslant 2000$ K	35
		$= 1.02 \times 10^{-10} \exp\left(-\frac{[illegible]}{T}\right)$	$T > 2000$ K	36
39	[illegible] $\rightarrow CH + H_2$	$k_{39} =$ [illegible] $\times 10^{-11}$		37
40	$CH_2 + O \rightarrow CO + H + H$	$k_{40} = 1.33 \times 10^{-10}$		38
41	$CH_2 + O \rightarrow CO + H_2$	$k_{41} = 8.0 \times 10^{-11}$		39
42	$C_2 + O \rightarrow CO + C$	$k_{42} = 5.0 \times 10^{-11} \left(\frac{T}{300}\right)^{0.5}$	$T \leqslant 300$ K	40
		$= 5.0 \times 10^{-11} \left(\frac{T}{300}\right)^{0.757}$	$T > 300$ K	41
43	$O + H_2 \rightarrow OH + H$	$k_{43} = 3.14 \times 10^{-13} \left(\frac{T}{300}\right)^{2.7} \exp\left(-\frac{3150}{T}\right)$		42
44	$OH + H \rightarrow O + H_2$	$k_{44} = 6.99 \times 10^{-14} \left(\frac{T}{300}\right)^{2.8} \exp\left(-\frac{1950}{T}\right)$		43
45	$OH + H_2 \rightarrow H_2O + H$	$k_{45} = 2.05 \times 10^{-12} \left(\frac{T}{300}\right)^{1.52} \exp\left(-\frac{1736}{T}\right)$		44
46	$OH + C \rightarrow CO + H$	$k_{46} = 1.0 \times 10^{-10}$		34
47	$OH + O \rightarrow O_2 + H$	$k_{47} = 3.50 \times 10^{-11}$	$T \leqslant 261$ K	45
		$= 1.77 \times 10^{-11} \exp\left(\frac{178}{T}\right)$	$T > 261$ K	33
48	$OH + OH \rightarrow H_2O + H$	$k_{48} = 1.65 \times 10^{-12} \left(\frac{T}{300}\right)^{1.14} \exp\left(-\frac{50}{T}\right)$		34
49	$H_2O + H \rightarrow H_2 + OH$	$k_{49} = 1.59 \times 10^{-11} \left(\frac{T}{300}\right)^{1.2} \exp\left(-\frac{9610}{T}\right)$		46
50	$O_2 + H \rightarrow OH + O$	$k_{50} = 2.61 \times 10^{-10} \exp\left(-\frac{8156}{T}\right)$		33
51	$O_2 + H_2 \rightarrow OH + OH$	$k_{51} = 3.16 \times 10^{-10} \exp\left(-\frac{21890}{T}\right)$		47
52	$O_2 + C \rightarrow CO + O$	$k_{52} = 4.7 \times 10^{-11} \left(\frac{T}{300}\right)^{-0.34}$	$T \leqslant 295$ K	34
		$= 2.48 \times 10^{-12} \left(\frac{T}{300}\right)^{1.54} \exp\left(\frac{613}{T}\right)$	$T > 295$ K	33
53	$CO + H \rightarrow C + OH$	$k_{53} = 1.1 \times 10^{-10} \left(\frac{T}{300}\right)^{0.5} \exp\left(-\frac{77700}{T}\right)$		28
54	$H_2^+ + H_2 \rightarrow H_3^+ + H$	$k_{54} = 2.24 \times 10^{-9} \left(\frac{T}{300}\right)^{0.042} \exp\left(-\frac{T}{46600}\right)$		48
55	$H_3^+ + H \rightarrow H_2^+ + H_2$	$k_{55} = 7.7 \times 10^{-9} \exp\left(-\frac{17560}{T}\right)$		49
56	$C + H_2^+ \rightarrow CH^+ + H$	$k_{56} = 2.4 \times 10^{-9}$		28
57	$C + H_3^+ \rightarrow CH^+ + H_2$	$k_{57} = 2.0 \times 10^{-9}$		28
58	$C^+ + H_2 \rightarrow CH^+ + H$	$k_{58} = 1.0 \times 10^{-10} \exp\left(-\frac{4640}{T}\right)$		50
59	$CH^+ + H \rightarrow C^+ + H_2$	$k_{59} = 7.5 \times 10^{-10}$		51
60	$CH^+ + H_2 \rightarrow CH_2^+ + H$	$k_{60} = 1.2 \times 10^{-9}$		51
61	$CH^+ + O \rightarrow CO^+ + H$	$k_{61} = 3.5 \times 10^{-10}$		52
62	$CH_2 + H^+ \rightarrow CH^+ + H_2$	$k_{62} = 1.4 \times 10^{-9}$		28
63	$CH_2^+ + H \rightarrow CH^+ + H_2$	$k_{63} = 1.0 \times 10^{-9} \exp\left(-\frac{7080}{T}\right)$		28
64	$CH_2^+ + H_2 \rightarrow CH_3^+ + H$	$k_{64} = 1.6 \times 10^{-9}$		53
65	$CH_2^+ + O \rightarrow HCO^+ + H$	$k_{65} = 7.5 \times 10^{-10}$		28
66	$CH_3^+ + H \rightarrow CH_2^+ + H_2$	$k_{66} = 7.0 \times 10^{-10} \exp\left(-\frac{10560}{T}\right)$		28
67	$CH_3^+ + O \rightarrow HCO^+ + H_2$	$k_{67} = 4.0 \times 10^{-10}$		54
68	$C_2 + O^+ \rightarrow CO^+ + C$	$k_{68} = 4.8 \times 10^{-10}$		28
69	$O^+ + H_2 \rightarrow OH^+ + H$	$k_{69} = 1.7 \times 10^{-9}$		55
70	$O + H_2^+ \rightarrow OH^+ + H$	$k_{70} = 1.5 \times 10^{-9}$		28
71	$O + H_3^+ \rightarrow OH^+ + H_2$	$k_{71} = 8.4 \times 10^{-10}$		56
72	$OH + H_3^+ \rightarrow H_2O^+ + H_2$	$k_{72} = 1.3 \times 10^{-9}$		28
73	$OH + C^+ \rightarrow CO^+ + H$	$k_{73} = 7.7 \times 10^{-10}$		28
74	$OH^+ + H_2 \rightarrow H_2O^+ + H$	$k_{74} = 1.01 \times 10^{-9}$		57
75	$H_2O^+ + H_2 \rightarrow H_3O^+ + H$	$k_{75} = 6.4 \times 10^{-10}$		58
76	$H_2O + H_3^+ \rightarrow H_3O^+ + H_2$	$k_{76} = 5.9 \times 10^{-9}$		59
77	$H_2O + C^+ \rightarrow HCO^+ + H$	$k_{77} = 9.0 \times 10^{-10}$		60
78	$H_2O + C^+ \rightarrow HOC^+ + H$	$k_{78} = 1.8 \times 10^{-9}$		60
79	$H_3O^+ + C \rightarrow HCO^+ + H_2$	$k_{79} = 1.0 \times 10^{-11}$		28
80	$O_2 + C^+ \rightarrow CO^+ + O$	$k_{80} = 3.8 \times 10^{-10}$		53
81	$O_2 + C^+ \rightarrow CO + O^+$	$k_{81} = 6.2 \times 10^{-10}$		53
82	$O_2 + CH_2^+ \rightarrow HCO^+ + OH$	$k_{82} = 9.1 \times 10^{-10}$		53
83	$O_2^+ + C \rightarrow CO^+ + O$	$k_{83} = 5.2 \times 10^{-11}$		28
84	$CO + H_3^+ \rightarrow HOC^+ + H_2$	$k_{84} = 2.7 \times 10^{-11}$		61
85	$CO + H_3^+ \rightarrow HCO^+ + H_2$	$k_{85} = 1.7 \times 10^{-9}$		61
86	$HCO^+ + C \rightarrow CO + CH^+$	$k_{86} = 1.1 \times 10^{-9}$		28
87	$HCO^+ + H_2O \rightarrow CO + H_3O^+$	$k_{87} = 2.5 \times 10^{-9}$		62

(Glover, Federrath, Mac Low, Klessen, 2010, MNRS, 404, 2)

chemical model 2

88	$H_2 + He^+ \rightarrow He + H_2^+$	$k_{88} = 7.2 \times 10^{-15}$	63
89	$H_2 + He^+ \rightarrow He + H + H^+$	$k_{89} = 3.7 \times 10^{-14} \exp\left(\frac{35}{T}\right)$	63
90	$CH + H^+ \rightarrow CH^+ + H$	$k_{90} = 1.9 \times 10^{-9}$	28
91	$CH_2 + H^+ \rightarrow CH_2^+ + H$	$k_{91} = 1.4 \times 10^{-9}$	28
92	$CH_2 + He^+ \rightarrow C^+ + He + H_2$	$k_{92} =$ [illegible]	28
93	$C_2 + He^+ \rightarrow C^+ + C + He$	$k_{93} =$ [illegible]	28
94	$OH + H^+ \rightarrow OH^+ + H$	$k_{94} = 2.1 \times 10^{-9}$	28
95	$OH + He^+ \rightarrow O^+ + He + H$	$k_{95} = 1.1 \times 10^{-9}$	28
96	$H_2O + H^+ \rightarrow H_2O^+ + H$	$k_{96} = 6.9 \times 10^{-9}$	64
97	$H_2O + He^+ \rightarrow OH + He + H^+$	$k_{97} = 2.04 \times 10^{-10}$	65
98	$H_2O + He^+ \rightarrow OH^+ + He + H$	$k_{98} = 2.86 \times 10^{-10}$	65
99	$H_2O + He^+ \rightarrow H_2O^+ + He$	$k_{99} = 6.05 \times 10^{-11}$	65
100	$O_2 + H^+ \rightarrow O_2^+ + H$	$k_{100} = 2.0 \times 10^{-9}$	64
101	$O_2 + He^+ \rightarrow O_2^+ + He$	$k_{101} = 3.3 \times 10^{-11}$	66
102	$O_2 + He^+ \rightarrow O^+ + O + He$	$k_{102} = 1.1 \times 10^{-9}$	66
103	$O_2^+ + C \rightarrow O_2 + C^+$	$k_{103} = 5.2 \times 10^{-11}$	28
104	$CO + He^+ \rightarrow C^+ + O + He$	$k_{104} = 1.4 \times 10^{-9} \left(\frac{T}{300}\right)^{-0.5}$	67
105	$CO + He^+ \rightarrow C + O^+ + He$	$k_{105} = 1.4 \times 10^{-16} \left(\frac{T}{300}\right)^{-0.5}$	67
106	$CO^+ + H \rightarrow CO + H^+$	$k_{106} = 7.5 \times 10^{-10}$	68
107	$C^- + H^+ \rightarrow C + H$	$k_{107} = 2.3 \times 10^{-7} \left(\frac{T}{300}\right)^{-0.5}$	28
108	$O^- + H^+ \rightarrow O + H$	$k_{108} = 2.3 \times 10^{-7} \left(\frac{T}{300}\right)^{-0.5}$	28
109	$He^+ + H^- \rightarrow He + H$	$k_{109} = 2.32 \times 10^{-7} \left(\frac{T}{300}\right)^{-0.52} \exp\left(\frac{T}{22400}\right)$	69
110	$H_3^+ + e^- \rightarrow H_2 + H$	$k_{110} = 2.34 \times 10^{-8} \left(\frac{T}{300}\right)^{-0.52}$	70
111	$H_3^+ + e^- \rightarrow H + H + H$	$k_{111} = 4.36 \times 10^{-8} \left(\frac{T}{300}\right)^{-0.52}$	70
112	$CH^+ + e^- \rightarrow C + H$	$k_{112} = 7.0 \times 10^{-8} \left(\frac{T}{300}\right)^{-0.5}$	71
113	$CH_2^+ + e^- \rightarrow CH + H$	$k_{113} = 1.6 \times 10^{-7} \left(\frac{T}{300}\right)^{-0.6}$	72
114	$CH_2^+ + e^- \rightarrow C + H + H$	$k_{114} = 4.03 \times 10^{-7} \left(\frac{T}{300}\right)^{-0.6}$	72
115	$CH_2^+ + e^- \rightarrow C + H_2$	$k_{115} = 7.68 \times 10^{-8} \left(\frac{T}{300}\right)^{-0.6}$	72
116	$CH_3^+ + e^- \rightarrow CH_2 + H$	$k_{116} = 7.75 \times 10^{-8} \left(\frac{T}{300}\right)^{-0.5}$	73
117	$CH_3^+ + e^- \rightarrow CH + H_2$	$k_{117} = 1.95 \times 10^{-7} \left(\frac{T}{300}\right)^{-0.5}$	73
118	$CH_3^+ + e^- \rightarrow CH + H + H$	$k_{118} = 2.0 \times 10^{-7} \left(\frac{T}{300}\right)^{-0.4}$	28
119	$OH^+ + e^- \rightarrow O + H$	$k_{119} = 6.3 \times 10^{-9} \left(\frac{T}{300}\right)^{-0.48}$	74
120	$H_2O^+ + e^- \rightarrow O + H + H$	$k_{120} = 3.05 \times 10^{-7} \left(\frac{T}{300}\right)^{-0.5}$	75
121	$H_2O^+ + e^- \rightarrow O + H_2$	$k_{121} = 3.9 \times 10^{-8} \left(\frac{T}{300}\right)^{-0.5}$	75
122	$H_2O^+ + e^- \rightarrow OH + H$	$k_{122} = 8.6 \times 10^{-8} \left(\frac{T}{300}\right)^{-0.5}$	75
123	$H_3O^+ + e^- \rightarrow H + H_2O$	$k_{123} = 1.08 \times 10^{-7} \left(\frac{T}{300}\right)^{-0.5}$	76
124	$H_3O^+ + e^- \rightarrow OH + H_2$	$k_{124} = 6.02 \times 10^{-8} \left(\frac{T}{300}\right)^{-0.5}$	76
125	$H_3O^+ + e^- \rightarrow OH + H + H$	$k_{125} = 2.58 \times 10^{-7} \left(\frac{T}{300}\right)^{-0.5}$	76
126	$H_3O^+ + e^- \rightarrow O + H + H_2$	$k_{126} = 5.6 \times 10^{-9} \left(\frac{T}{300}\right)^{-0.5}$	76
127	$O_2^+ + e^- \rightarrow O + O$	$k_{127} = 1.95 \times 10^{-7} \left(\frac{T}{300}\right)^{-0.7}$	77
128	$CO^+ + e^- \rightarrow C + O$	$k_{128} = 2.75 \times 10^{-7} \left(\frac{T}{300}\right)^{-0.55}$	78
129	$HCO^+ + e^- \rightarrow CO + H$	$k_{129} = 2.76 \times 10^{-7} \left(\frac{T}{300}\right)^{-0.64}$	79
130	$HCO^+ + e^- \rightarrow OH + C$	$k_{130} = 2.4 \times 10^{-8} \left(\frac{T}{300}\right)^{-0.64}$	79
131	$HOC^+ + e^- \rightarrow CO + H$	$k_{131} = 1.1 \times 10^{-7} \left(\frac{T}{300}\right)^{-1.0}$	28
132	$H^- + C \rightarrow CH + e^-$	$k_{132} = 1.0 \times 10^{-9}$	28
133	$H^- + O \rightarrow OH + e^-$	$k_{133} = 1.0 \times 10^{-9}$	28
134	$H^- + OH \rightarrow H_2O + e^-$	$k_{134} = 1.0 \times 10^{-10}$	28
135	$C^- + H \rightarrow CH + e^-$	$k_{135} = 5.0 \times 10^{-10}$	28
136	$C^- + H_2 \rightarrow CH_2 + e^-$	$k_{136} = 1.0 \times 10^{-13}$	28
137	$C^- + O \rightarrow CO + e^-$	$k_{137} = 5.0 \times 10^{-10}$	28
138	$O^- + H \rightarrow OH + e^-$	$k_{138} = 5.0 \times 10^{-10}$	28
139	$O^- + H_2 \rightarrow H_2O + e^-$	$k_{139} = 7.0 \times 10^{-10}$	28
140	$O^- + C \rightarrow CO + e^-$	$k_{140} = 5.0 \times 10^{-10}$	28

87	$HCO^+ + H_2O \rightarrow CO + H_3O^+$	$k_{87} = 2.5 \times 10^{-9}$	62

(Glover, Federrath, Mac Low, Klessen, 2010, MNRS, 404, 2)

chemical model 2

(Glover, Federrath, Mac Low, Klessen, 2010, MNRS, 404, 2)

Table B1.

14	$H^- + H \rightarrow H + H + e^-$			
87	$HCO^+ + H_2O \rightarrow CO + H_3O^+$	$k_{87} = 2.5 \times 10^{-9}$		62
88	$H_2 + He^+ \rightarrow He + H_2^+$	$k_{88} = 7.2 \times 10^{-15}$		63
89	$H_2 + He^+ \rightarrow He + H + H^+$	$k_{89} = 3.7 \times 10^{-14} \exp\left(\frac{35}{T}\right)$		63
90	$CH + H^+ \rightarrow CH^+ + H$	$k_{90} = 1.9 \times 10^{-9}$		28
91	$CH_2 + H^+ \rightarrow CH_2^+ + H$	$k_{91} = 1.4 \times 10^{-9}$		28
94	$OH + H^+ \rightarrow OH^+ + H$	$k_{94} = 2.1 \times 10^{-9}$		28
95	$OH + He^+ \rightarrow O^+ + He + H$	$k_{95} = 1.1 \times 10^{-9}$		28
96	$H_2O + H^+ \rightarrow H_2O^+ + H$	$k_{96} = 6.9 \times 10^{-9}$		64
97	$H_2O + He^+ \rightarrow OH + He + H^+$	$k_{97} = 2.04 \times 10^{-10}$		65
129	$HCO^+ + e^- \rightarrow CO + H$	$k_{129} = 2.76 \times 10^{-7} \left(\frac{T}{300}\right)^{-0.64}$		79
130	$HCO^+ + e^- \rightarrow OH + C$	$k_{130} = 2.4 \times 10^{-8} \left(\frac{T}{300}\right)^{-0.64}$		79
131	$HOC^+ + e^- \rightarrow CO + H$	$k_{131} = 1.1 \times 10^{-7} \left(\frac{T}{300}\right)^{-1.0}$		28
132	$H^- + C \rightarrow CH + e^-$	$k_{132} = 1.0 \times 10^{-9}$		28
133	$H^- + O \rightarrow OH + e^-$	$k_{133} = 1.0 \times 10^{-9}$		28
134	$H^- + OH \rightarrow H_2O + e^-$	$k_{134} = 1.0 \times 10^{-10}$		28
135	$C^- + H \rightarrow CH + e^-$	$k_{135} = 5.0 \times 10^{-10}$		28
136	$C^- + H_2 \rightarrow CH_2 + e^-$	$k_{136} = 1.0 \times 10^{-13}$		28
137	$C^- + O \rightarrow CO + e^-$	$k_{137} = 5.0 \times 10^{-10}$		28
138	$O^- + H \rightarrow OH + e^-$	$k_{138} = 5.0 \times 10^{-10}$		28
139	$O^- + H_2 \rightarrow H_2O + e^-$	$k_{139} = 7.0 \times 10^{-10}$		28
140	$O^- + C \rightarrow CO + e^-$	$k_{140} = 5.0 \times 10^{-10}$		28
142	$C + e^- \rightarrow C^- + \gamma$	$k_{142} = 2.25 \times 10^{-15}$		81
143	$C + H \rightarrow CH + \gamma$	$k_{143} = 1.0 \times 10^{-17}$		82
144	$C + H_2 \rightarrow CH_2 + \gamma$	$k_{144} = 1.0 \times 10^{-17}$		82
145	$C + C \rightarrow C_2 + \gamma$	$k_{145} = 4.36 \times 10^{-18} \left(\frac{T}{300}\right)^{0.35} \exp\left(-\frac{161.3}{T}\right)$		83
146	$C + O \rightarrow CO + \gamma$	$k_{146} = 2.1 \times 10^{-19}$	$T \leqslant 300$ K	84
		$= 3.09 \times 10^{-17} \left(\frac{T}{300}\right)^{0.33} \exp\left(-\frac{1629}{T}\right)$	$T > 300$ K	85
147	$C^+ + H \rightarrow CH^+ + \gamma$	$k_{147} = 4.46 \times 10^{-16} T^{-0.5} \exp\left(-\frac{4.93}{T^{2/3}}\right)$		86
148	$C^+ + H_2 \rightarrow CH_2^+ + \gamma$	$k_{148} = 4.0 \times 10^{-16} \left(\frac{T}{300}\right)^{-0.2}$		87
149	$C^+ + O \rightarrow CO^+ + \gamma$	$k_{149} = 2.5 \times 10^{-18}$	$T \leqslant 300$ K	84
		$= 3.14 \times 10^{-18} \left(\frac{T}{300}\right)^{-0.15} \exp\left(\frac{68}{T}\right)$	$T > 300$ K	85
150	$O + e^- \rightarrow O^- + \gamma$	$k_{150} = 1.5 \times 10^{-15}$		28
151	$O + H \rightarrow OH + \gamma$	$k_{151} = 9.9 \times 10^{-19} \left(\frac{T}{300}\right)^{-0.38}$		28
152	$O + O \rightarrow O_2 + \gamma$	$k_{152} = 4.9 \times 10^{-20} \left(\frac{T}{300}\right)^{1.58}$		82
153	$OH + H \rightarrow H_2O + \gamma$	$k_{153} = 5.26 \times 10^{-18} \left(\frac{T}{300}\right)^{-5.22} \exp\left(-\frac{90}{T}\right)$		88
154	$H + H + H \rightarrow H_2 + H$	$k_{154} = 1.32 \times 10^{-32} \left(\frac{T}{300}\right)^{-0.38}$	$T \leqslant 300$ K	89
		$= 1.32 \times 10^{-32} \left(\frac{T}{300}\right)^{-1.0}$	$T > 300$ K	90
155	$H + H + H_2 \rightarrow H_2 + H_2$	$k_{155} = 2.8 \times 10^{-31} T^{-0.6}$		91
156	$H + H + He \rightarrow H_2 + He$	$k_{156} = 6.9 \times 10^{-32} T^{-0.4}$		92
157	$C + C + M \rightarrow C_2 + M$	$k_{157} = 5.99 \times 10^{-33} \left(\frac{T}{5000}\right)^{-1.6}$	$T \leqslant 5000$ K	93
		$= 5.99 \times 10^{-33} \left(\frac{T}{5000}\right)^{-0.64} \exp\left(\frac{5255}{T}\right)$	$T > 5000$ K	94
158	$C + O + M \rightarrow CO + M$	$k_{158} = 6.16 \times 10^{-29} \left(\frac{T}{300}\right)^{-3.08}$	$T \leqslant 2000$ K	35
		$= 2.14 \times 10^{-29} \left(\frac{T}{300}\right)^{-3.08} \exp\left(\frac{2114}{T}\right)$	$T > 2000$ K	67
159	$C^+ + O + M \rightarrow CO^+ + M$	$k_{159} = 100 \times k_{210}$		67
160	$C + O^+ + M \rightarrow CO^+ + M$	$k_{160} = 100 \times k_{210}$		67
161	$O + H + M \rightarrow OH + M$	$k_{161} = 4.33 \times 10^{-32} \left(\frac{T}{300}\right)^{-1.0}$		43
162	$OH + H + M \rightarrow H_2O + M$	$k_{162} = 2.56 \times 10^{-31} \left(\frac{T}{300}\right)^{-2.0}$		35
163	$O + O + M \rightarrow O_2 + M$	$k_{163} = 9.2 \times 10^{-34} \left(\frac{T}{300}\right)^{-1.0}$		37
164	$O + CH \rightarrow HCO^+ + e^-$	$k_{164} = 2.0 \times 10^{-11} \left(\frac{T}{300}\right)^{0.44}$		95
165	$H + H(s) \rightarrow H_2$	$k_{165} = 3.0 \times 10^{-18} T^{0.5} f_A [1.0 + 0.04(T + T_d)^{0.5} + 0.002\,T + 8 \times 10^{-6} T^2]^{-1}$	$f_A = \left[1.0 + 10^4 \exp\left(-\frac{600}{T_d}\right)\right]^{-1}$	96

chemical model 2

Table B2. List of photochemical reactions included in our chemical model

No.	Reaction	Optically thin rate (s^{-1})	γ	Ref.
166	$H^- + \gamma \rightarrow H + e^-$	$R_{166} = 7.1 \times 10^{-7}$	0.5	1
167	$H_2^+ + \gamma \rightarrow H + H^+$	$R_{167} = 1.1 \times 10^{-9}$	1.9	2
168	$H_2 + \gamma \rightarrow H + H$	$R_{168} = 5.6 \times 10^{-11}$	See §2.2	3
169	$H_3^+ + \gamma \rightarrow H_2 + H^+$	$R_{169} = 4.9 \times 10^{-13}$	1.8	4
170	$H_3^+ + \gamma \rightarrow H_2^+ + H$	$R_{170} = 4.9 \times 10^{-13}$	2.3	4
171	$C + \gamma \rightarrow C^+ + e^-$	$R_{171} = 3.1 \times 10^{-10}$	3.0	5
172	$C^- + \gamma \rightarrow C + e^-$	$R_{172} = 2.4 \times 10^{-7}$	0.9	6
173	$CH + \gamma \rightarrow C + H$	$R_{173} = 8.7 \times 10^{-10}$	1.2	7
174	$CH + \gamma \rightarrow CH^+ + e^-$	$R_{174} = 7.7 \times 10^{-10}$	2.8	8
175	$CH^+ + \gamma \rightarrow C + H^+$	$R_{175} = 2.6 \times 10^{-10}$	2.5	7
176	$CH_2 + \gamma \rightarrow CH + H$	$R_{176} = 7.1 \times 10^{-10}$	1.7	7
177	$CH_2 + \gamma \rightarrow CH_2^+ + e^-$	$R_{177} = 5.9 \times 10^{-10}$	2.3	6
178	$CH_2^+ + \gamma \rightarrow CH^+ + H$	$R_{178} = 4.6 \times 10^{-10}$	1.7	9
179	$CH_3^+ + \gamma \rightarrow CH_2^+ + H$	$R_{179} = 1.0 \times 10^{-9}$	1.7	6
180	$CH_3^+ + \gamma \rightarrow CH^+ + H_2$	$R_{180} = 1.0 \times 10^{-9}$	1.7	6
181	$C_2 + \gamma \rightarrow C + C$	$R_{181} = 1.5 \times 10^{-10}$	2.1	7
182	$O^- + \gamma \rightarrow O + e^-$	$R_{182} = 2.4 \times 10^{-7}$	0.5	6
183	$OH + \gamma \rightarrow O + H$	$R_{183} = 3.7 \times 10^{-10}$	1.7	10
184	$OH + \gamma \rightarrow OH^+ + e^-$	$R_{184} = 1.6 \times 10^{-12}$	3.1	6
185	$OH^+ + \gamma \rightarrow O + H^+$	$R_{185} = 1.0 \times 10^{-12}$	1.8	4
186	$H_2O + \gamma \rightarrow OH + H$	$R_{186} = 6.0 \times 10^{-10}$	1.7	11
187	$H_2O + \gamma \rightarrow H_2O^+ + e^-$	$R_{187} = 3.2 \times 10^{-11}$	3.9	8
188	$H_2O^+ + \gamma \rightarrow H_2^+ + O$	$R_{188} = 5.0 \times 10^{-11}$	See §2.2	12
189	$H_2O^+ + \gamma \rightarrow H^+ + OH$	$R_{189} = 5.0 \times 10^{-11}$	See §2.2	12
190	$H_2O^+ + \gamma \rightarrow O^+ + H_2$	$R_{190} = 5.0 \times 10^{-11}$	See §2.2	12
191	$H_2O^+ + \gamma \rightarrow OH^+ + H$	$R_{191} = 1.5 \times 10^{-10}$	See §2.2	12
192	$H_3O^+ + \gamma \rightarrow H^+ + H_2O$	$R_{192} = 2.5 \times 10^{-11}$	See §2.2	12
193	$H_3O^+ + \gamma \rightarrow H_2^+ + OH$	$R_{193} = 2.5 \times 10^{-11}$	See §2.2	12
194	$H_3O^+ + \gamma \rightarrow H_2O^+ + H$	$R_{194} = 7.5 \times 10^{-12}$	See §2.2	12
195	$H_3O^+ + \gamma \rightarrow OH^+ + H_2$	$R_{195} = 2.5 \times 10^{-11}$	See §2.2	12
196	$O_2 + \gamma \rightarrow O_2^+ + e^-$	$R_{196} = 5.6 \times 10^{-11}$	3.7	7
197	$O_2 + \gamma \rightarrow O + O$	$R_{197} = 7.0 \times 10^{-10}$	1.8	7
198	$CO + \gamma \rightarrow C + O$	$R_{198} = 2.0 \times 10^{-10}$	See §2.2	13

(Glover, Federrath, Mac Low, Klessen, 2010, MNRS, 404, 2)

chemical model 2

(Glover, Federrath, Mac Low, Klessen, 2010, MNRS, 404, 2)

No.	Reaction	Rate	Ref.
88	$H_2 + He^+ \rightarrow He + H_2^+$	$k_{88} = 7.2 \times 10^{-15}$	63
89	$H_2 + He^+ \rightarrow He + H + H^+$	$k_{89} = 3.7 \times 10^{-14} \exp\left(\frac{35}{T}\right)$	63
90	$CH + H^+ \rightarrow CH^+ + H$	$k_{90} = 1.9 \times 10^{-9}$	28
94	$OH + H^+ \rightarrow OH^+ + H$	$k_{94} = 2.1 \times 10^{-9}$	28
95	$OH + He^+ \rightarrow O^+ + He + H$	$k_{95} = 1.1 \times 10^{-9}$	28
96	$H_2O + H^+ \rightarrow H_2O^+ + H$	$k_{96} = 6.9 \times 10^{-9}$	64
97	$H_2O + He^+ \rightarrow OH + He + H^+$	$k_{97} = 2.04 \times 10^{-10}$	65
87	$HCO^+ + H_2O \rightarrow CO + H_3O^+$	$k_{87} = 2.5 \times 10^{-9}$	62
140	$O^- + C \rightarrow CO + e^-$	$k_{140} = 5.0 \times 10^{-10}$	28

Table B2. List of photochemical reactions included in our chemical model

No.	Reaction	Optically thin rate (s^{-1})	γ	Ref.
166	$H^- + \gamma \rightarrow H + e^-$	$R_{166} = 7.1 \times 10^{-7}$	0.5	1
167	$H_2^+ + \gamma \rightarrow H + H^+$	$R_{167} = 1.1 \times 10^{-9}$	1.9	2
168	$H_2 + \gamma \rightarrow H + H$	$R_{168} = 5.6 \times 10^{-11}$	See §2.2	3
169	$H_3^+ + \gamma \rightarrow H_2 + H^+$	$R_{169} = 4.9 \times 10^{-13}$	1.8	4
170	$H_3^+ + \gamma \rightarrow H_2^+ + H$	$R_{170} = 4.9 \times 10^{-13}$	2.3	4
197	$O_2 + \gamma \rightarrow O + O$	$R_{197} = 7.0 \times 10^{-10}$	1.8	7
198	$CO + \gamma \rightarrow C + O$	$R_{198} = 2.0 \times 10^{-10}$	See §2.2	13

Table B3. List of reactions included in our chemical model that involve cosmic rays or cosmic-ray induced UV emission

No.	Reaction	Rate ($s^{-1}\zeta_H^{-1}$)	Ref.
199	$H + c.r. \rightarrow H^+ + e^-$	$R_{199} = 1.0$	—
200	$He + c.r. \rightarrow He^+ + e^-$	$R_{200} = 1.1$	1
201	$H_2 + c.r. \rightarrow H^+ + H + e^-$	$R_{201} = 0.037$	1
202	$H_2 + c.r. \rightarrow H + H$	$R_{202} = 0.22$	1
203	$H_2 + c.r. \rightarrow H^+ + H^-$	$R_{203} = 6.5 \times 10^{-4}$	1
204	$H_2 + c.r. \rightarrow H_2^+ + e^-$	$R_{204} = 2.0$	1
205	$C + c.r. \rightarrow C^+ + e^-$	$R_{205} = 3.8$	1
206	$O + c.r. \rightarrow O^+ + e^-$	$R_{206} = 5.7$	1
207	$CO + c.r. \rightarrow CO^+ + e^-$	$R_{207} = 6.5$	1
208	$C + \gamma_{c.r.} \rightarrow C^+ + e^-$	$R_{208} = 2800$	2
209	$CH + \gamma_{c.r.} \rightarrow C + H$	$R_{209} = 4000$	3
210	$CH^+ + \gamma_{c.r.} \rightarrow C^+ + H$	$R_{210} = 960$	3
211	$CH_2 + \gamma_{c.r.} \rightarrow CH_2^+ + e^-$	$R_{211} = 2700$	1
212	$CH_2 + \gamma_{c.r.} \rightarrow CH + H$	$R_{212} = 2700$	1
213	$C_2 + \gamma_{c.r.} \rightarrow C + C$	$R_{213} = 1300$	3
214	$OH + \gamma_{c.r.} \rightarrow O + H$	$R_{214} = 2800$	3
215	$H_2O + \gamma_{c.r.} \rightarrow OH + H$	$R_{215} = 5300$	3
216	$O_2 + \gamma_{c.r.} \rightarrow O + O$	$R_{216} = 4100$	3
217	$O_2 + \gamma_{c.r.} \rightarrow O_2^+ + e^-$	$R_{217} = 640$	3
218	$CO + \gamma_{c.r.} \rightarrow C + O$	$R_{218} = 0.21 T^{1/2} x_{H_2} x_{CO}^{-1/2}$	4


example:
^{12}CO / ^{13}CO ratio

CO chemistry in GMCs

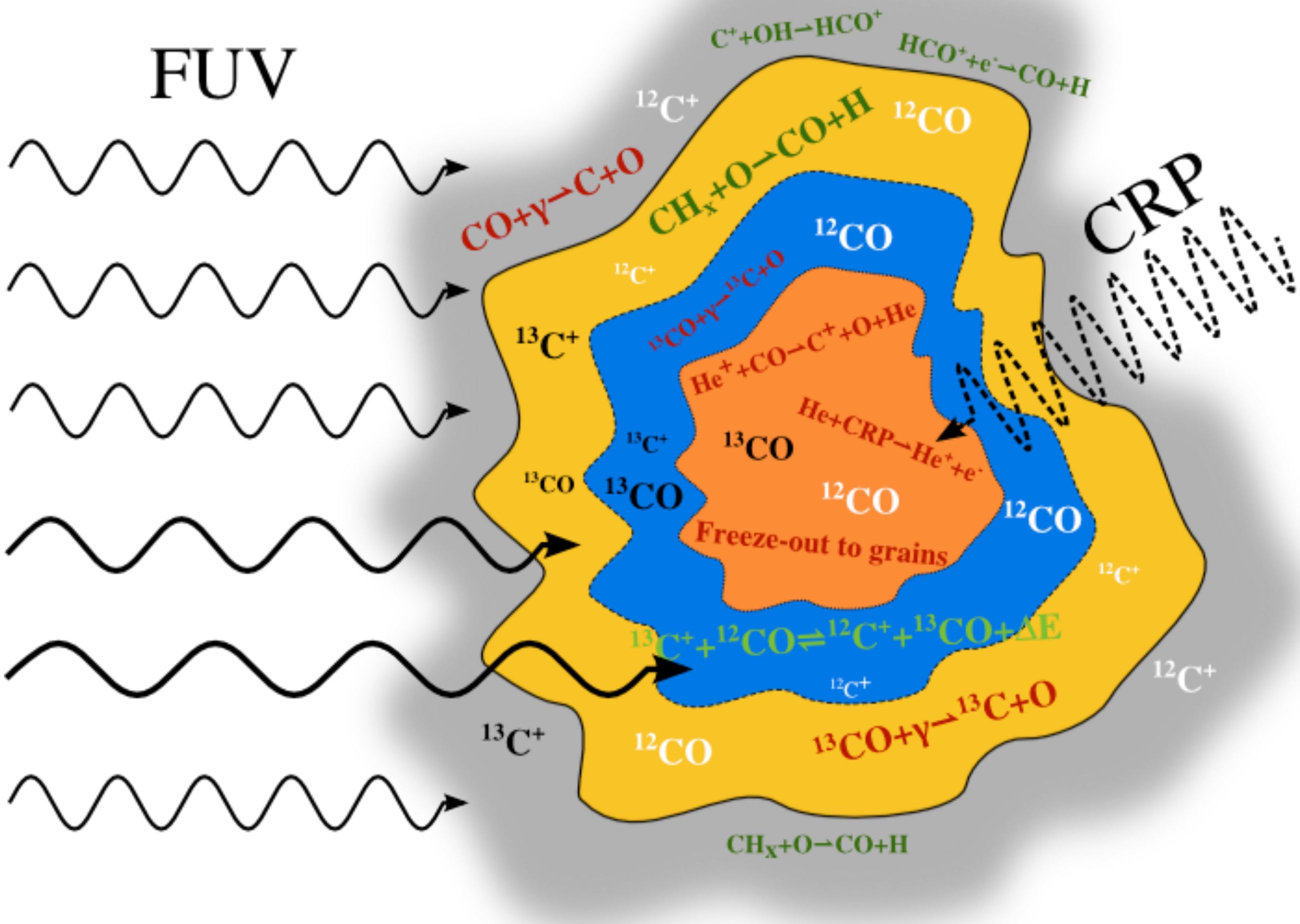

(Szűcs, Glover, Klessen 2014, MNRAS 445, 4055-4072)

Non-isotope selective reactions

Reaction	
$C^+ + OH \rightarrow HCO^+$	**Production**
$HCO^+ + e^- \rightarrow H + CO$	**Production**
$CH_x + O \rightarrow CO + H_x$	**Production**
$He + CRP \rightarrow He^+ + e^-$	**Destruction**
$He^+ + CO \rightarrow C^+ + O + He$	**Destruction**
Accretion to grains	**Depletion**

I. Diffuse region ($A_V < 0.5^m$)

$CO + \gamma \rightarrow C + O$

II. Translucent region ($1^m < A < 2^m$)

a) **preferential ^{13}CO photo-dissociation**

b) **Fractionation reaction**

$^{12}CO + ^{13}C \leftarrow\rightarrow ^{13}CO + ^{12}C + 36K$

III. Dense core ($A_V \approx 5^m$)

C^+ depletes

Freeze-out & CRP destruction

Detailed thermodynamic analysis

6 different models:

Model	n_0 [cm^{-3}]	Metallicity [$Z_\odot$]	ISRF [G_0]	Time [Myr]
a	300	0.3	1	2.046
b	300	0.6	1	1.930
c	300	1	0.1	2.124
d	300	1	1	2.150
e	300	1	10	2.022
f	1000	1	1	0.973

all relevant heating and cooling processes:

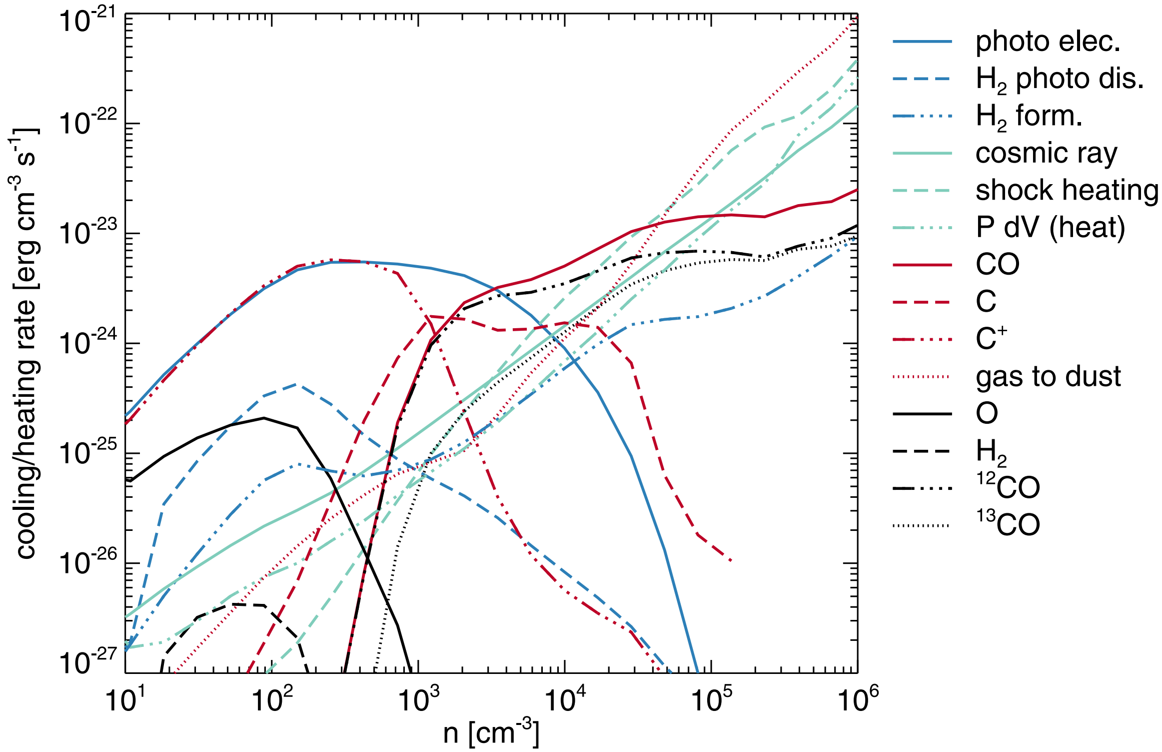

(Szücs et al. 2014, MNRAS 445, 4055)

(also Glover & Clark 2012, MNRAS, 421, 9)

Results – $N(^{12}CO)/N(^{13}CO)$ column densities ratio

N_0 = 300 cm^{-3}
ISRF = 1 G_0
Z = 1 $Z_\odot$
Before first sink particle forms

White contour shows 5×10^{21} cm^{-2}

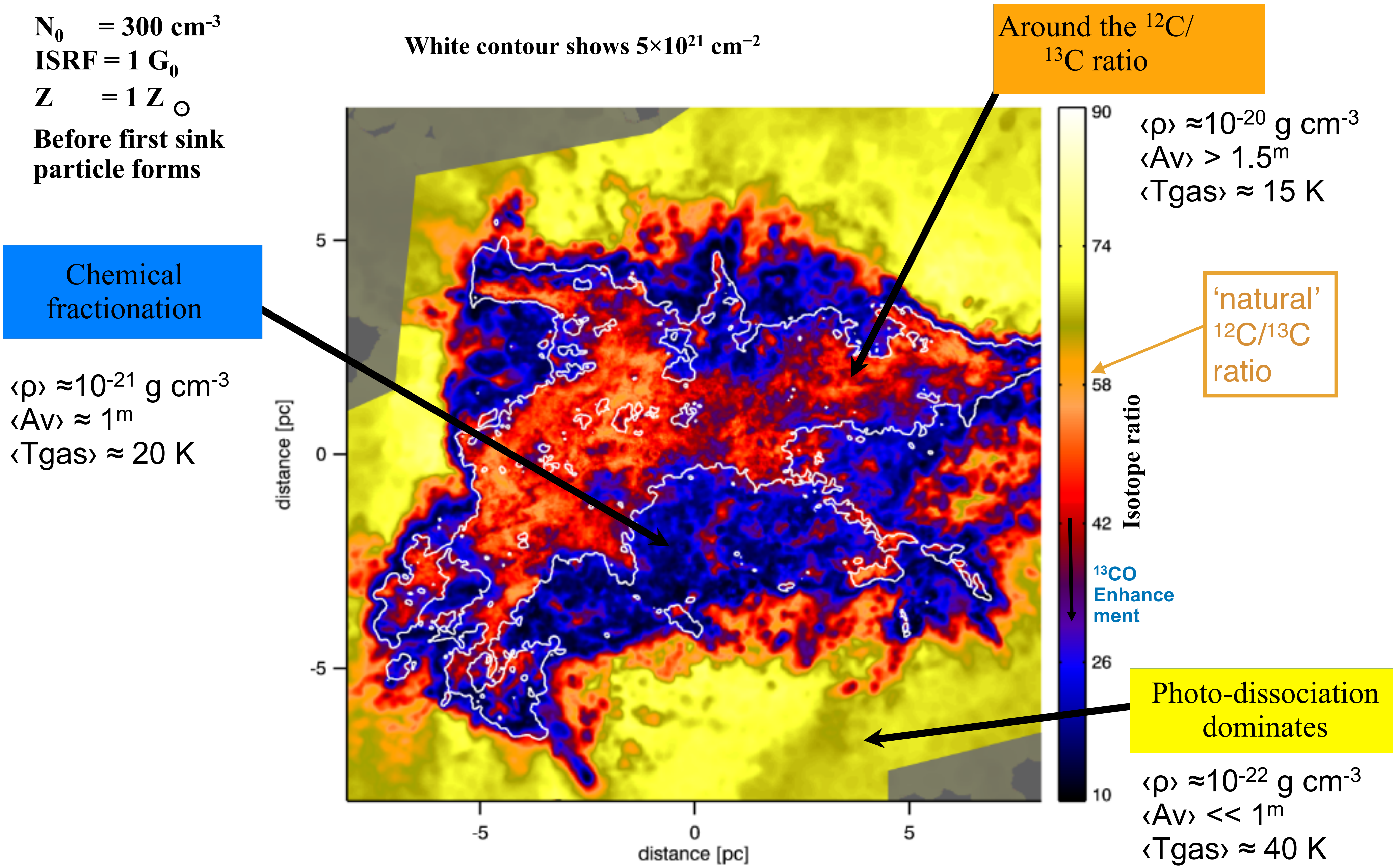

$\langle\rho\rangle \approx 10^{-21}$ g cm^{-3}
$\langle Av\rangle \approx 1^m$
$\langle Tgas\rangle \approx$ 20 K

$\langle\rho\rangle \approx 10^{-20}$ g cm^{-3}
$\langle Av\rangle > 1.5^m$
$\langle Tgas\rangle \approx$ 15 K

$\langle\rho\rangle \approx 10^{-22}$ g cm^{-3}
$\langle Av\rangle << 1^m$
$\langle Tgas\rangle \approx$ 40 K

(Szücs et al. 2014, MNRAS 445, 4055-4072)

Results – N(^{12}CO)/N(^{13}CO) column densities ratio

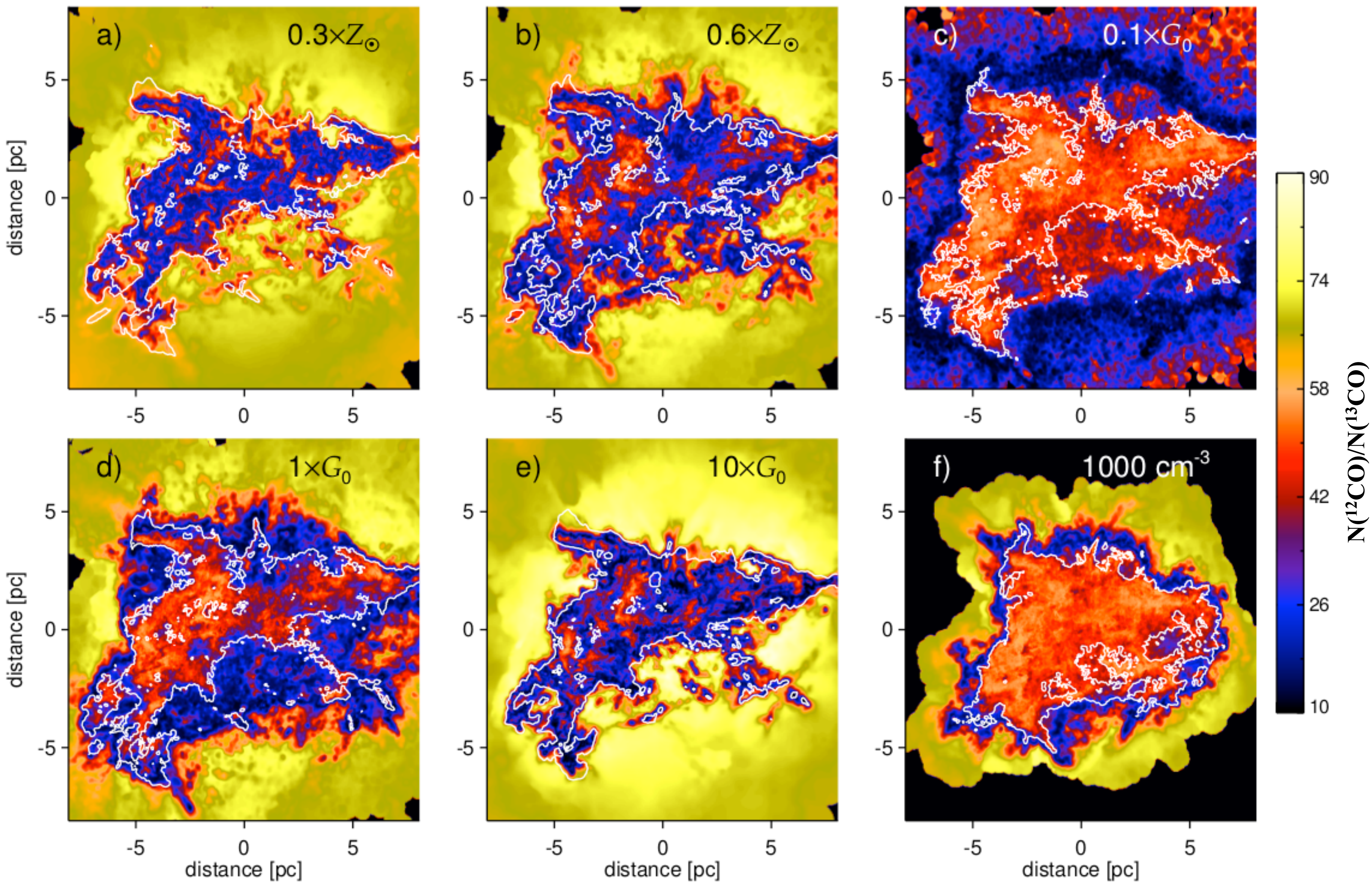

(Szücs et al. 2014, MNRAS 445, 4055-4072)

White contour shows 5×10^{21} cm^{-2}
→ overall density is not changing significantly

Results – N(^{12}CO)/N(^{13}CO) column densities ratio

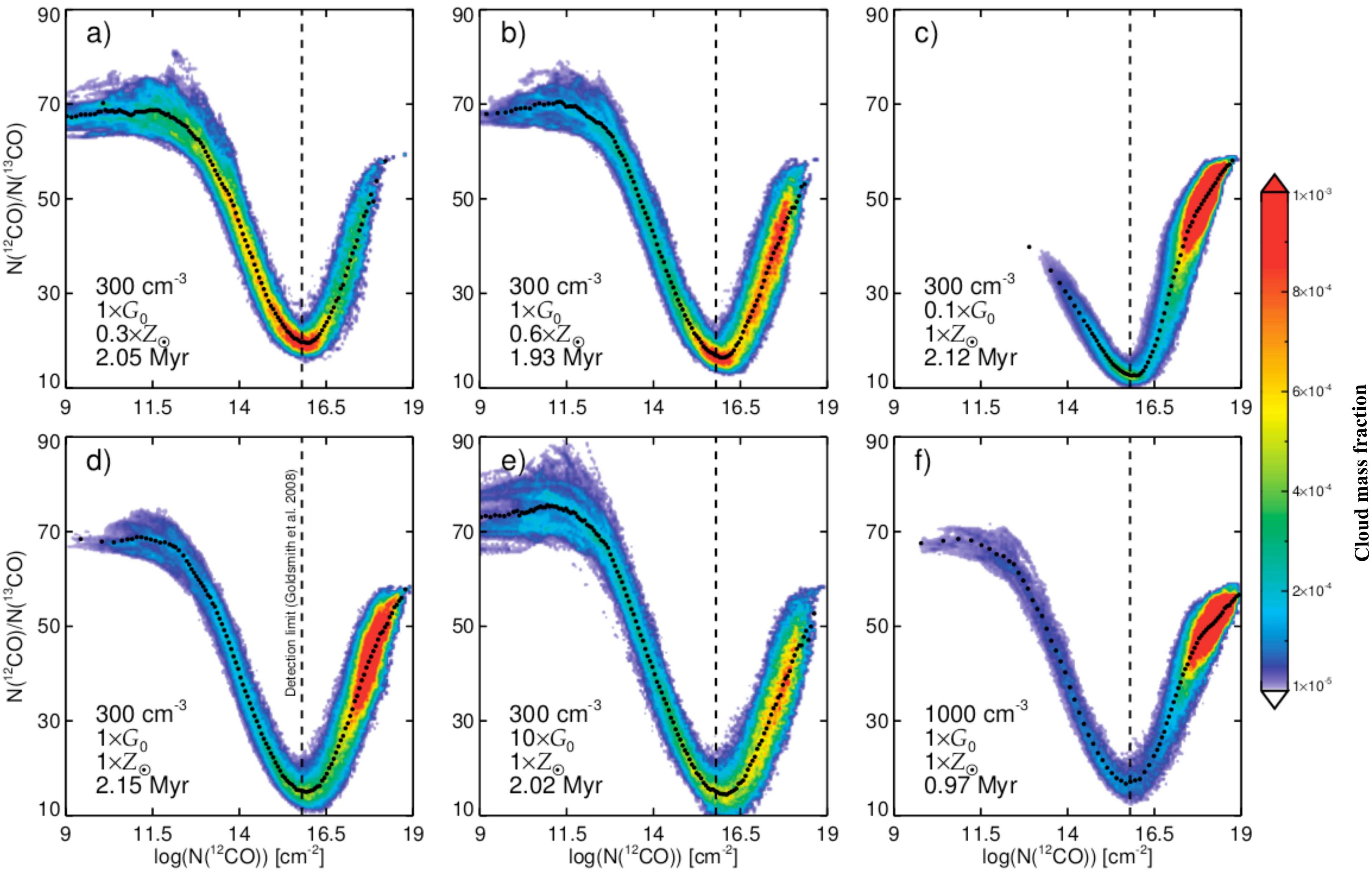

(Szücs et al. 2014, MNRAS 445, 4055-4072)

Fitting formula

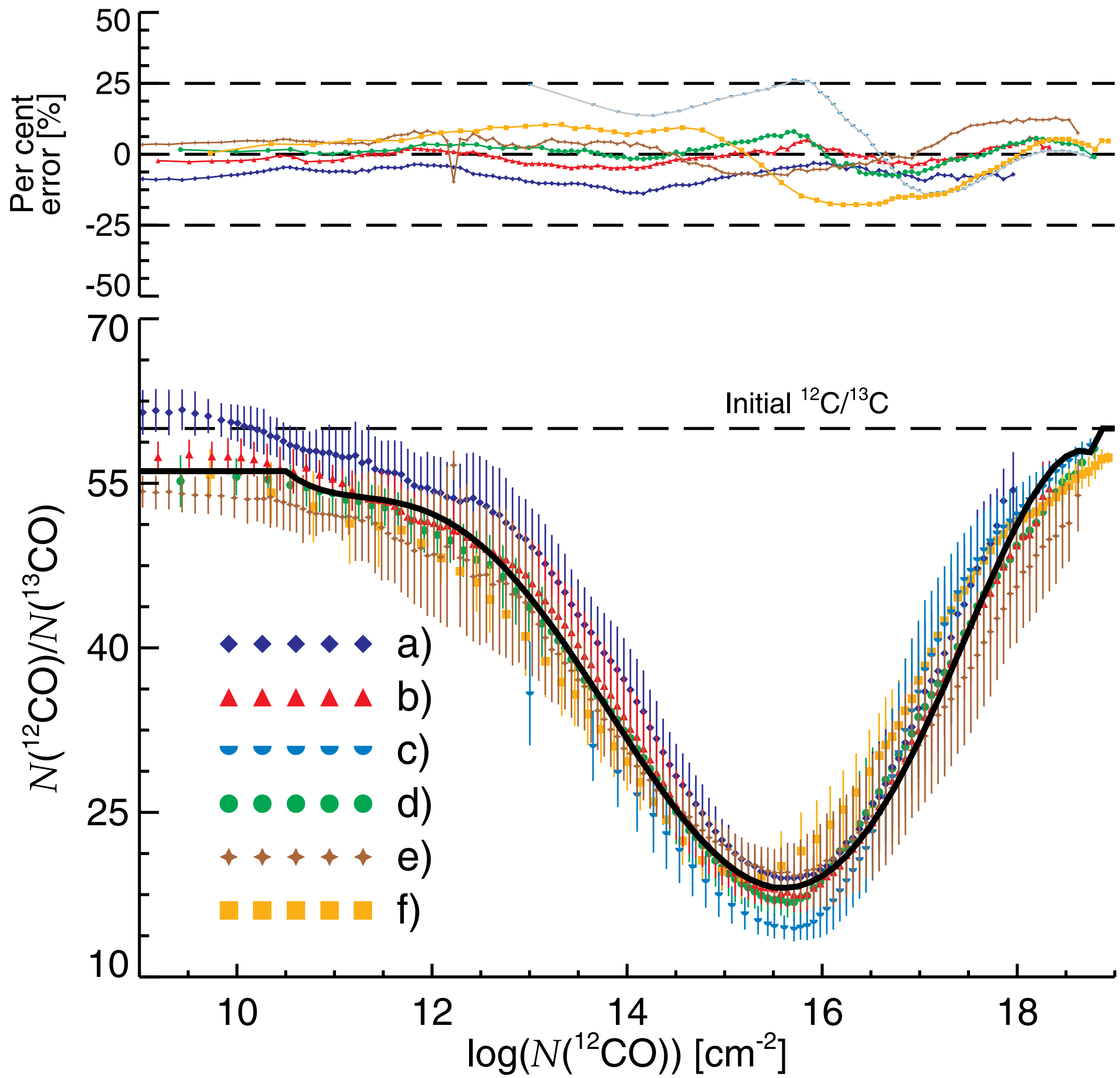

(Szücs et al. 2014, MNRAS 445, 4055-4072)

Fitting formula

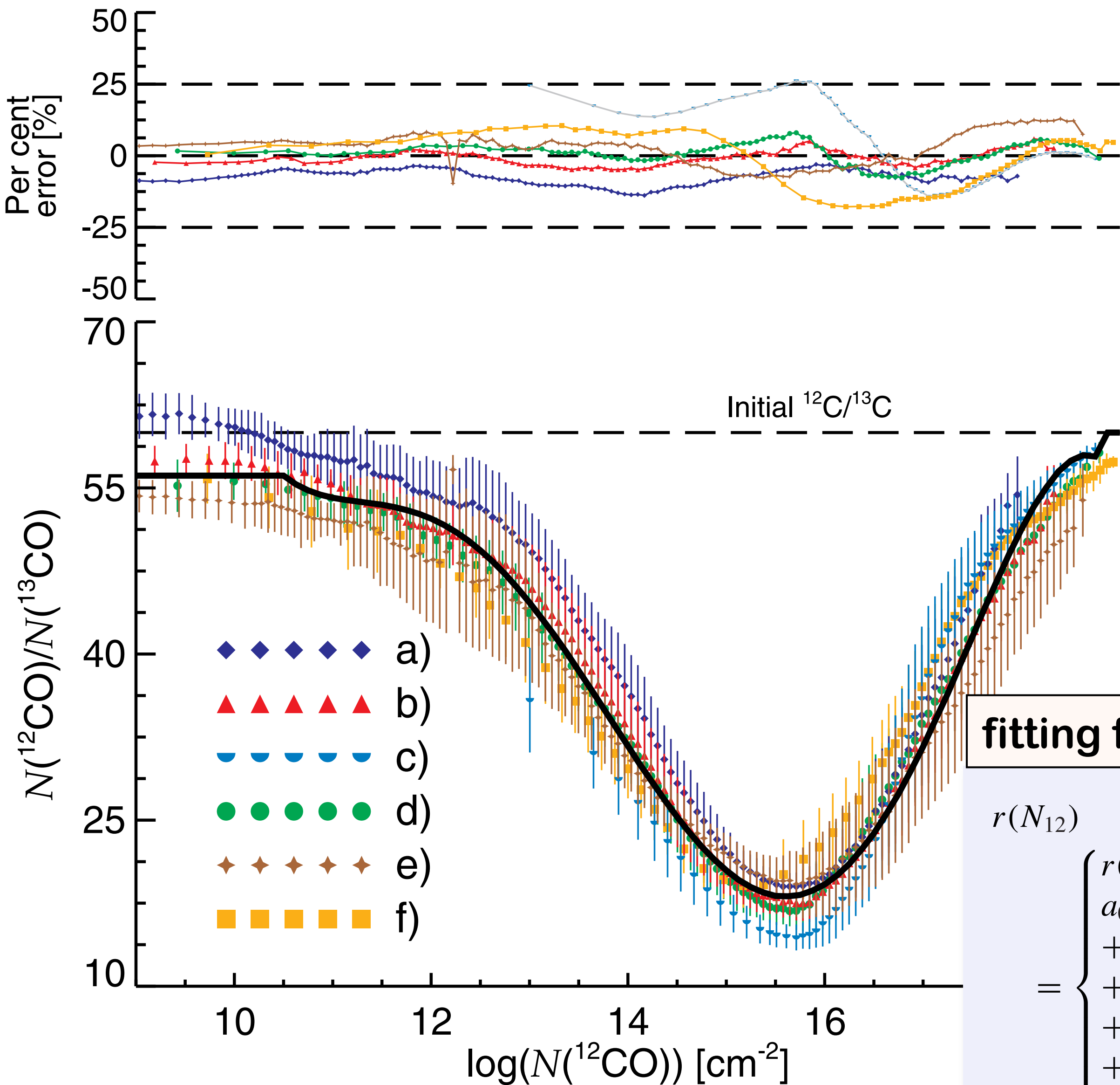

fitting formula:

$$r(N_{12}) = \begin{cases} r(N_{12} = 3.2 \times 10^{10}) & \text{if } N_{12} < 3.2 \times 10^{10} \\ a_{0,12} + a_{1,12} \log_{10}(N_{12}) & \\ +a_{2,12} \log_{10}(N_{12})^2 & \\ +a_{3,12} \log_{10}(N_{12})^3 & \\ +a_{4,12} \log_{10}(N_{12})^4 & \\ +a_{5,12} \log_{10}(N_{12})^5 & \text{if } 3.2 \times 10^{10} \le N_{12} \le 6 \times 10^{18} \\ 60 & \text{if } N_{12} > 6 \times 10^{18} \end{cases}$$

(Szücs et al. 2014, MNRAS 445, 4055-4072)


application:
global SF relations

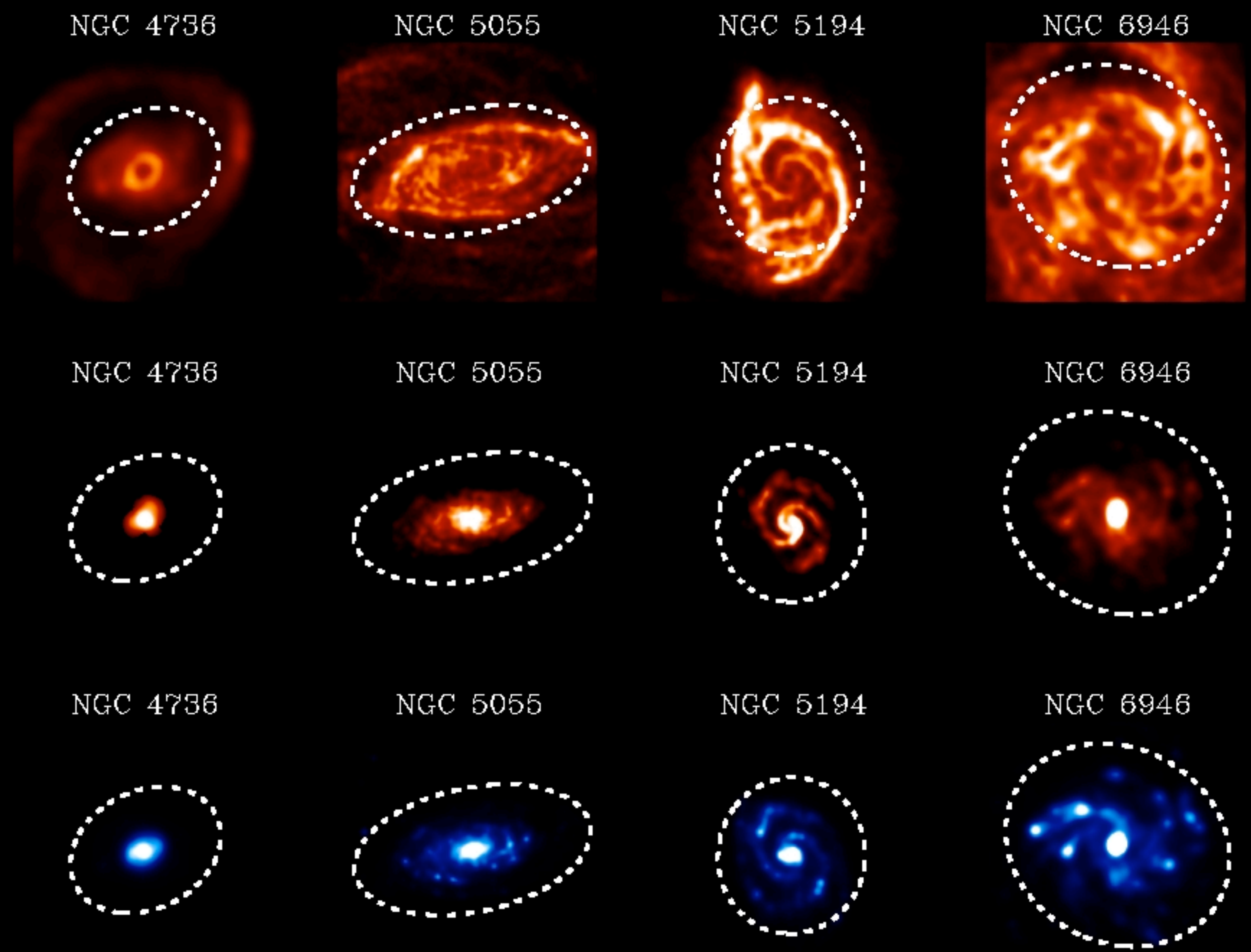

atomic hydrogen

molecular hydrogen

star formation

- HI gas more extended
- H2 and SF well correlated

galaxies from THINGS and HERACLES survey
(images from Frank Bigiel, ZAH/ITA)

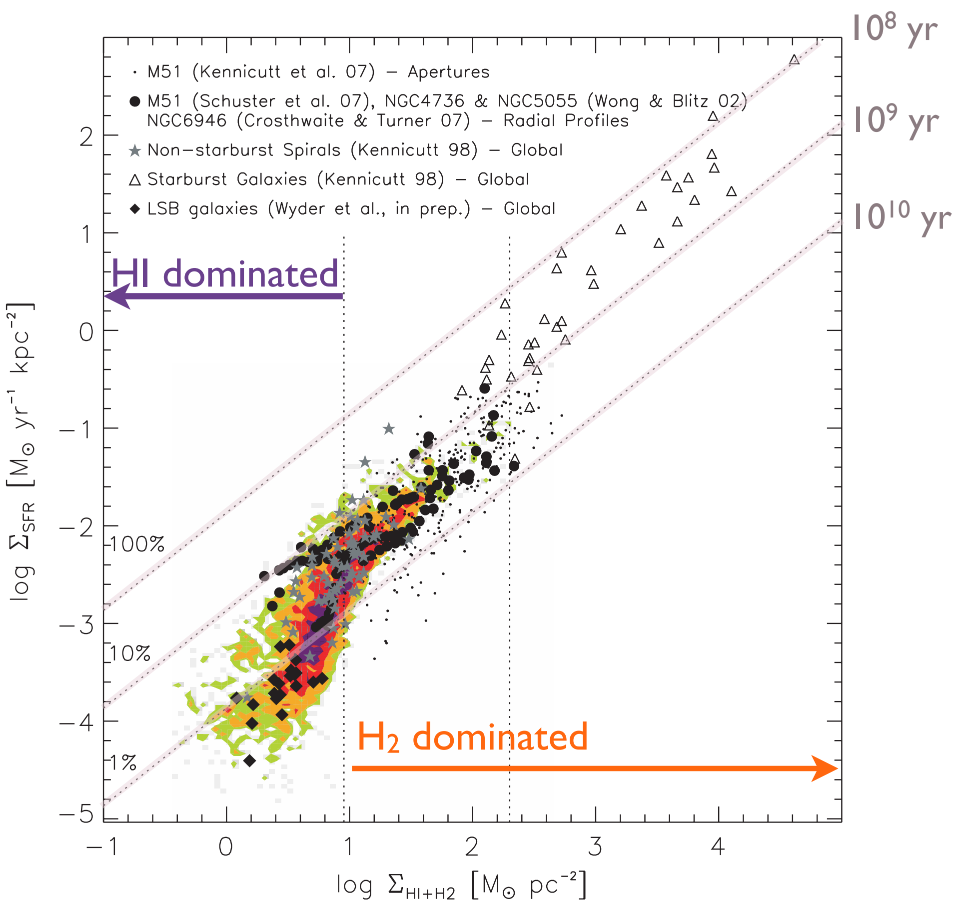

Bigiel et al. (2008, AJ, 136, 2846)

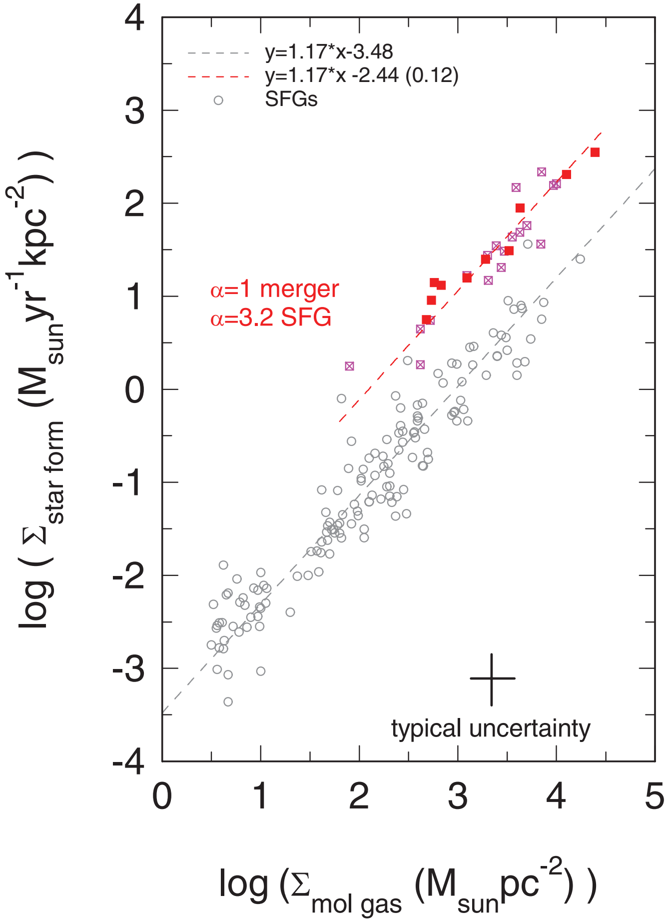

Genzel et al. (2010, MNRAS, AJ, 407, 2091)

- standard model: roughly linear relation between H
- standard model: roughly constant depletion time: few x 10
- super linear relation between total gas and SFR

data from STING survey (Rahman et al. 2011, 2012)

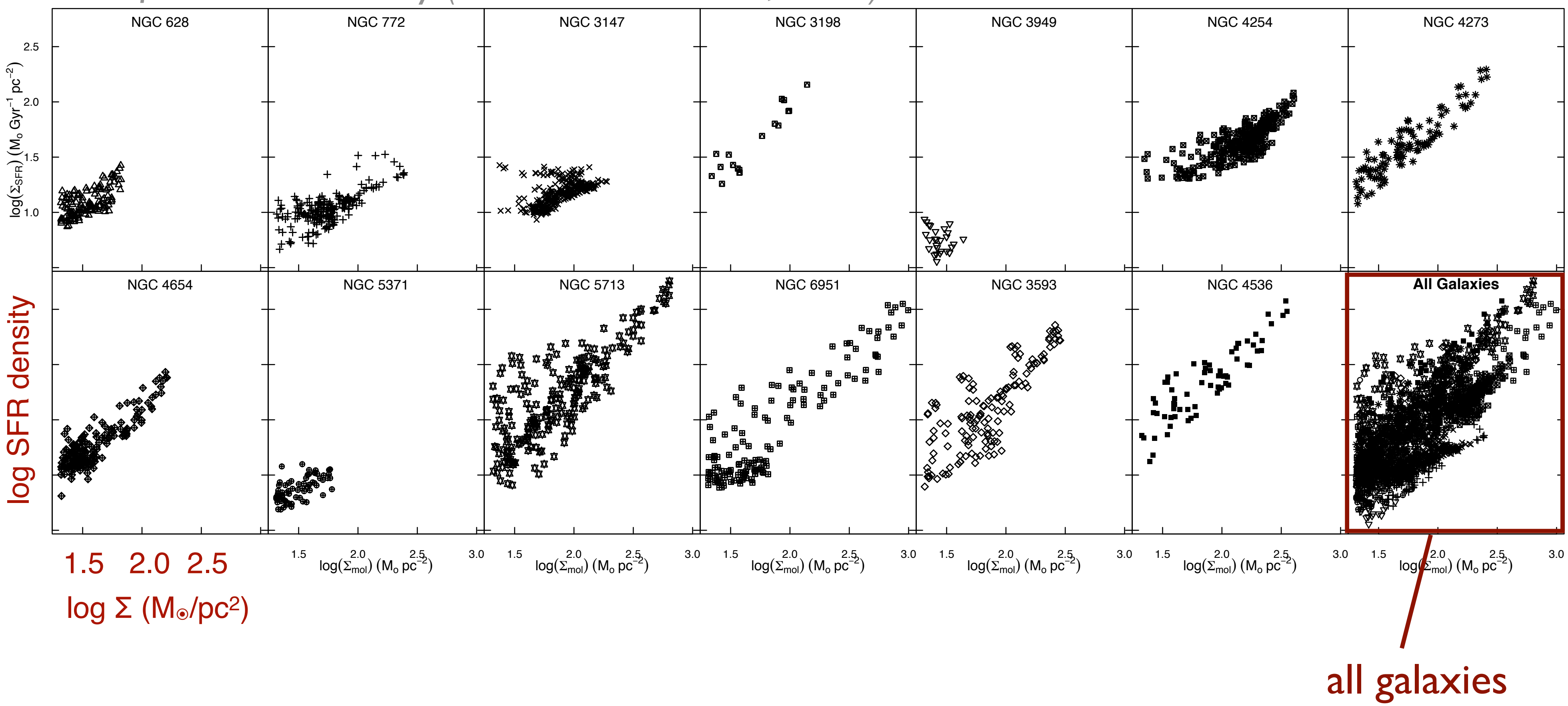

- QUIZ: do you see a universal

Shetty et al. (2014, MNRAS, 437, L61, see also Shetty, Kelly, Bigiel, 2013, MNRAS, 430, 288)

data from STING survey (Rahman et al. 2011, 2012)

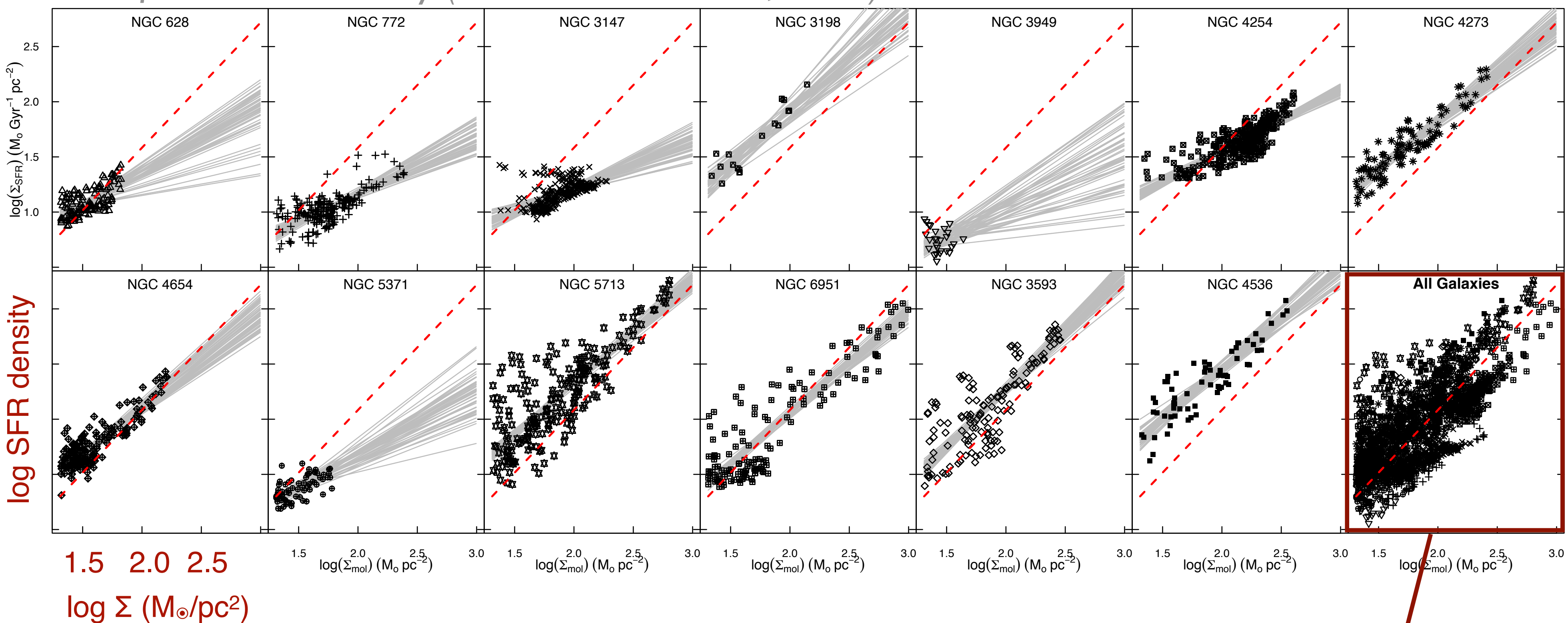

all galaxies

- QUIZ: do you see a universal
- ANSWER: - probably not
  - in addition, the relation often is sublinear

Shetty et al. (2014, MNRAS, 437, L61, see also Shetty, Kelly, Bigiel, 2013, MNRAS, 430, 288)

data from STING survey (Rahman et al. 2011, 2012)

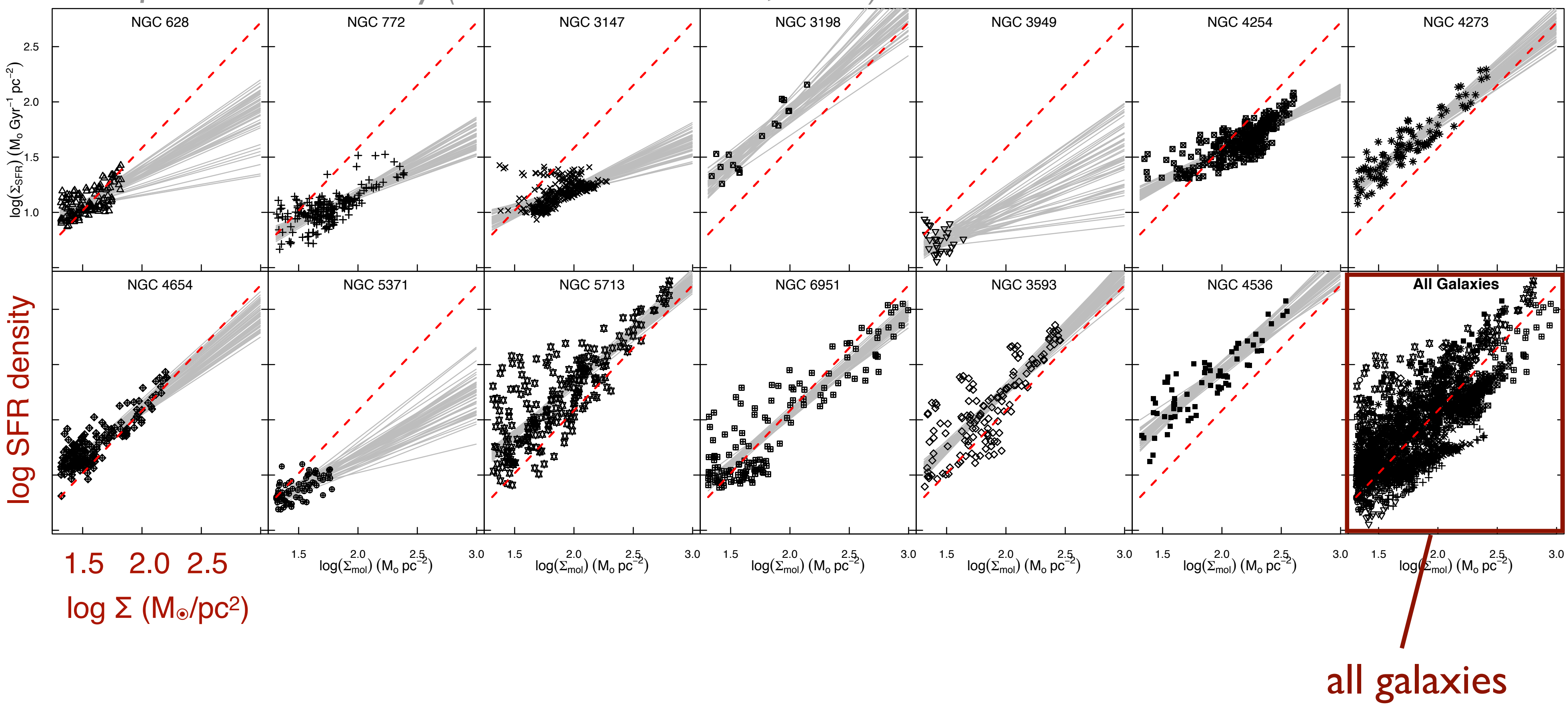

Shetty et al. (2014, MNRAS, 437, L61, see also Shetty, Kelly, Bigiel, 2013, MNRAS, 430, 288)

data from STING survey (Rahman et al. 2011, 2012)

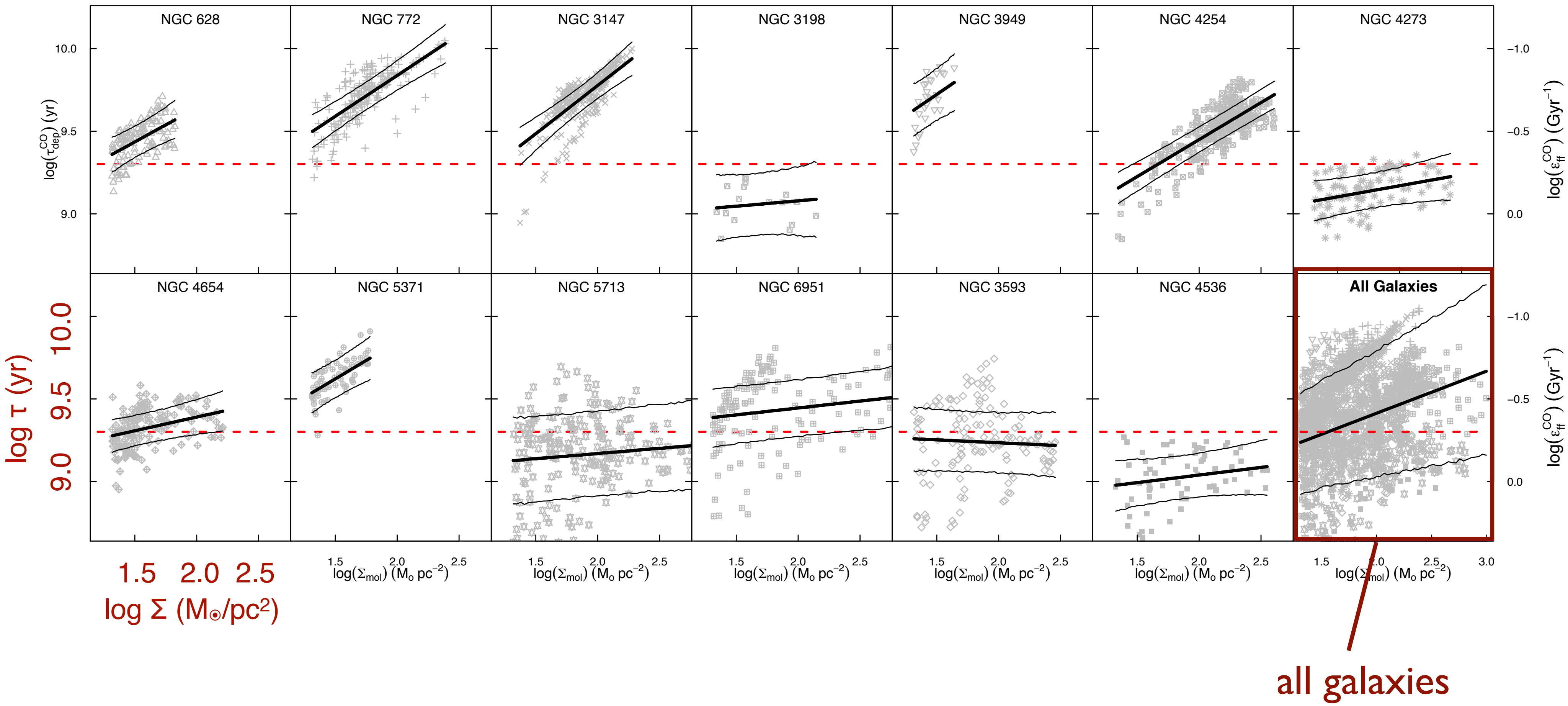

Hierarchical Bayesian model for STING galaxies indicate *varying depleting times.*

Shetty et al. (2014, MNRAS, 437, L61)

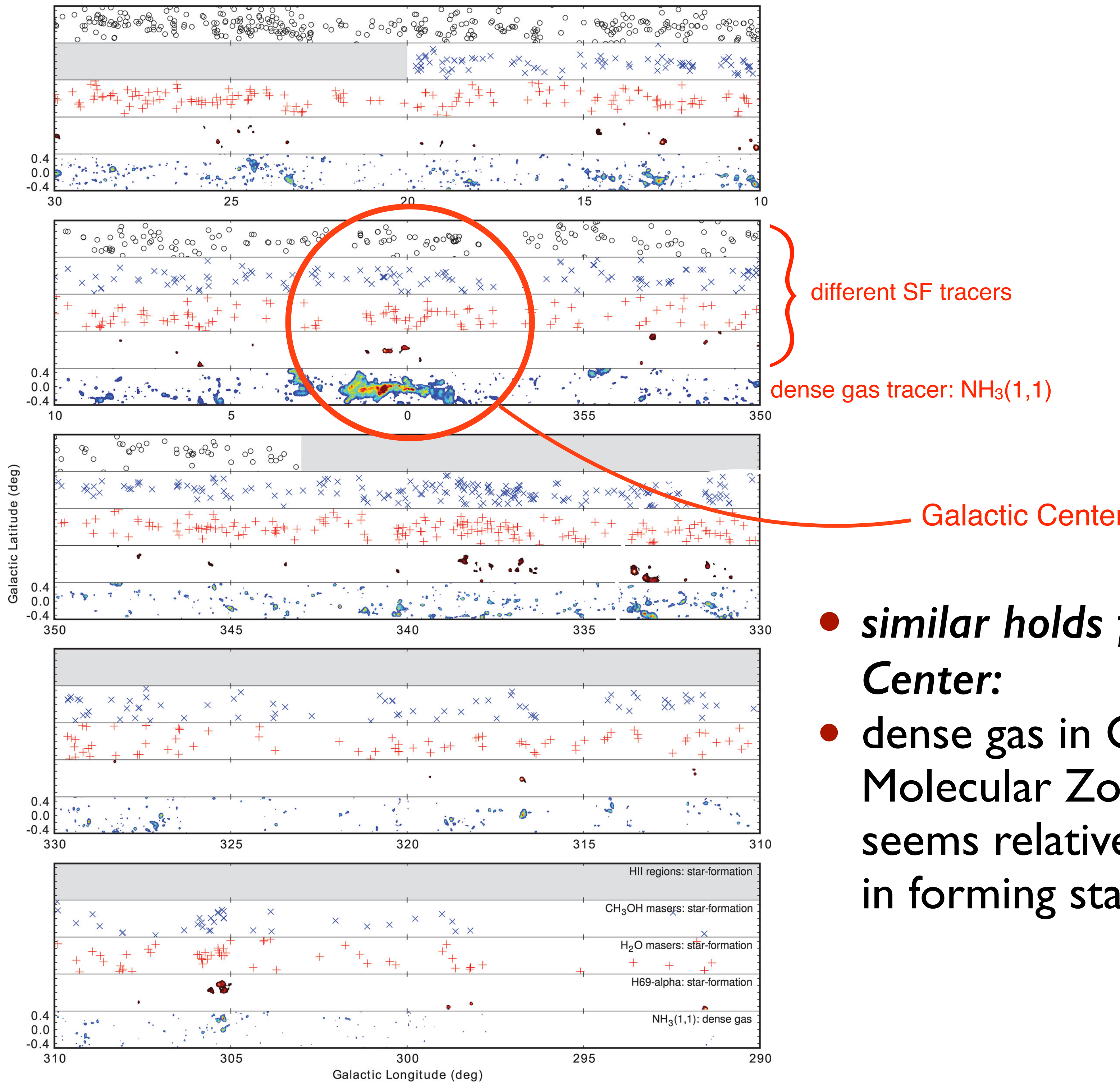

- ***similar holds for Galactic Center:***
- dense gas in Central Molecular Zone (CMZ) seems relative inefficient in forming stars

987)

data from STING survey (Rahman et al. 2011, 2012)

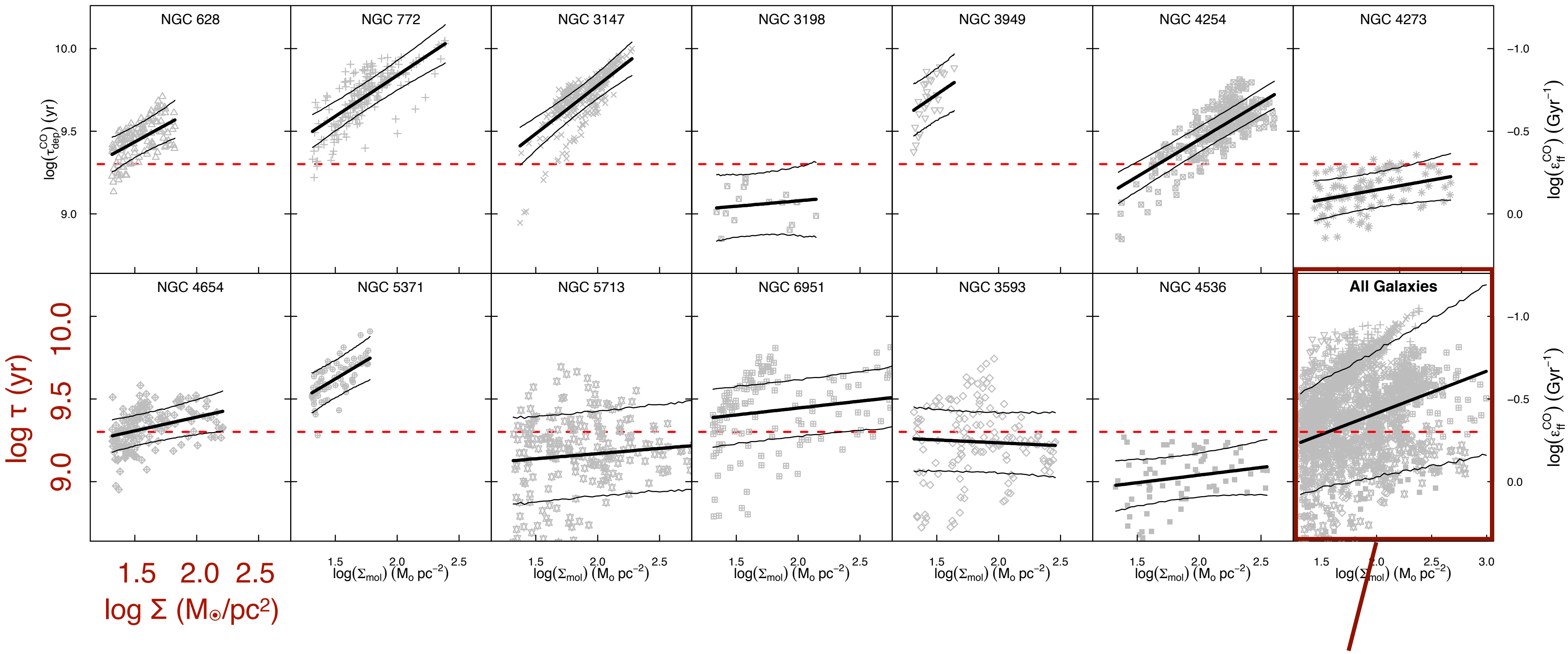

physical origin of this behavior?

- maybe strong shear in dense arms (example M51, Meidt et al. 2013)...
- maybe non-star forming H densities (recall H

Shetty et al. (2013, MNRAS, 437, L61, see also Shetty, Kelly, Bigiel, 2013, MNRAS, 430, 288)

data from STING survey (Rahman et al. 2011, 2012)

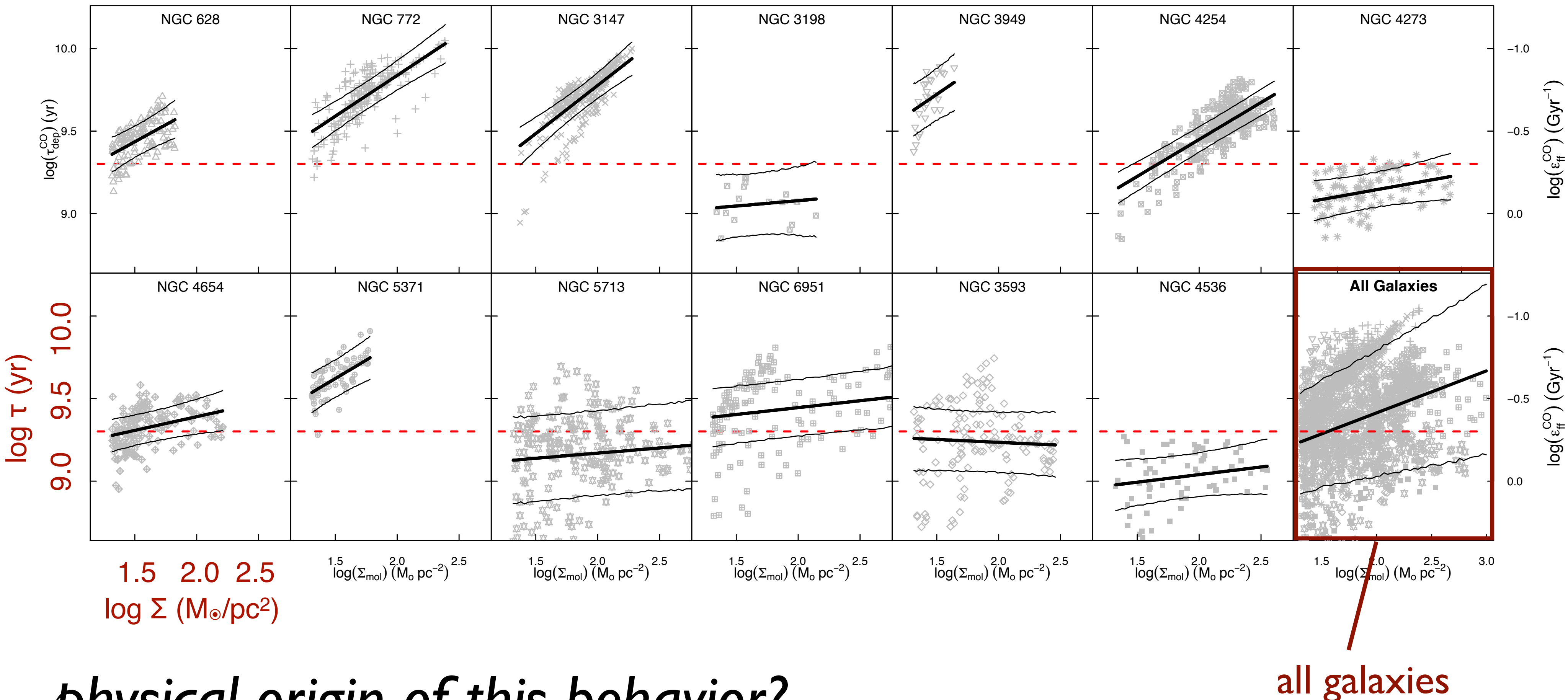

physical origin of this behavior?

SEARCH FOR CO-dark H_2 GAS

Shetty et al. (2013, MNRAS, 437, L61, see also Shetty, Kelly, Bigiel, 2013, MNRAS, 430, 288)


application:
CO-dark gas

modeling Galactic-scale ISM dynamics

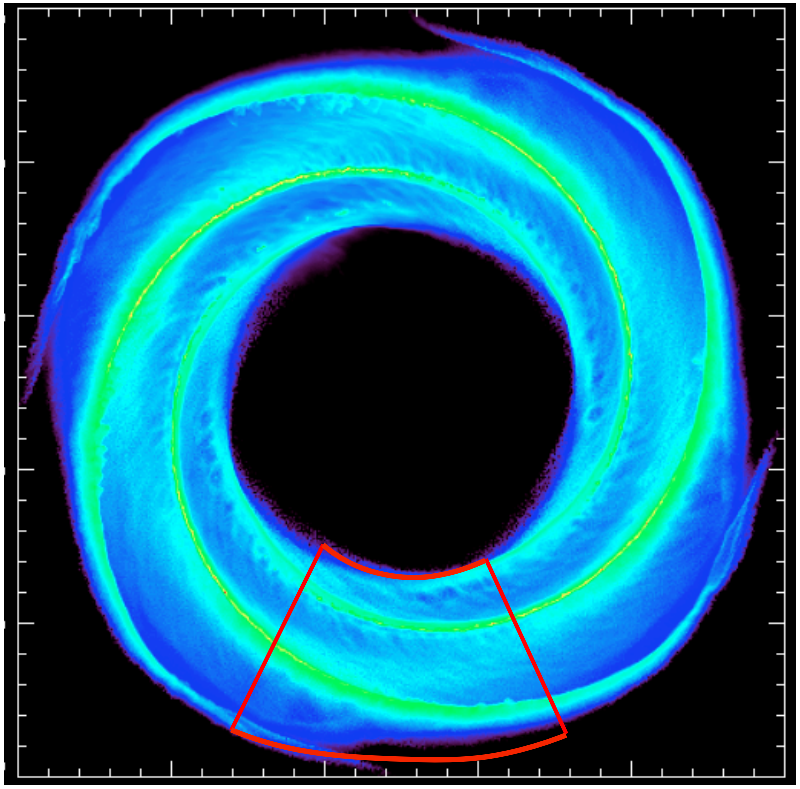

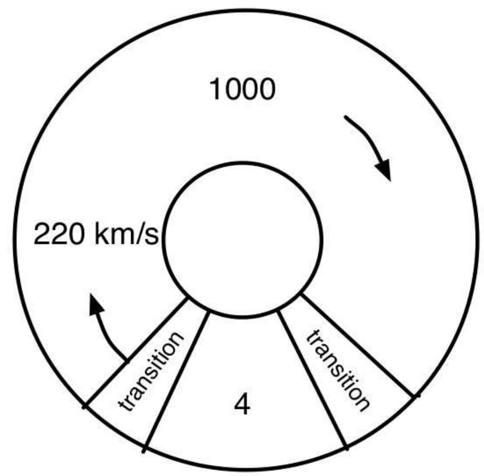

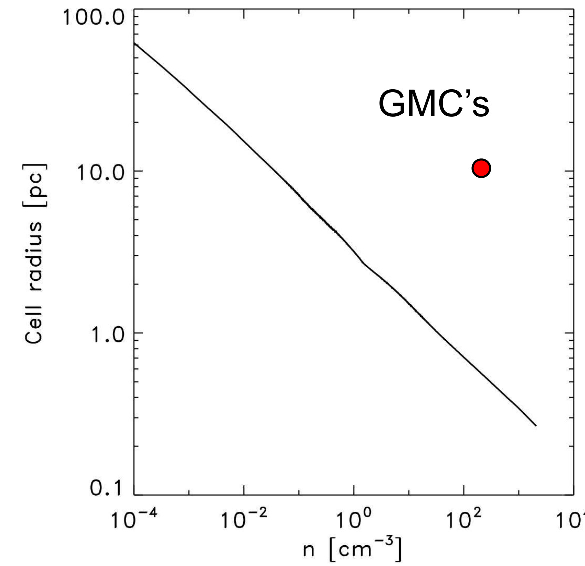

Simulation	Surface Density $M_\odot\ pc^{-2}$	Radiation Field G_0
Milky Way	10	1
Low Density	4	1
Strong Field	10	10
Low & Weak	4	0.1

(Smith et al., 2014, MNRAS, 441, 1628)

- Arepo moving mesh code *(Springel 2010)*
- time dependent chemistry *(Glover et al. 2007)* gives heating & cooling in a 2 phase medium
- two layers of refinement with mass resolution down to 4 $M_\odot$ in full Galaxy simulation
- UV field and cosmic rays
- TreeCol *(Clark et al. 2012)*
- external spiral potential *(Dobbs & Bonnell 2006)*
- no gas self-gravity, SN, or magnetic fields yet

numerical method

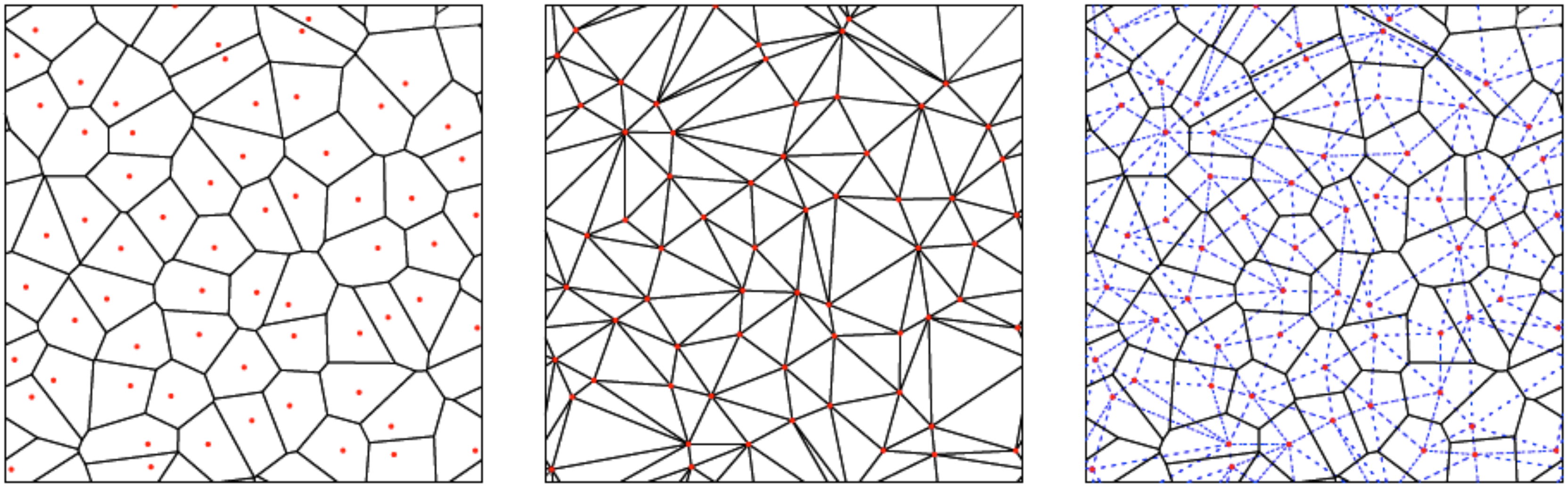

*moving mesh code **Arepo**:*

- semi-Lagrangian
- flexible refinement
- fluid instabilities and no artificial clumping
  (Agertz et al. 2007)
- can also handle sub-sonic turbulence
  (Bauer & Springel 2012)
- no preferred geometry

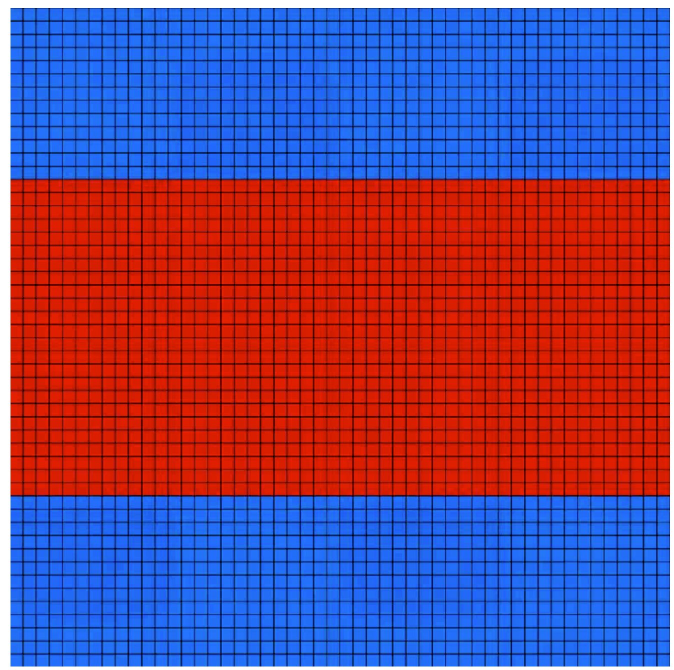

Springel (2010, MNRAS, 401, 791)

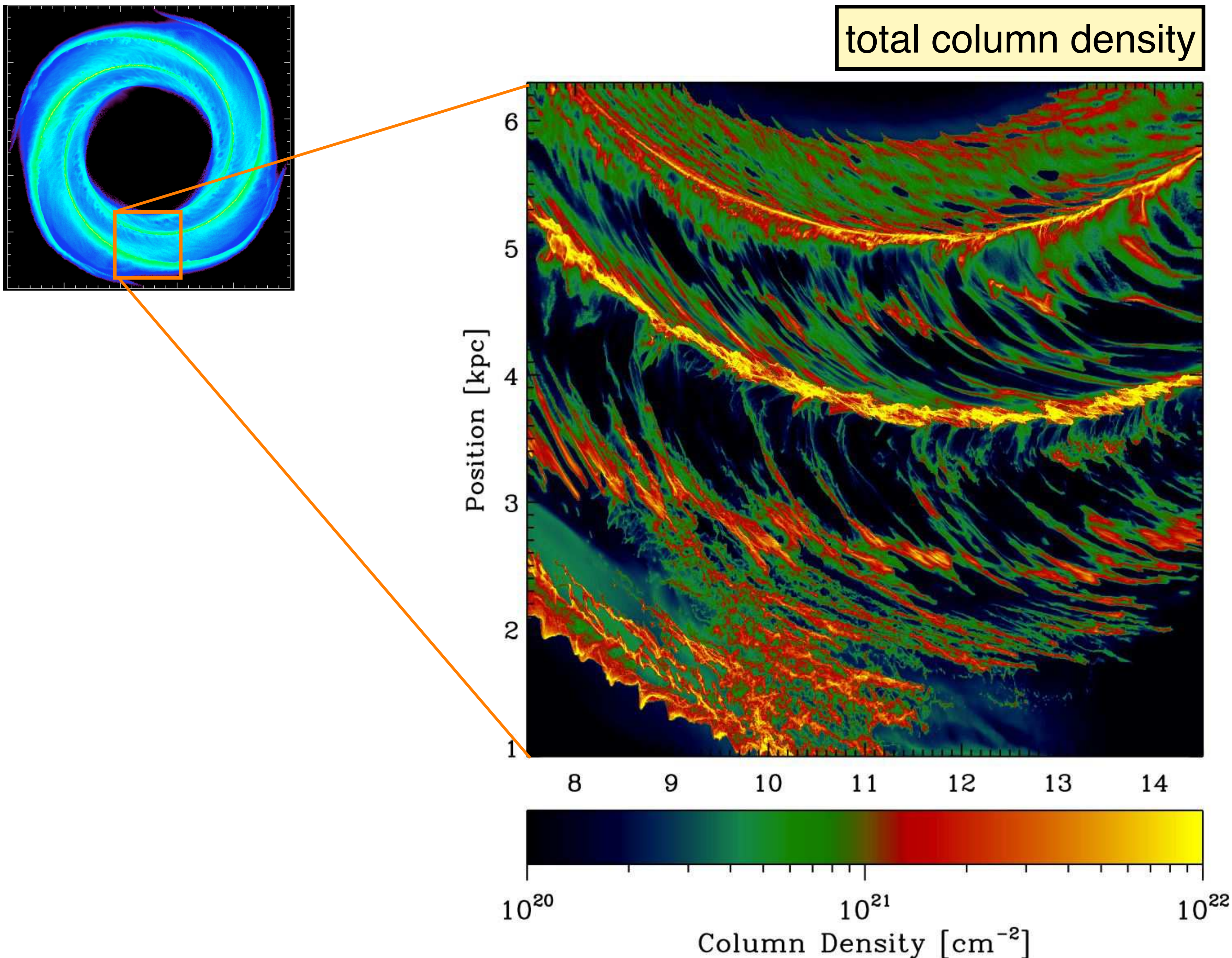

(Smith et al., 2014, MNRAS, 441, 1628)

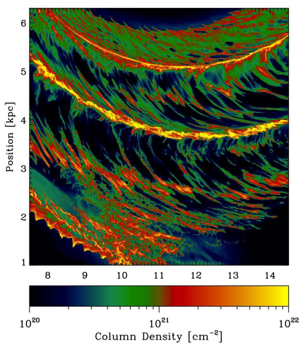

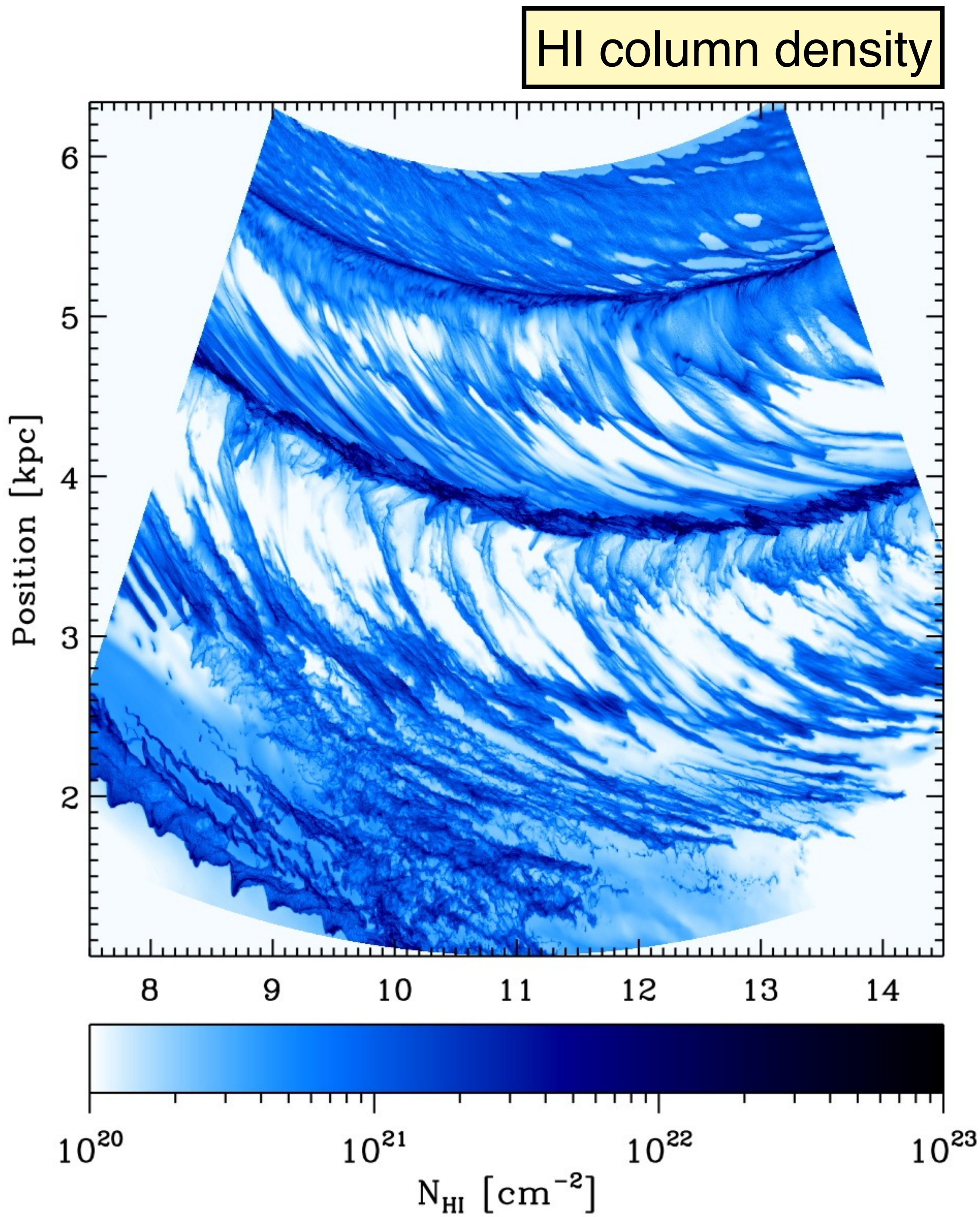

(Smith et al., 2014, MNRAS, 441, 1628)

preliminary image from THOR Galactic plane survey (PI H. Beuther): continuum emission around 21 cm

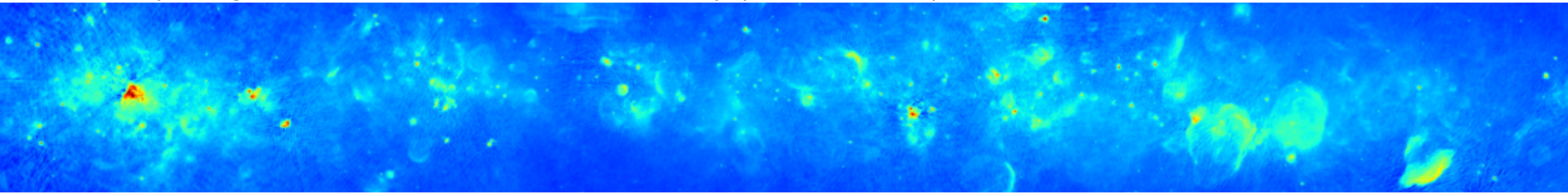

next step: produce all sky maps at various positions in the model galaxy (use RADMC-3D)

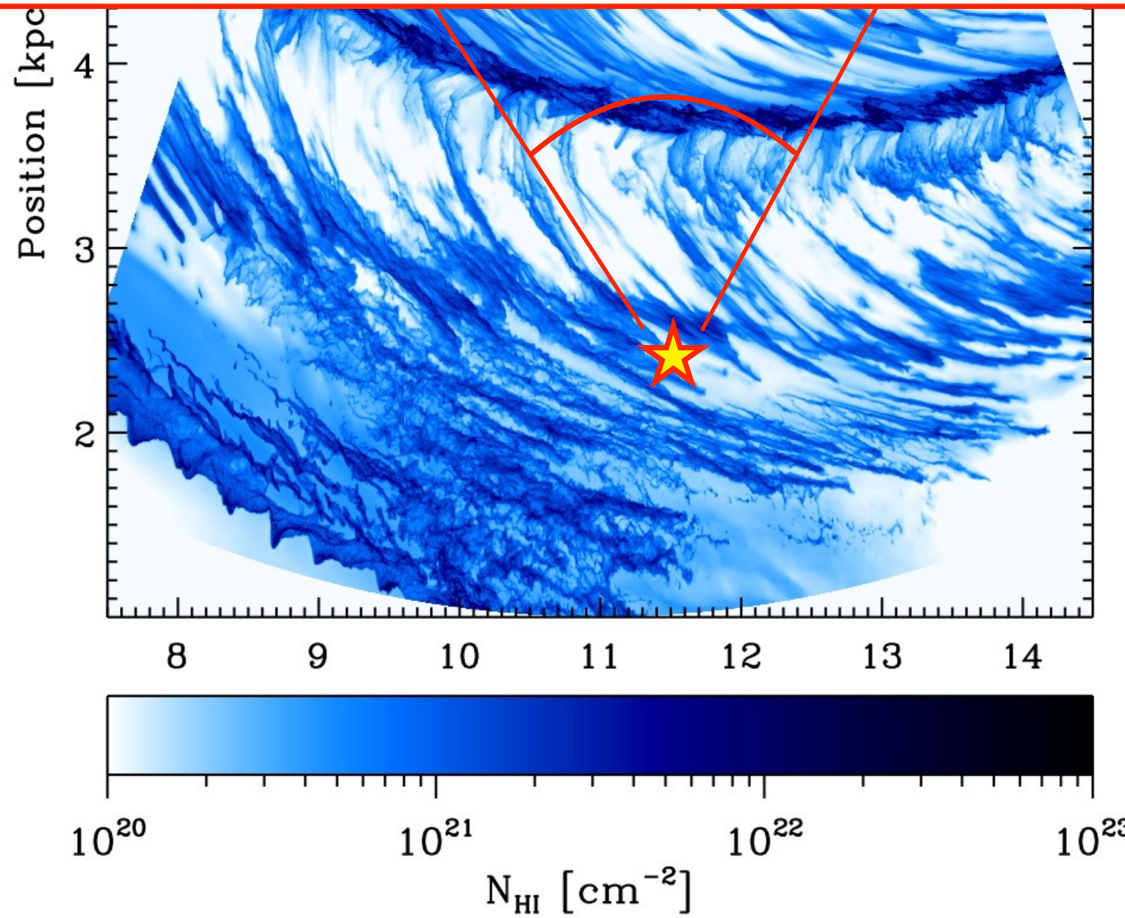

(Smith et al., 2014, MNRAS, 441, 1628)

preliminary image from THOR Galactic plane survey (PI H. Beuther): continuum emission around 21 cm

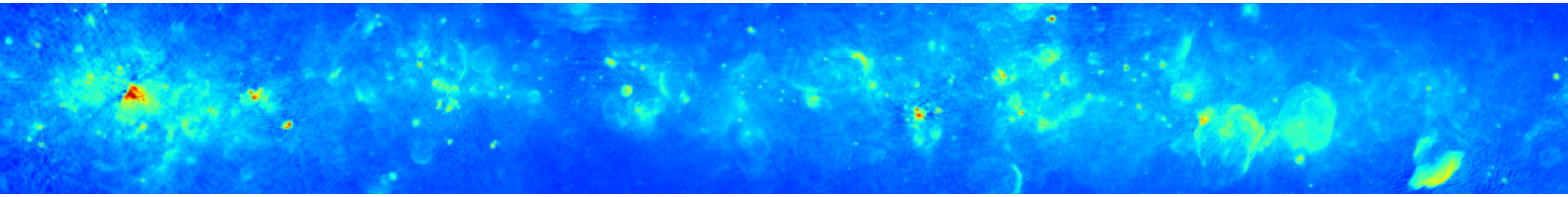

next step: produce all sky maps at various positions in the model galaxy (use RADMC-3D)

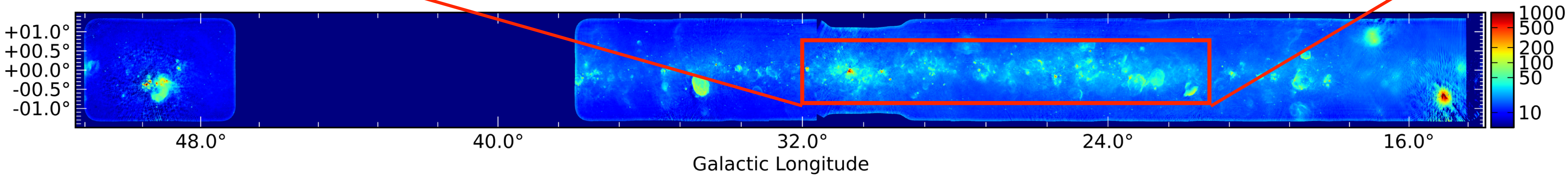

http://www.mpia.de/thor/Overview.html

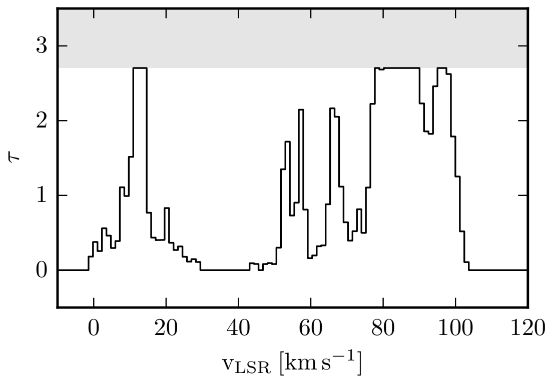

Fig. 10. Optical depth of W43-Main, calculated using equation 6. The grey shaded area indicates the maximum measurable optical depth of $\tau_{lower-limit} = 2.7$ calculated using equation 7.

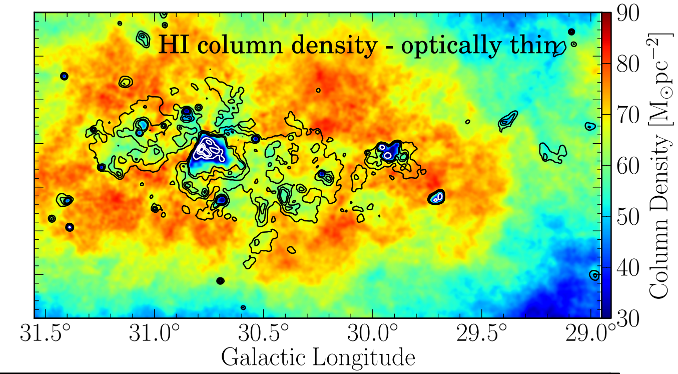

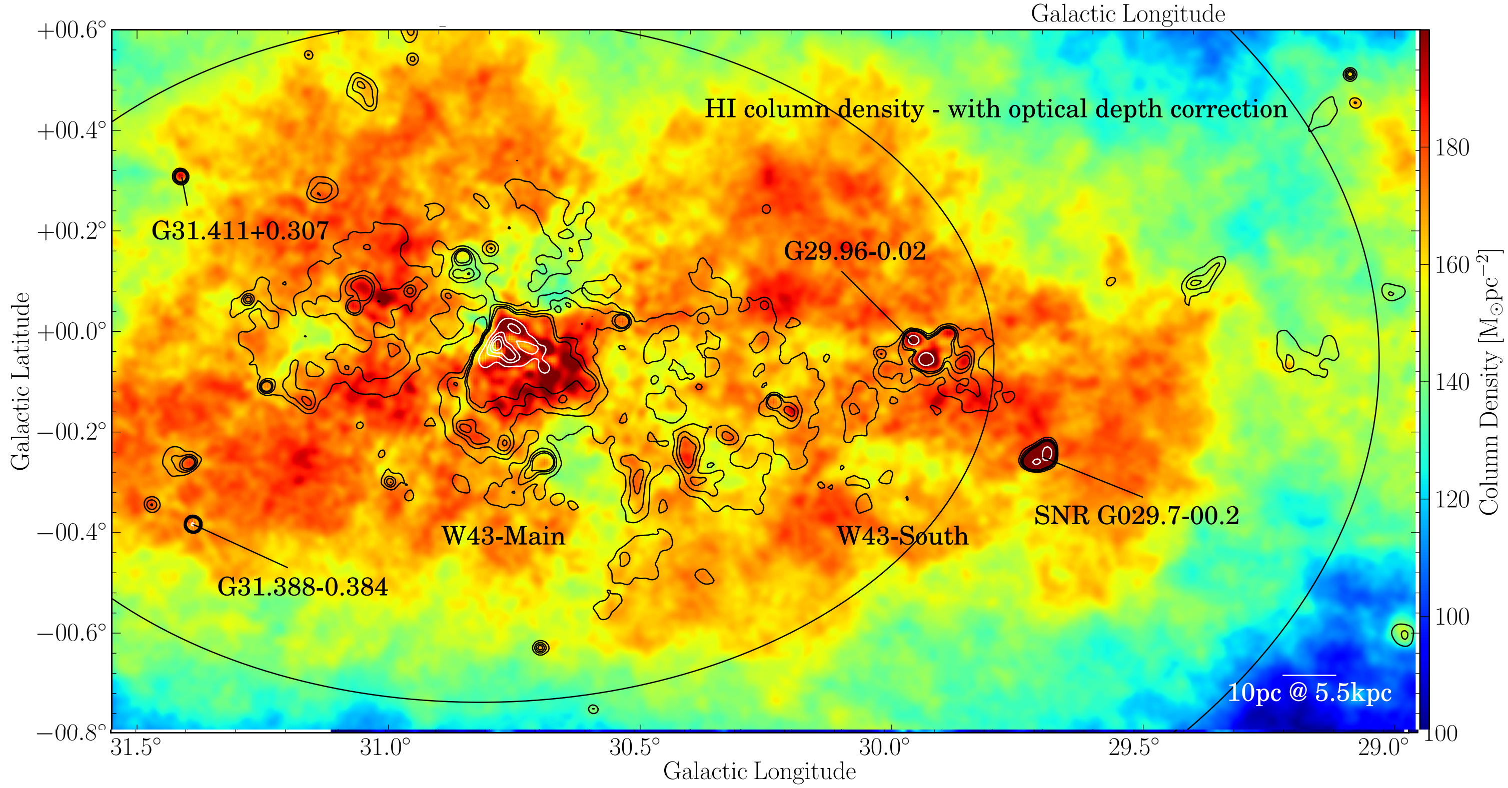

Some first results from the THOR pilot study:

HI emission in the Galactic disk may have large regions with $\tau > 0$ (even $\tau \gtrsim 1$).

Bihr et al. (2015, A&A in press, arXiv:1505.05176)

http://www.mpia.de/thor/Overview.html

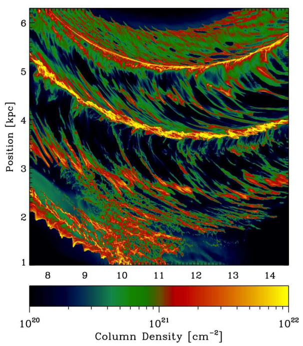

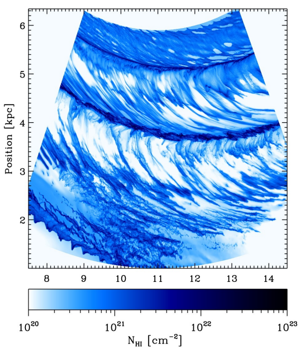

H_2 column density

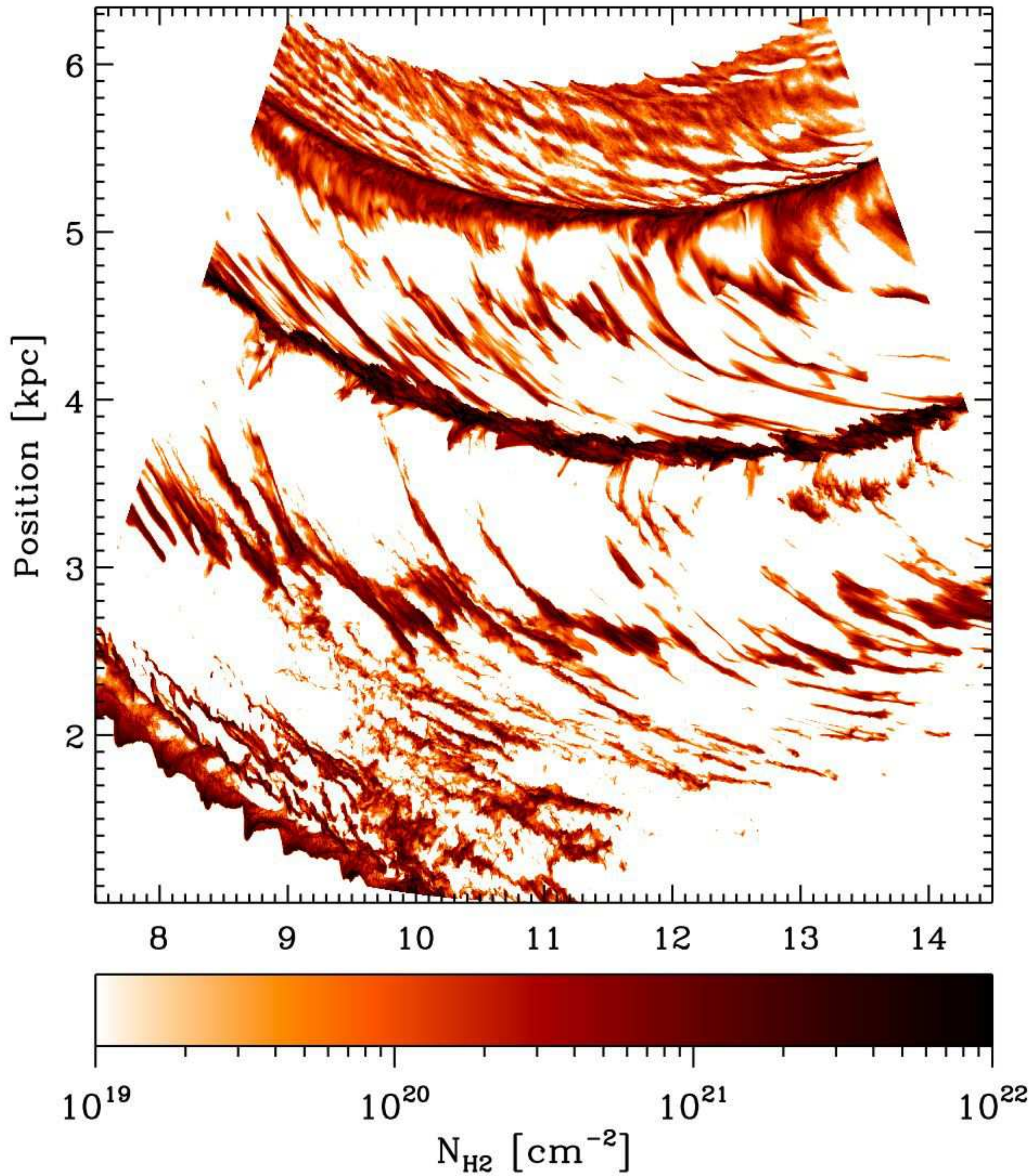

(Smith et al., 2014, MNRAS, 441, 1628)

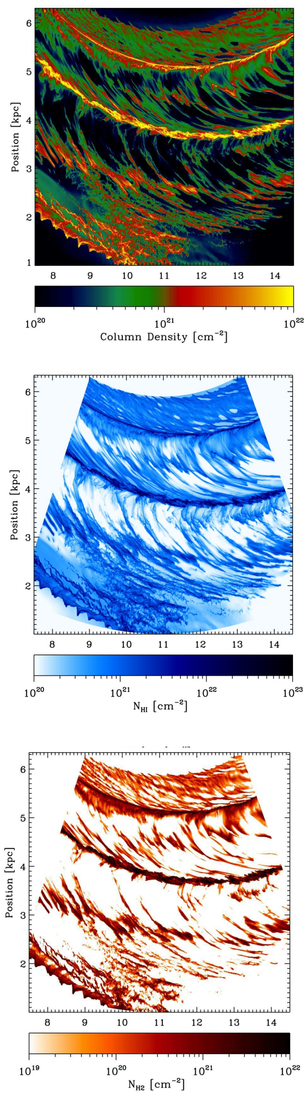

CO column density

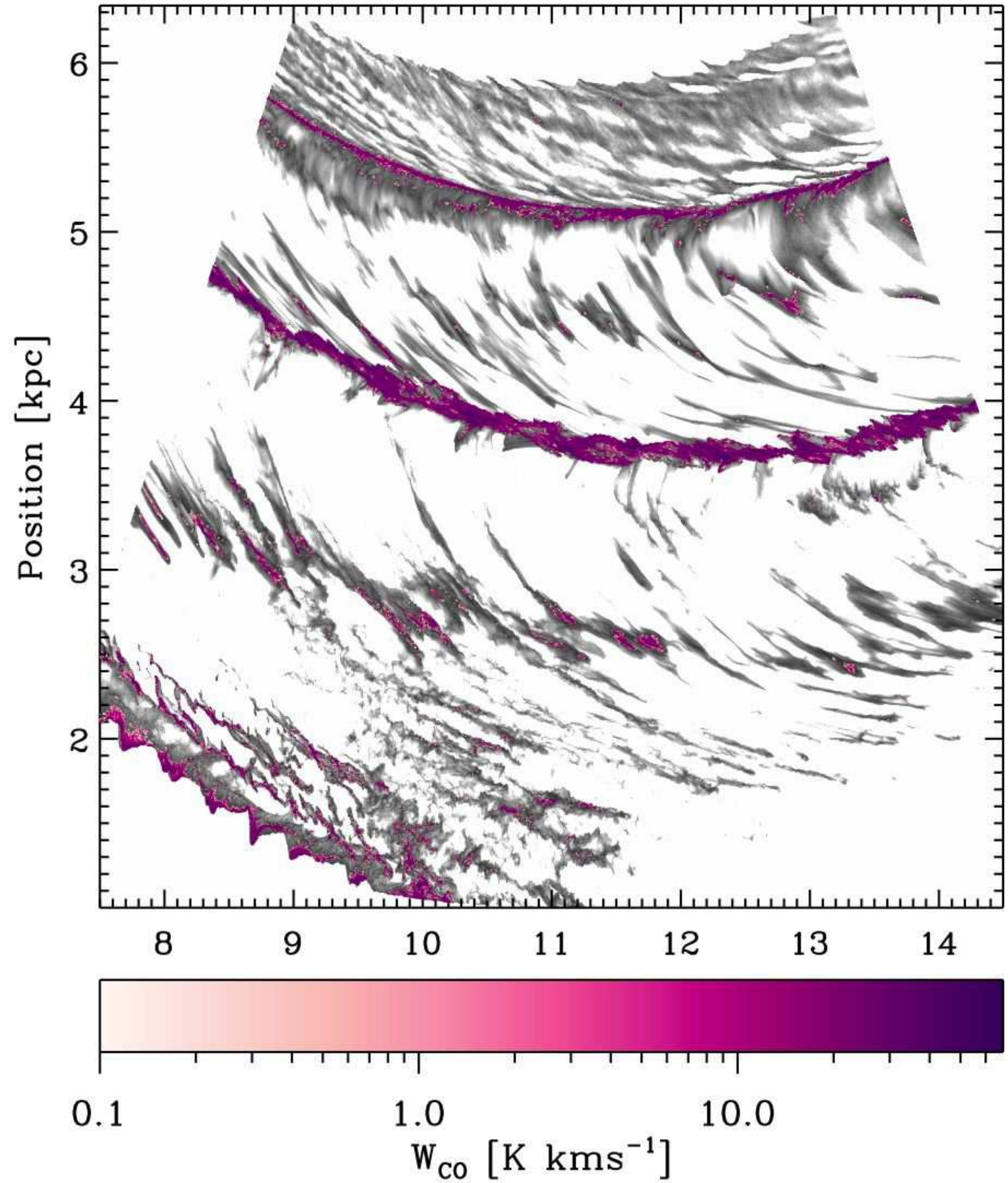

(Smith et al., 2014, MNRAS, 441, 1628)

H$_2$ fraction vs. column density N

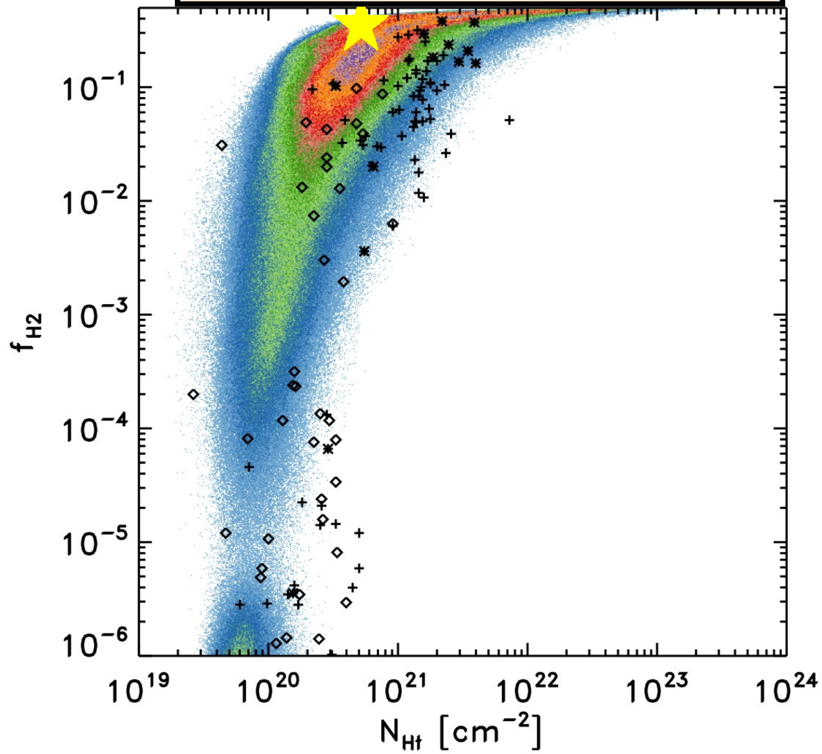

CO col. density vs. H$_2$ col. density

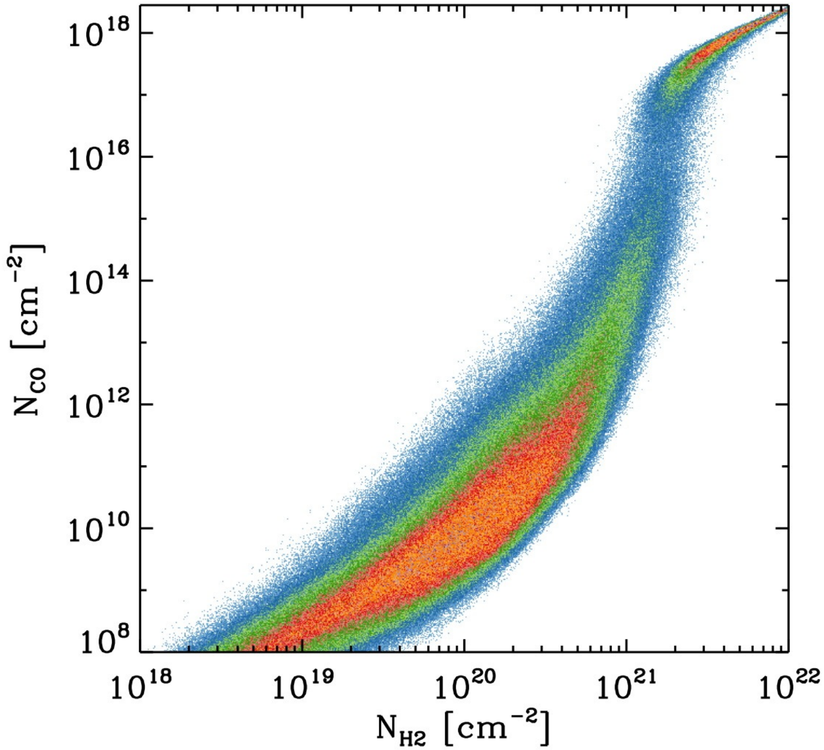

H$_2$ forms above column densities of 10^{20} cm^{-2}

CO columns jump after $N_{H2} \sim 10^{21}$ cm^{-2}

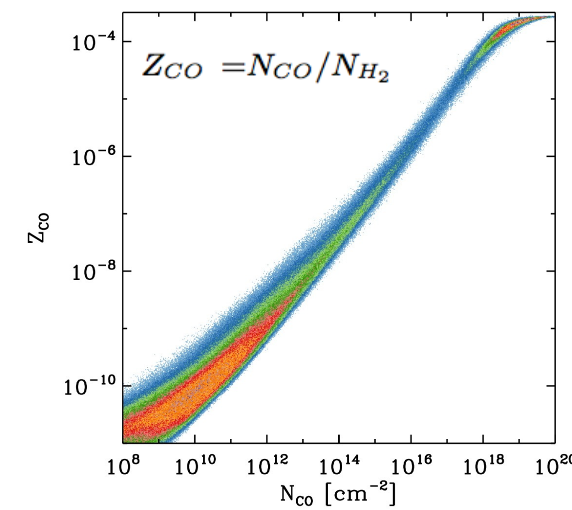

$$log(Z_{CO}[cm^{-2}]) = -18.1 log(N_{CO}[cm^{-2}]) + 0.8.$$

(Smith et al., 2014, MNRAS, 441, 1628)

details of CO emission

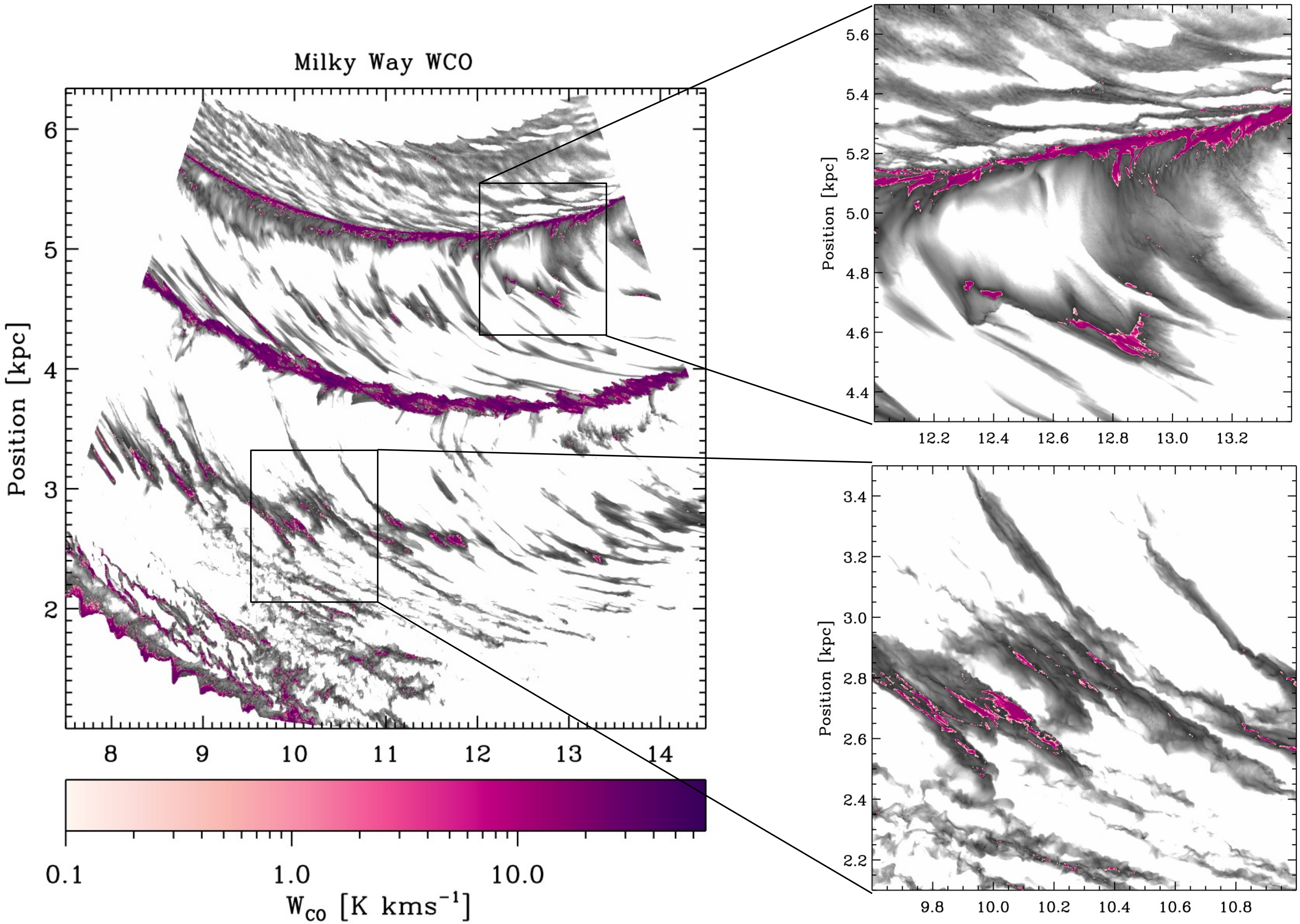

(Smith et al., 2014, MNRAS, 441, 1628)

relation between CO and H_2

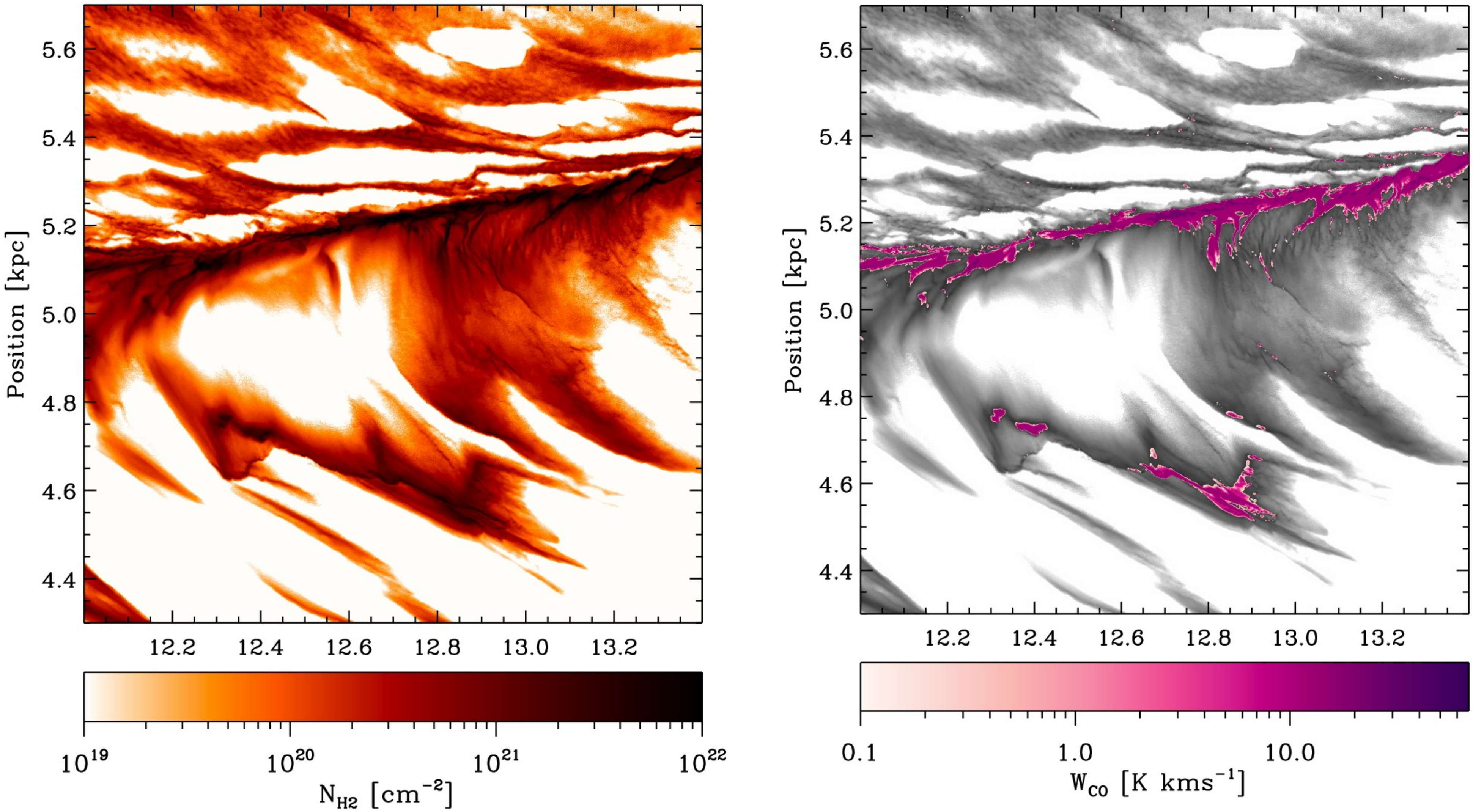

(Smith et al., 2014, MNRAS, 441, 1628)

relation between CO and H_2

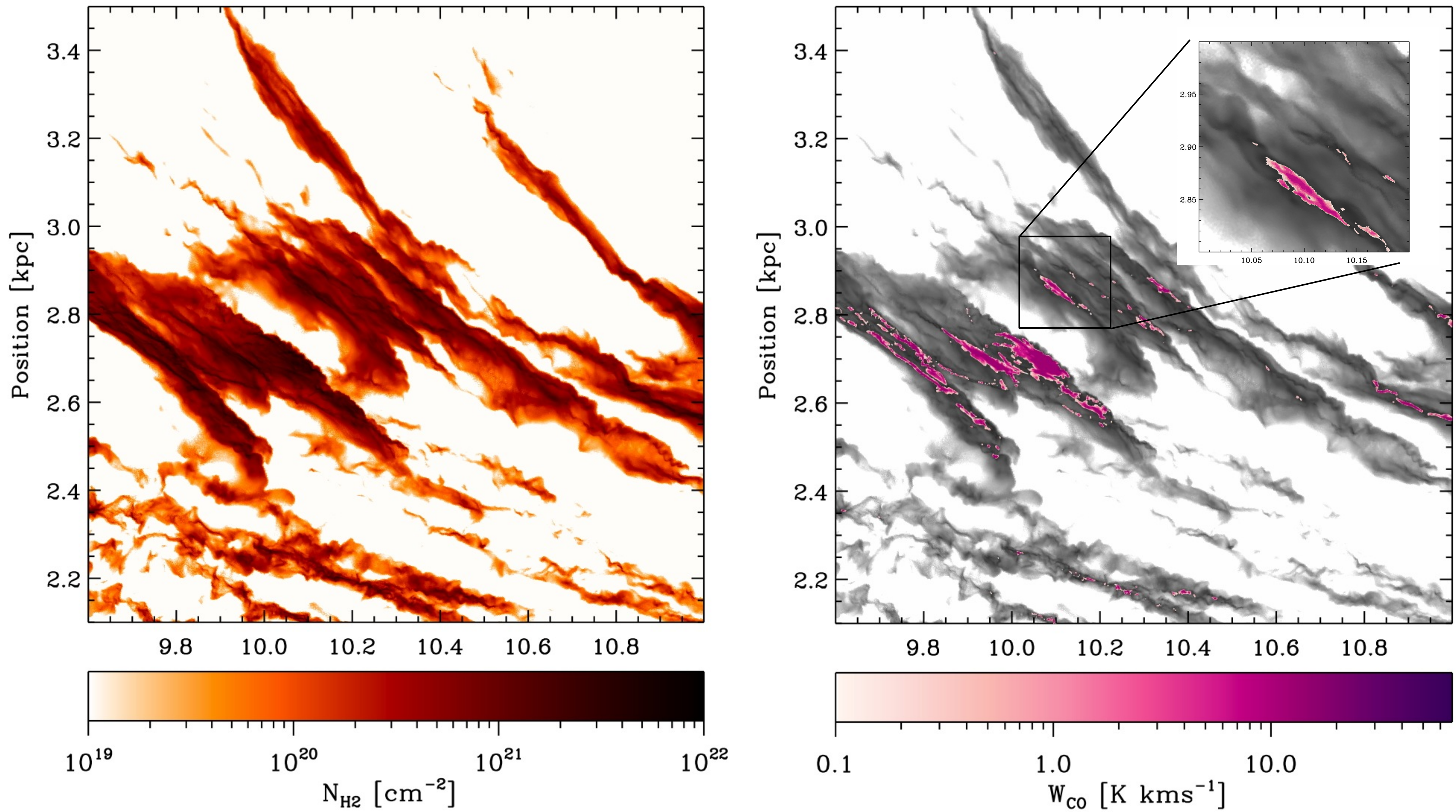

Filamentary molecular clouds in inter-arm regions are likely only the observable parts of much larger structures.

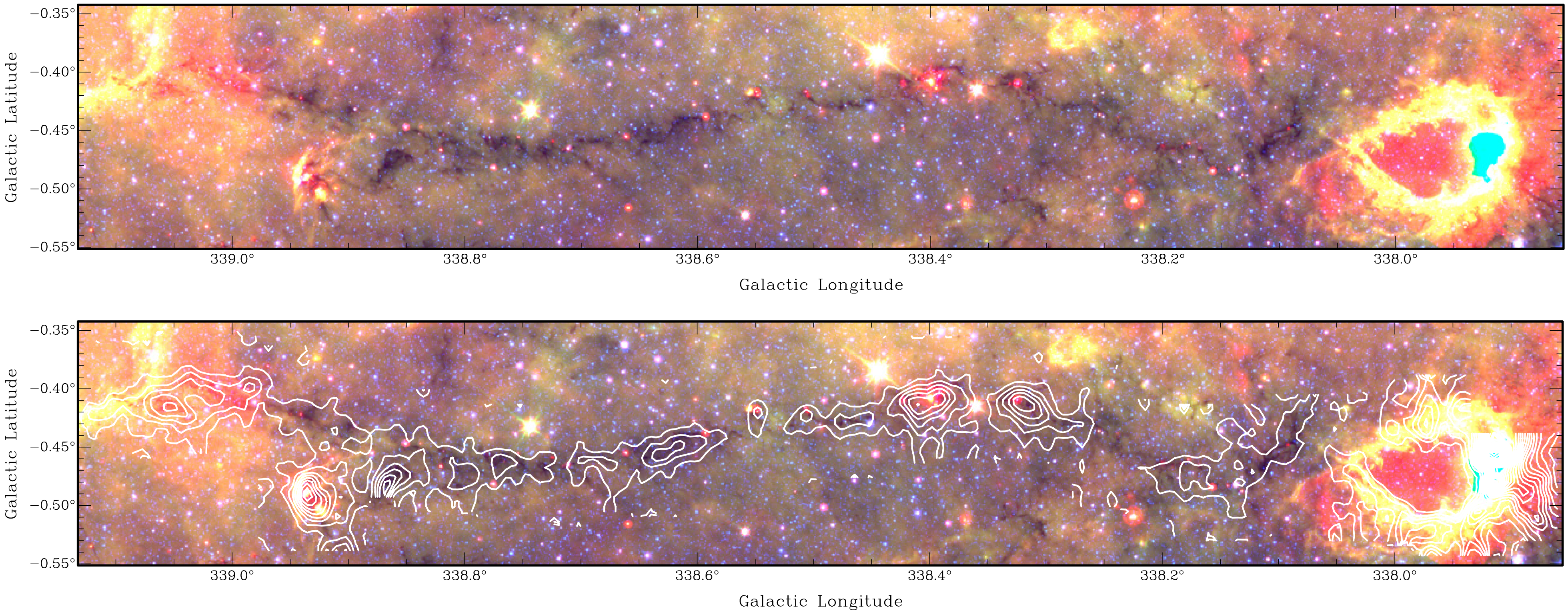

Nessie filament (Jackson et al. 2010, Goodman et al, 2014)

(Jackson et al. 2010, ApJ, 719, L185)

Filamentary molecular clouds in inter-arm regions are likely only the observable parts of much larger structures.

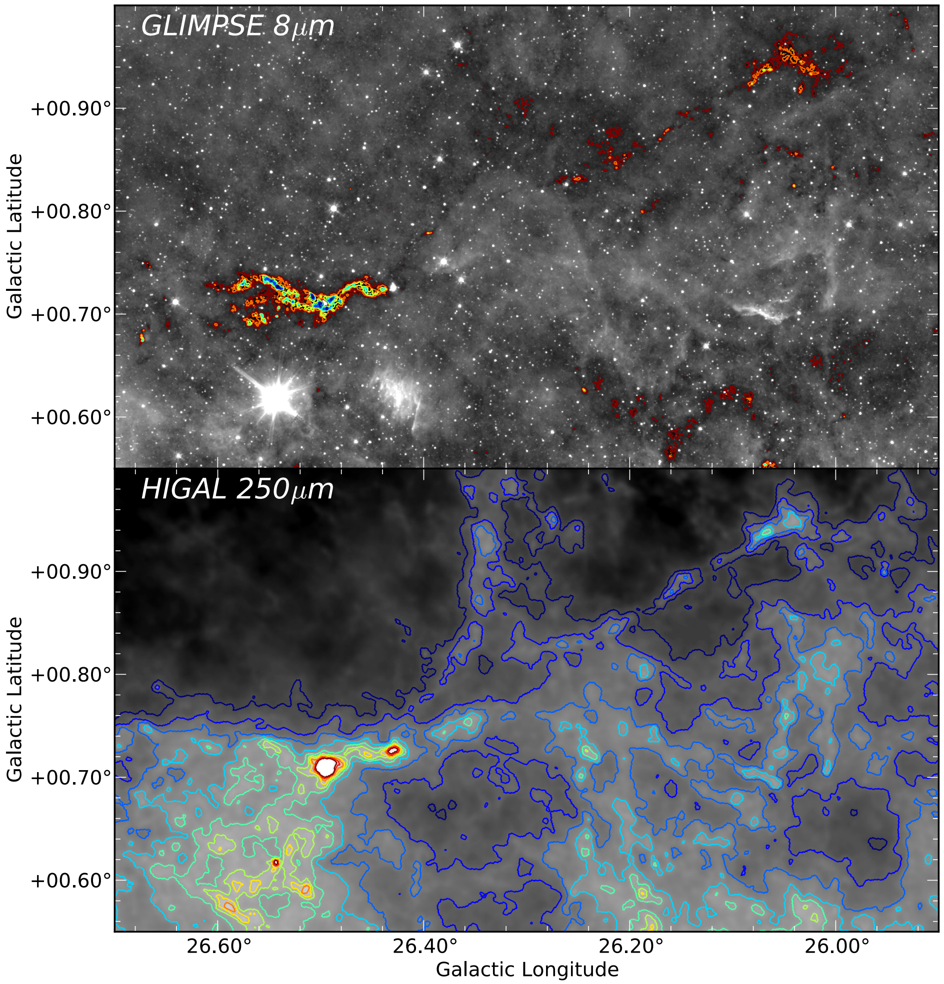

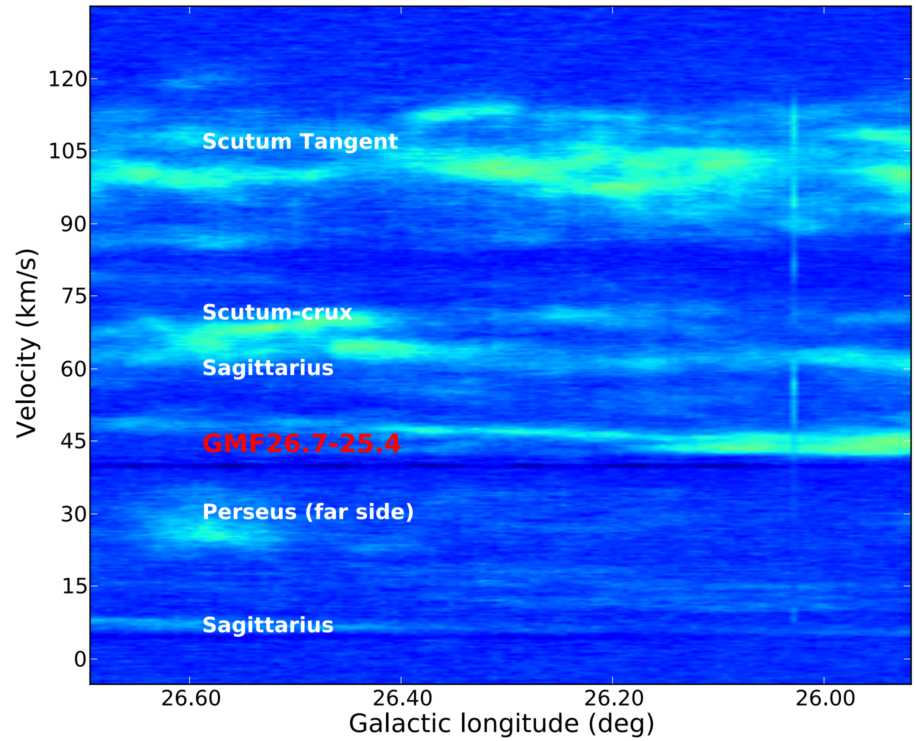

Filamentary molecular clouds in inter-arm regions are likely only the observable parts of much larger structures.

Name	Cloud mass $[M_\odot]$	Dense gas mass $[M_\odot]$	DGMF [%]	R_{gal} [kpc]	β [degrees]	$\langle z \rangle$ [pc]	Assoc.
GMF 18.0-16.8	1.5e+5	3.9e+3	2.7	6.3	4.6	55	M 16, W 37
GMF 20.0-17.9	4.0e+5	4.8e+4	12.0	5.0	7.7	(12)	W 39, SC-arm
GMF 26.7-25.4	2.0e+5	1.3e+4	6.5	5.7	9.4	68	
GMF 38.1-32.4a	7.0e+5	3.7e+4[a]	5.3	5.9	12.8	(24)	W 44
GMF 38.1-32.4b	7.7e+4	5.0e+3[a]	6.5	6.2	11.5	(5)	
GMF 41.0-41.3	4.9e+4	7.7e+2	1.6	6.5	12.5	19	
GMF 54.0-52.0	6.8e+4	2.4e+3	3.5	7.3	11.2	25	W 52
Nessie	–	3.9e+5	–	5.6	−7.8	–	SC-arm
G32.02+0.06	2.0e+5	3.0e+4	15.0	4.7	19.7	48	

Ragan et al. (2014 A&A 568, A73)

Many of the long filaments are indeed located at inter-arm regions.

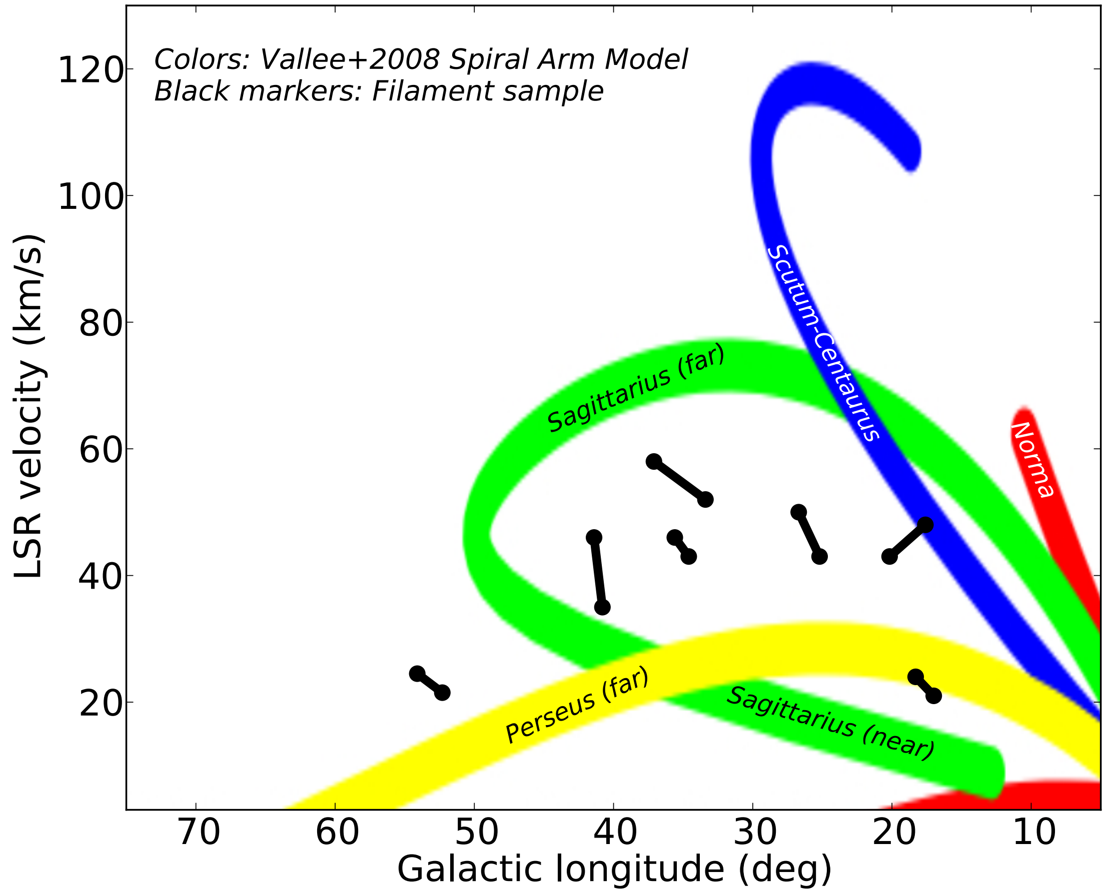

Name	Cloud mass $[M_\odot]$	Dense gas mass $[M_\odot]$	DGMF [%]	R_{gal} [kpc]	β [degrees]	$\langle z \rangle$ [pc]	Assoc.
GMF 18.0-16.8	1.5e+5	3.9e+3	2.7	6.3	4.6	55	M 16, W 37
GMF 20.0-17.9	4.0e+5	4.8e+4	12.0	5.0	7.7	(12)	W 39, SC-arm
GMF 26.7-25.4	2.0e+5	1.3e+4	6.5	5.7	9.4	68	
GMF 38.1-32.4a	7.0e+5	3.7e+4[a]	5.3	5.9	12.8	(24)	W 44
GMF 38.1-32.4b	7.7e+4	5.0e+3[a]	6.5	6.2	11.5	(5)	
GMF 41.0-41.3	4.9e+4	7.7e+2	1.6	6.5	12.5	19	
GMF 54.0-52.0	6.8e+4	2.4e+3	3.5	7.3	11.2	25	W 52
Nessie	–	3.9e+5	–	5.6	−7.8	–	SC-arm
G32.02+0.06	2.0e+5	3.0e+4	15.0	4.7	19.7	48	

Filamentary molecular clouds in inter-arm regions are likely only the observable parts of much larger structures.

Ragan et al. (2014 A&A 568, A73)

dark gas fraction

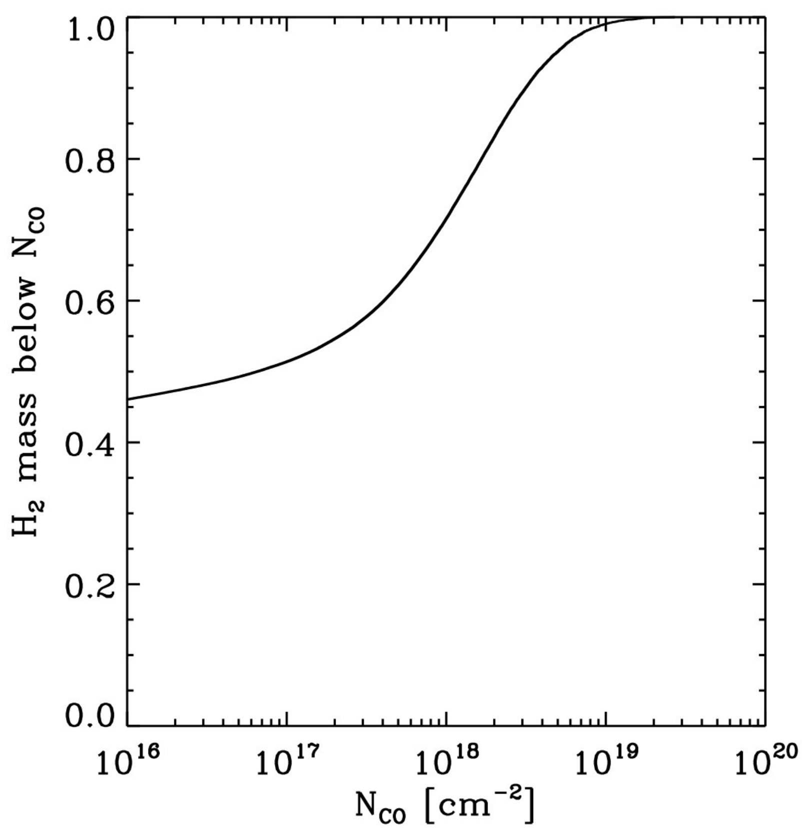

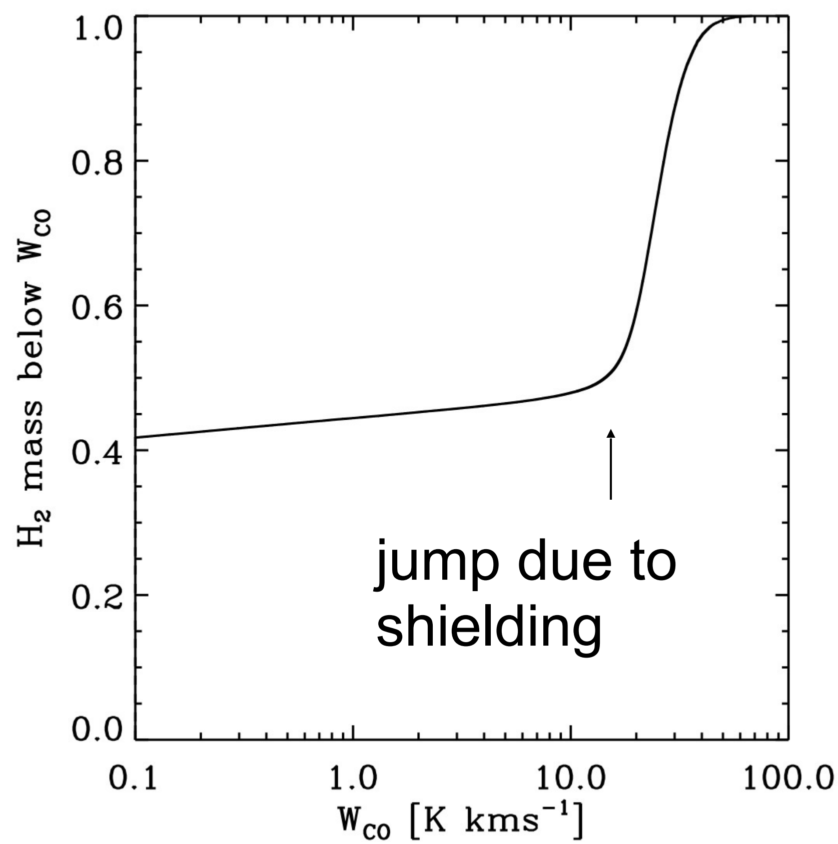

46% molecular gas below CO column densities of 10^{16} cm^{-2}

42% has an integrated CO emission of less than 0.1 K kms^{-1}

$f_{DG} = 0.42$ $\quad$ X_{co}=2.2 × 10^{20} $cm^{-2}K^{-1}km^{-1}s$

(Smith et al., 2014, MNRAS, 441, 1628)

dark gas fraction

Observational estimates:

Grenier et al. (2005)	f_{DG} = 0.33-0.5
Planck coll. (2011)*	f_{DG} = 0.54
Paradis et al. (2012)*	f_{DG} = 0.62
(inner f_{DG} = 0.71, outer f_{DG} = 0.43)	
Pineda et al. (2013)	f_{DG}= 0.3
Roman-Duval et al. (in prep.)	f_{DG} ~ 0.5

* dust methods have large uncertainties.

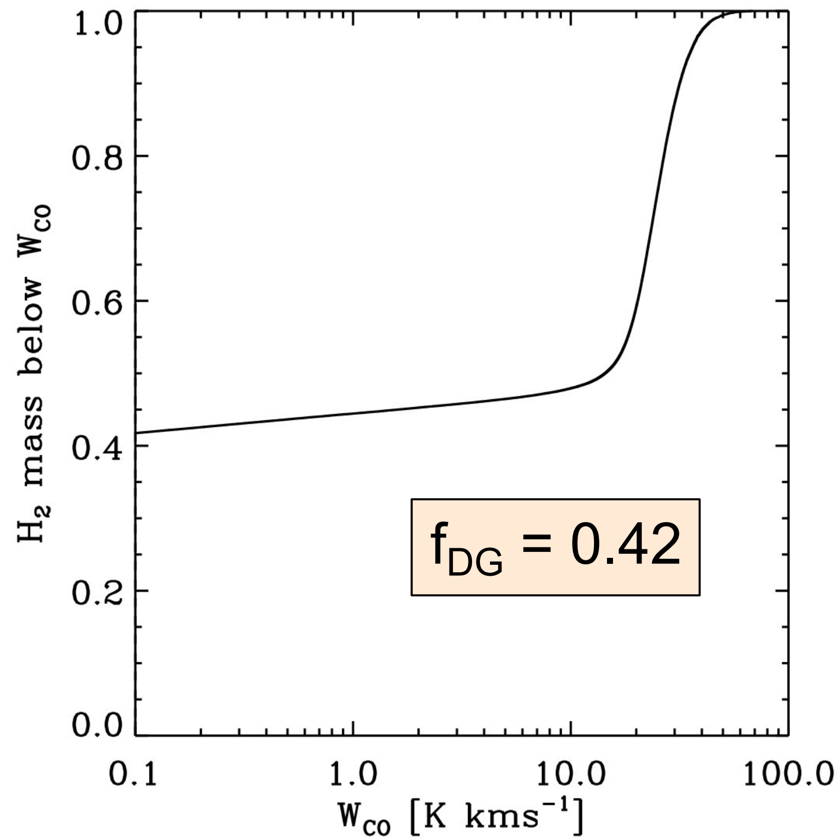

(Smith et al., 2014, MNRAS, 441, 1628)

further evidence

- there is increasing evidence, that a significant fraction of the H_2 gas in galaxies is not traced by CO (e.g. Pringle, Allen, Lubov 2001, Hosokawa & Inutsuka 2007, Clark et al. 2012)

- 3D simulations of colliding HI gas forming molecular clouds at the stagnation region performed by Paul Clark in Heidelberg
  - SPH (also with FLASH)
  - full fledged CO chemistry
  - TREECOL for calculating extinction
  - ‘standard’ dust model
  - sink particles to account for local collapse (star formation)
  - two models: slow and fast flow

further evidence form detailed colliding flow calculations

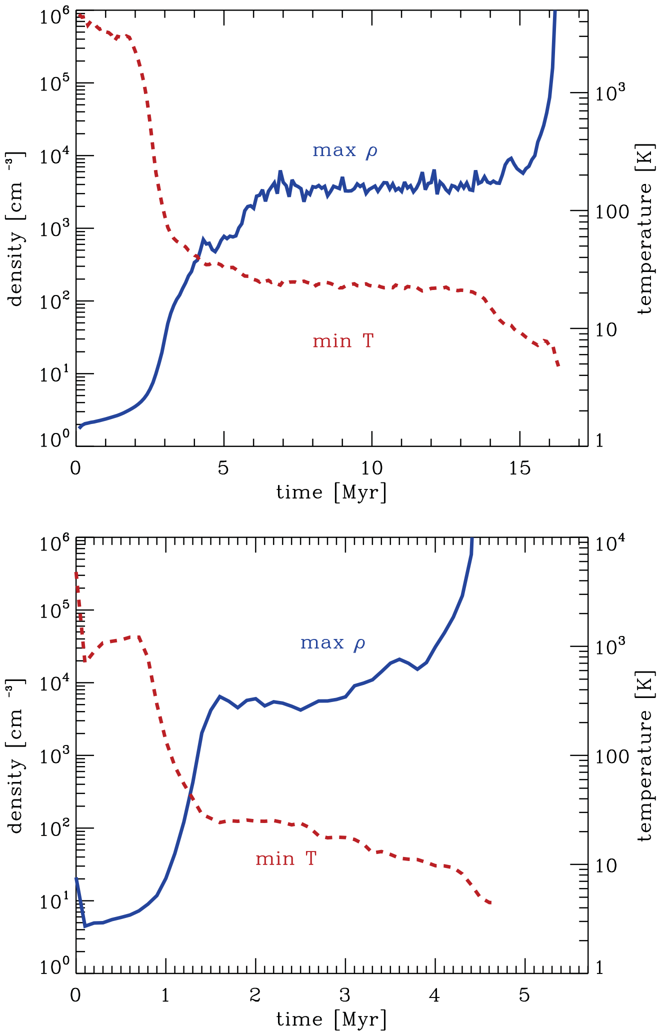

Figure 3. Evolution with time of the maximum density (blue, solid line) and minimum temperature (red, dashed line) in the slow flow (top panel) and the fast flow (bottom panel). Note that at any given instant, the coldest SPH particle is not necessarily the densest, and so the lines plotted are strictly independent of one another.

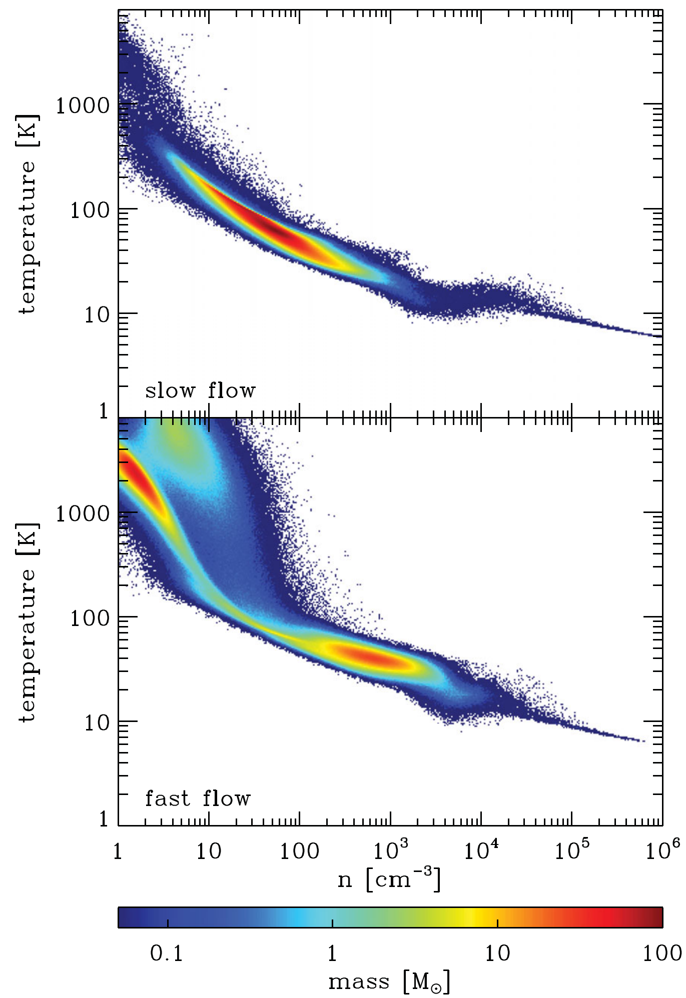

Figure 5. The gas temperature–density distribution in the flows at the onset of star formation.

slow flow

fast flow

Clark et al. (2012,MNRAS, 424, 2599)

see also Pringle, Allen, Lubov (2001), Hosokawa & Inutsuka (2007)

further evidence form detailed colliding flow calculations

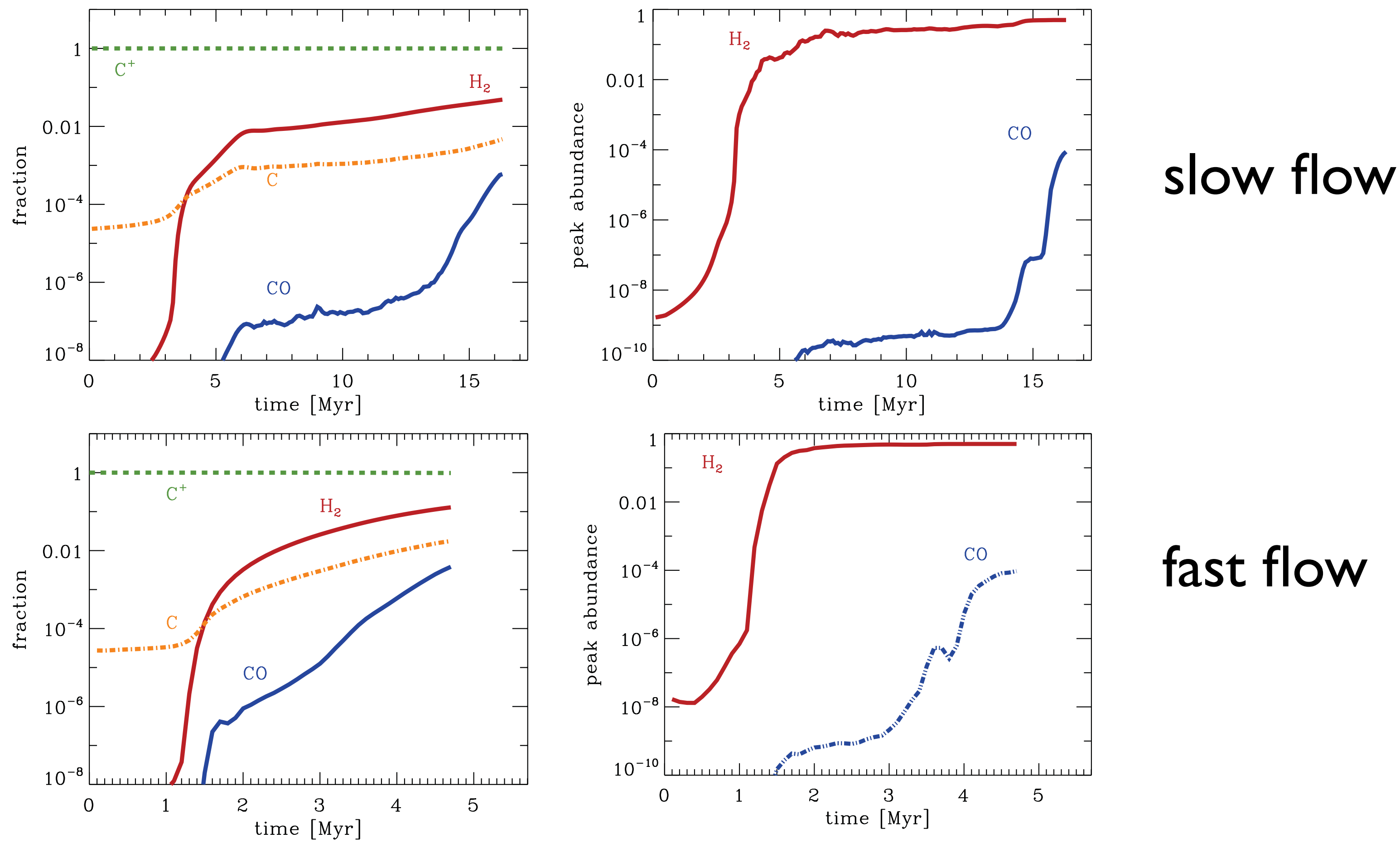

Figure 6. Chemical evolution of the gas in the flow. In the left-hand column, we show the time evolution of the fraction of the total mass of hydrogen that is in the form of H_2 (red solid line) for the 6.8 km s^{-1} flow (upper panel) and the 13.6 km s^{-1} flow (lower panel). We also show the time evolution of the fraction of the total mass of carbon that is in the form of C^+ (green dashed line), C (orange dot–dashed line) and CO (blue double-dot–dashed line). In the right-hand column, we show the peak values of the fractional abundances of H_2 and CO. These are computed relative to the total number of hydrogen nuclei, and so the maximum fractional abundances of H_2 and CO are 0.5 and 1.4×10^{-4}, respectively. Again, we show results for the 6.8 km s^{-1} flow in the upper panel and the 13.6 km s^{-1} flow in the lower panel. Note that the scale of the horizontal axis differs between the upper and lower panels.

Clark et al. (2012,MNRAS, 424, 2599)

see also Pringle, Allen, Lubov (2001), Hosokawa & Inutsuka (2007)

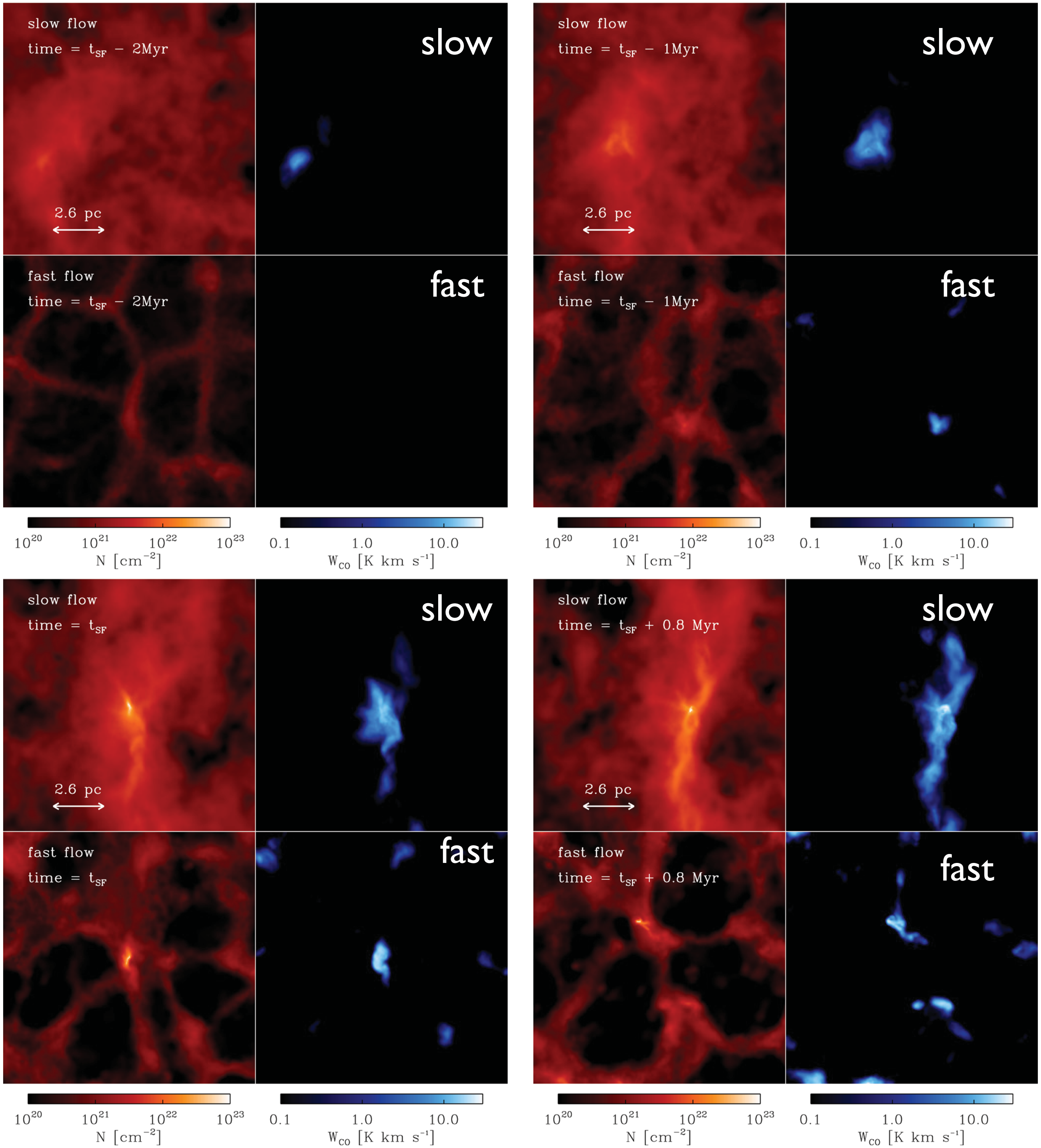

H_2 column

CO emission

fraction of CO dark gas will also change with metallicity and with ambient radiation field

Clark et al. (2012,MNRAS, 424, 2599)


properties of star
forming filaments

large-scale filaments

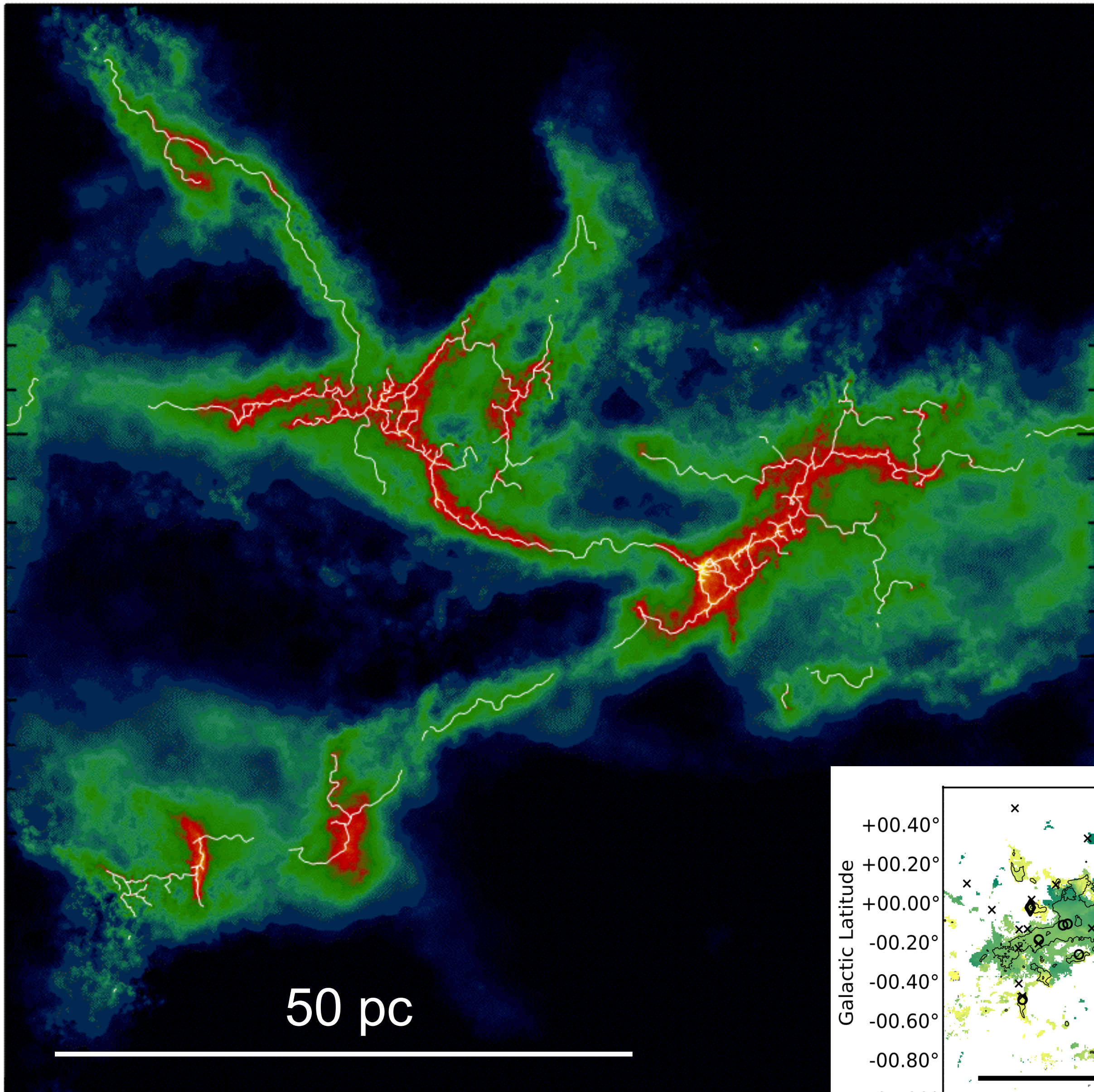

Smith et al. (2014, MNRAS, 445, 2900)

next steps:

studying details of ISM morphology and star formation in dedicated zoom-in simulation

example:
giant molecular cloud complex (~10^6 $M_\odot$) viewed in the plane of the disk.

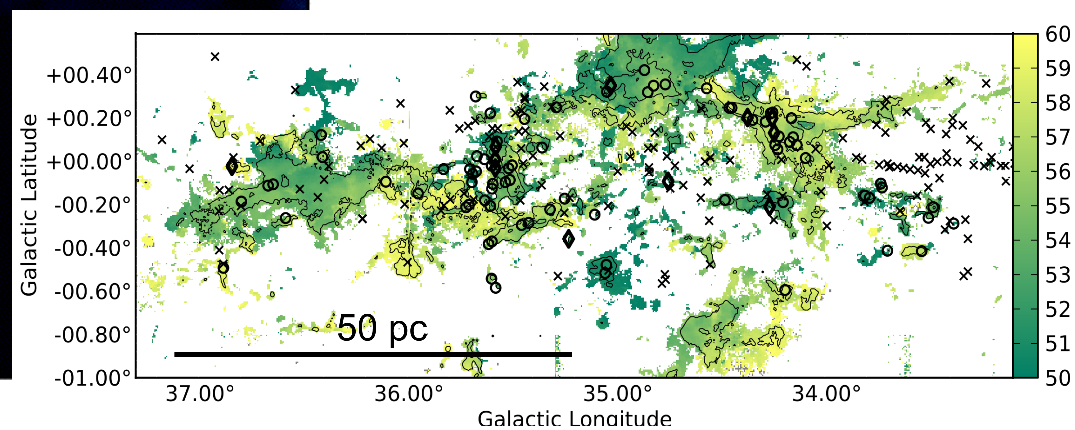

Ragan et al., 2014, A&A, 568, A73)

zoom-in on filaments

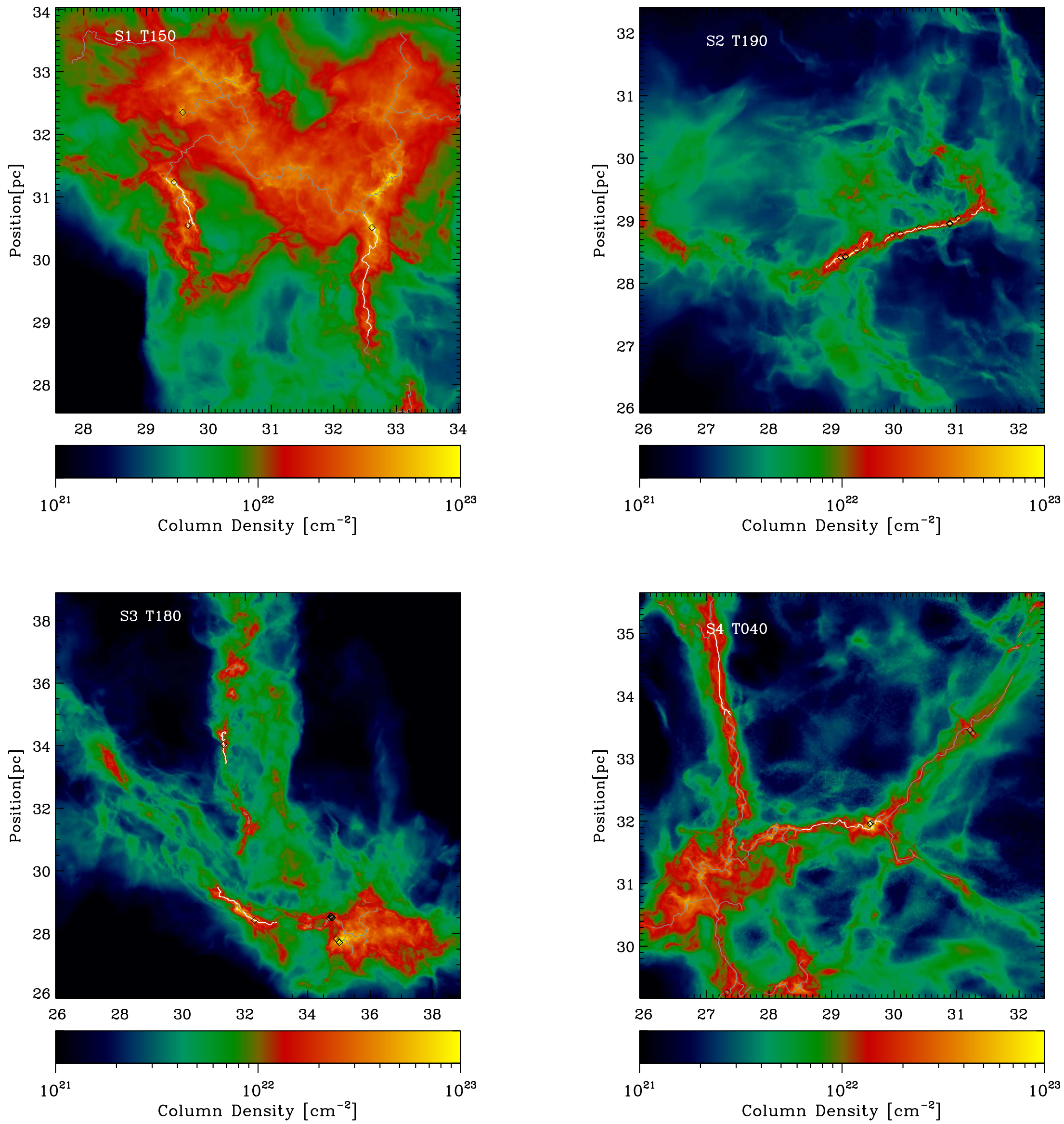

next steps:

studying details of ISM morphology and star formation in dedicated zoom-in simulation *(resolution $\lesssim$2000 AU, with full chemistry)*

analysis:

- morphology
- velocity
- chemistry
- observations (dust maps for Herschel, CO, N_2H+, HCN, etc. for line obs.)

Smith et al. (2014, MNRAS, 445, 2900,
also Smith et al. 2012, ApJ, 750, 64, Smith et al. 2013, ApJ, 771, 24, Chira et al., 2014, MNRAS, 444, 874)

filaments do not have universal width

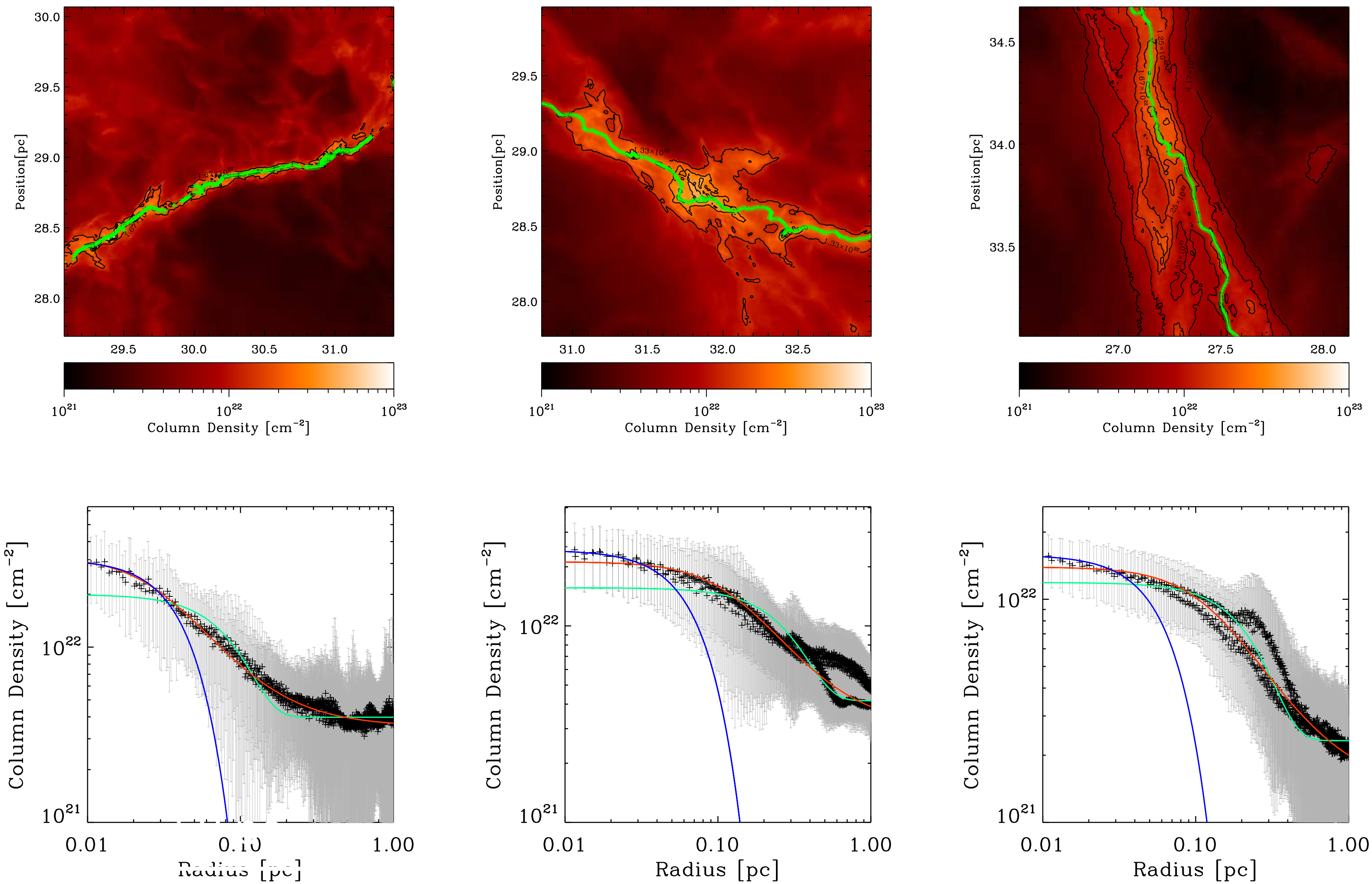

Smith et al. (2014, MNRAS, 445, 2900)

filaments do not have universal width

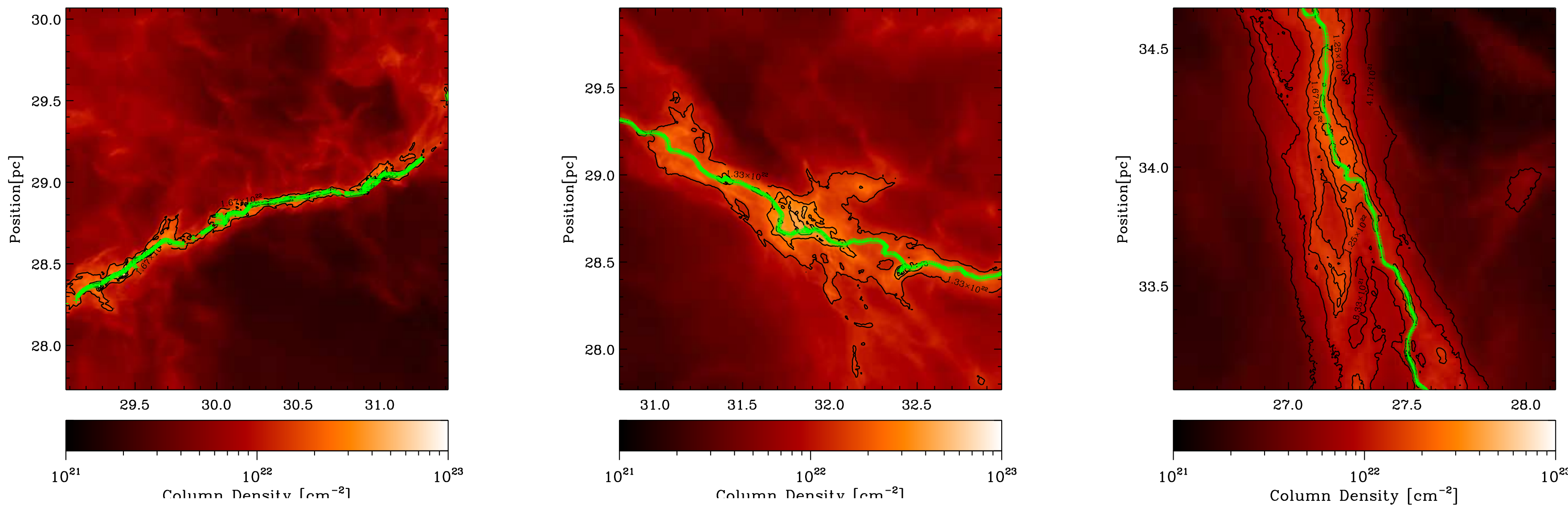

Arzoumanian, et al., 2011, A&A, 529, L6

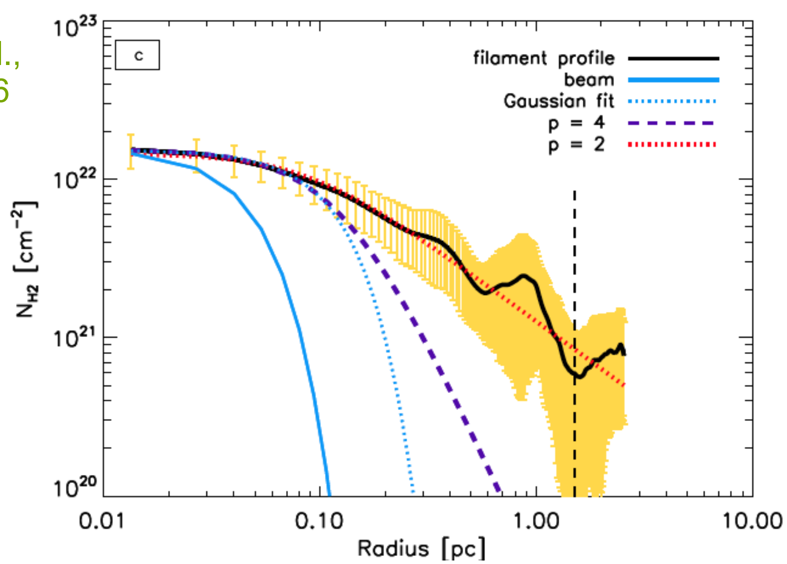

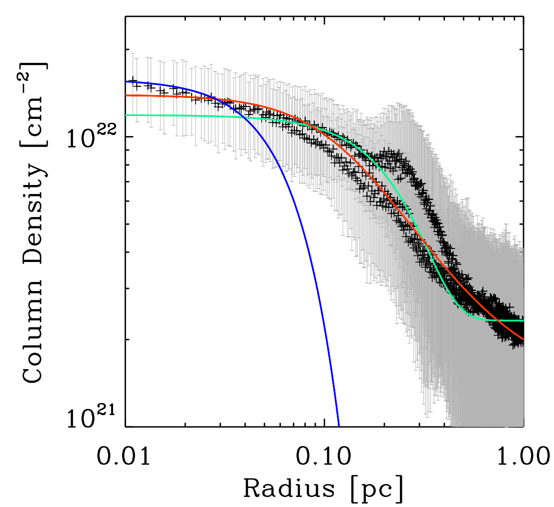

Smith et al. (2014, MNRAS, 445, 2900)

3D filaments have complex structure

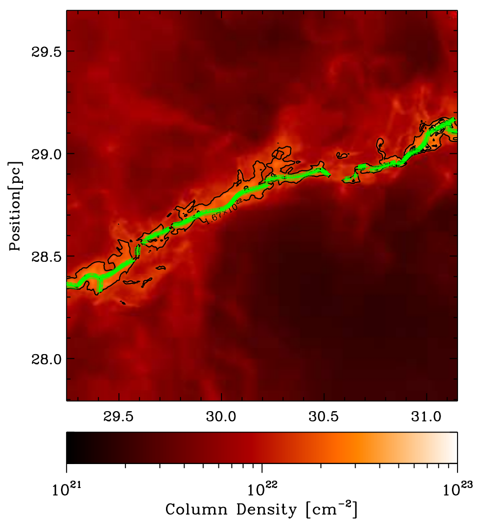

2D filament detection shows nice coherent filament

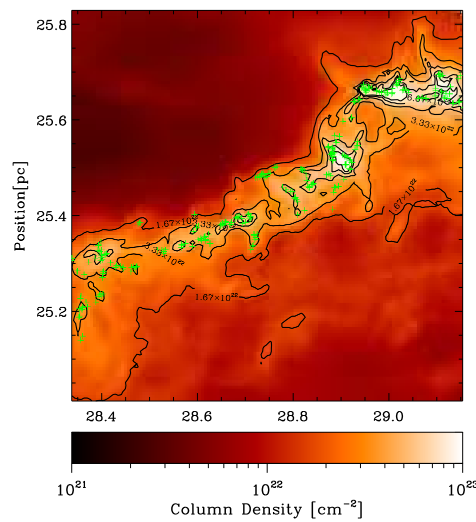

2D + LOS peak detection shows complex structure

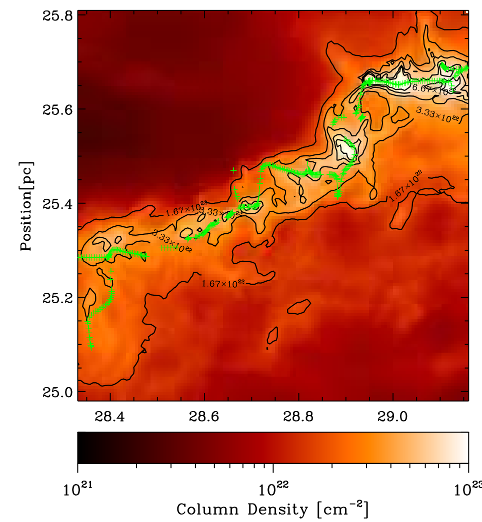

full 3D filament analysis confirms this picture

Smith et al. (2014, MNRAS, 445, 2900)

walk along the filament

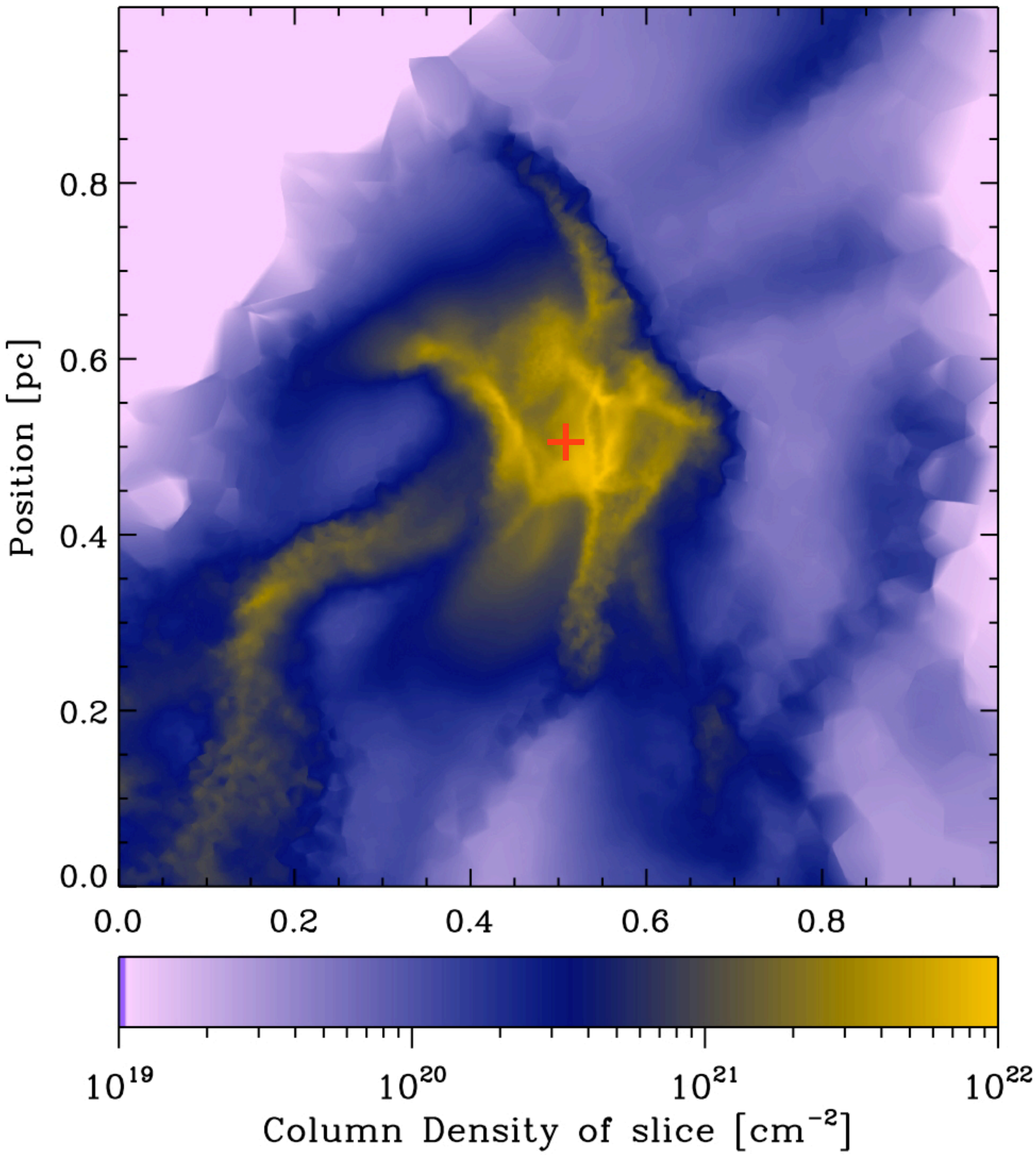

- walking along the filament exhibits complex 3D structure that is now (fully) seen in projected density
- is this similar to the filament fibers proposed by Hacar et al. (2013, A&A, 554, 55)

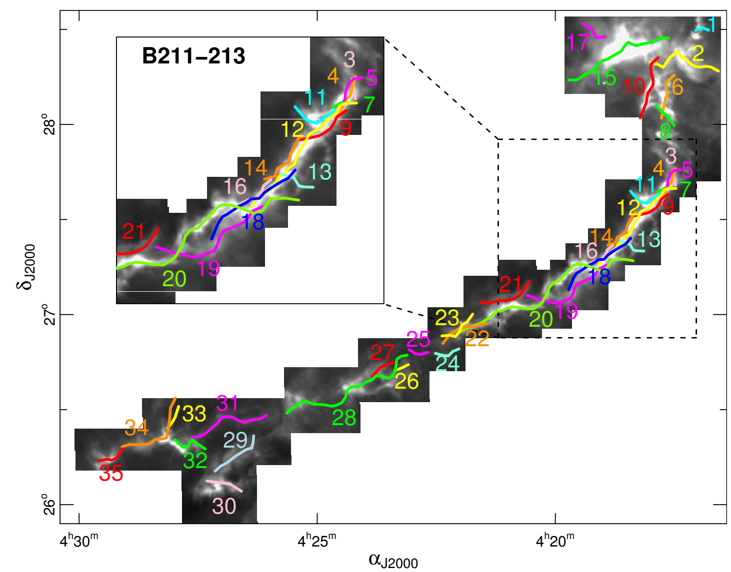

Smith et al. (2014, MNRAS, 445, 2900)


summary

Star formation is intrinsically a multi-scale and multi-physics problem.
Many different processes need to be considered simultaneously.

NGC 3324 (Hubble, NASA/ESA)

Star formation is intrinsically a multi-scale and multi-physics problem. Many different processes need to be considered simultaneously.

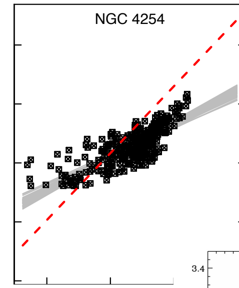

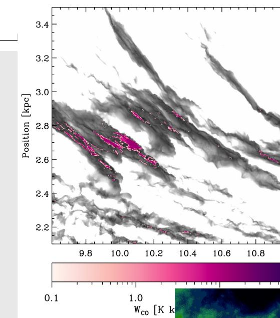

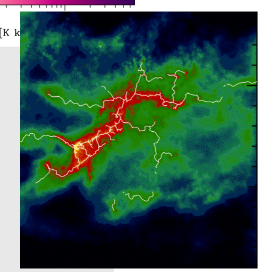

- hierarchical Bayesian statistics indicated galaxy to galaxy variations in the KS relation with typically sublinear slope
  → *how much diffuse CO gas is there*
- detailed (M)HD calculations with time-dependent chemistry allow us to study the properties of CO-dark H2 gas
  → *implications for interpreting observational data?*
- molecular clouds are filamentary, but filament parameters (width, slope, central density) may vary significantly
  → *what does it mean for star cluster formation?*
- next steps:
  multi-physics simulations with Arepo and FLASH for comparison with existing survey data

NGC 3324 (Hubble, NASA/ESA)


thanks